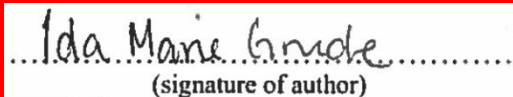




FACULTY OF SCIENCE AND TECHNOLOGY

MASTER'S THESIS

Study programme/specialisation: Environmental Engineering/Offshore Environmental Technology	Spring semester, 2018 Confidential until 15.06.2020
Author: Ida Marie Grude	 (signature of author)
Programme coordinator: Roald Kommedal Supervisor(s): Malcolm A. Kelland – University of Stavanger Tore Nordvik – Schlumberger	
Title of master's thesis: Development of new corrosion inhibitors	
Credits: 30	
Keywords: HPHT corrosion inhibitors, corrosion rate, corrosion prevention, LPR technique, Kettle- test, types of corrosion	Number of pages: 60 + supplemental material/other: 41 Stavanger, 15.06/2018

Acknowledgments

This thesis was the final step in completing my master's degree in Environmental Engineering at the University of Stavanger, Norway spring 2018. As the master program was mostly theoretical I wanted to do some practical work for my thesis, as well as continue in the direction of my bachelor thesis where I wrote about scale inhibitors. Malcolm Kelland was my supervisor during my bachelor thesis and also my internal supervisor for this thesis. I wished to carry out my master thesis in cooperation with a company and was very lucky to get the chance to do this at Schlumberger with Tore Nordvik as my supervisor.

Almost all of the laboratory work and writing process was carried out at Schlumberger, while all the NMR-samples was carried out in the laboratory at the University of Stavanger.

I would like to give thanks to Tore Nordvik for giving me the opportunity to carry out my thesis at Schlumberger, and for the outstanding help and motivation during the process.

Moreover, I want to thank all of the employees at PT R&D for having met me with open arms in January and continued to be very including and helpful every day of this period. A special thanks to Melisa Strenitz for excellent training and guidance at the laboratories, but also for a wonderful mood, engagement, and support throughout the thesis.

A big thank you also goes to Paul Barnes for testing all my products in Aberdeen and for your expertise, and to Lucian Popa and Karen Molde Immerstein for your training and guidance on Kettle-test.

I would also like to thank professor Malcolm A. Kelland for being my supervisor from the University of Stavanger.

Finally, I would like to thank my family and fiancé Erlend for supporting me through the years of studying.

Abstract

Pipelines are an essential part of the oil and gas industry as they are the main means of transportation. As the offshore technology advances, subsea pipelines are being operated in more demanding environments. In field operations where corrosion occurs, chemicals called inhibitors can be employed. Corrosion inhibitors (CI) are injected in small amounts with low concentrations to ensure flow assurance and controlling corrosion, especially CO₂ corrosion. Currently there are no CIs that function well at elevated temperatures, so the purpose of this master thesis was to synthesize CIs for that purpose. The master thesis was divided into two projects, one screening process to see whether or not it was possible to synthesize CIs below 100, and if the presence of a catalyst would help. The second project was a small experimental design project where three aldehydes and three catalysts were used in different combinations. The goal was to achieve a six-membered ring in these CIs as the theory indicates that this is crucial for the performance.

Two kinds of test were performed to evaluate the chemical performance of the synthesized products; High pressure, high temperature (HPHT), static autoclave testing and kettle-testing. The HPHT Autoclave tests were executed at Schlumberger in Aberdeen. Kettle-testing was done using the Linear Polarization Resistance (LPR) technique. Time (hours) and Corrosion rate (mils per year) were the parameters which were compared among the tests to reveal the best corrosion inhibitor. To characterize the synthesized products infrared (IR) spectroscopy and nuclear magnetic resonance (NMR) were performed.

NMR spectra of the products related to structure III show that these compounds do not have the expected six-membered ring which was the target for the synthesis. HPHT, static autoclave tests revealed that these products do not perform well as expected considering the NMR results. The same is shown in the Kettle-test where product 24 does not perform well as a CI, with the best inhibition efficiency of 37.7%. Product 12 on the other hand shows mixed results, but product 12 injected with formulation with 1% 2-mercaptoethanol (2-ME) tested in a cell with 80% NaCl (3%) brine and 20% kerosene have a performance of 93.6 % efficiency inhibition.

There were also some other interesting results from the HPHT, static autoclave test. Product 6 with an average performance of 7.205 mpy, with half the amount of active product in the formulation injected.

Further research after this thesis could be on dose response (in context of the HPHT static autoclave test) to find the cut off points in performance in terms of corrosion rate and surface conditions. Further characterization of the products related to structure III is also work that should be done in order to characterize the actual product. It would also be interesting to optimize the synthesis ratios and order of executing synthesis steps in order to optimize costs related to the final product(s). Additional testing of the products at Schlumberger (Forus) with Rotating Cylinder Electrode (RCE) is also of interest as this test adds medium stress-shear.

Contents

Acknowledgments.....	ii
Abstract.....	iii
Contents.....	iv
Abbreviations.....	viii
List of Figures.....	ix
List of Tables.....	xi
Chapter 1 - Introduction to Corrosion.....	1
What is corrosion?.....	1
Types of corrosion.....	2
General corrosion.....	3
Localized corrosion.....	3
Crevice corrosion.....	3
Pitting corrosion.....	3
Intergranular corrosion.....	3
Galvanic corrosion.....	4
Erosion-corrosion.....	4
Corrosion due to variation in fluid flows.....	4
Stress corrosion.....	4
Cracking corrosion.....	5
Microbial influenced corrosion (MIC).....	5
Corrosive behaviour.....	5
Immune behavior.....	5
Active behavior.....	5
Passive behavior.....	5
Effects of corrosion.....	6
The Economic impact of Corrosion.....	6
Corrosion control.....	9
Materials.....	9
Coatings.....	9
Inhibitors.....	10
Cathodic protection.....	10
Design.....	10
Chapter 2 - Corrosion inhibitors.....	12
Classification.....	12

Fields of application	12
Application of Corrosion Inhibitors.....	13
Batch application vs. Continuous Application	13
Emulsions	13
Application in Solid Form	13
Film-Forming Corrosion Inhibitors.....	13
How does FFCIs work?	13
Classes of FFCIs	14
Chapter 3 – Testing of Corrosion Inhibitors.....	18
High Pressure, High Temperature Static Autoclave Test	19
Corrosion testing by LPR – Kettle test.....	19
Purpose	19
Calculation	19
Chapter 4 – Catalysts	20
Reaction rates: How fast does a Reaction go?.....	20
Catalysts	21
The use of catalyst in this thesis	21
Chapter 5 – Synthesis of Hexahydropyrimidine.....	23
Selection of starting materials	24
Characterization of products	25
Purification.....	27
Chapter 6 – Results	29
High Pressure, High Temperature Static Autoclave Test.....	29
Kettle-test	31
Chapter 7 - Discussion.....	33
High Pressure, High Temperature Static Autoclave Test	33
Kettle-test	34
Economic aspects.....	35
Chapter 8 – Conclusions and further work	36
Chapter 9 – Experimental	38
Analysis	38
IR	38
NMR	38
Synthesis details.....	38
Method 1 – Vacuum synthesis.....	38
Method 2 – Dean Stark	39

Product 1.....	39
Product 2.....	39
Product 3.....	40
Product 4.....	40
Product 5.....	40
Product 6.....	40
Product 7.....	40
Product 8.....	40
Product 9.....	41
Product 10.....	41
Product 11.....	41
Product 12.....	41
Product 13.....	41
Product 14.....	42
Product 15.....	42
Product 16.....	42
Product 17.....	42
Product 18.....	42
Product 19.....	43
Product 20.....	43
Product 21.....	43
Product 22.....	43
Product 23.....	43
Product 24.....	44
Product 25.....	44
Product 26.....	44
Product 27.....	44
Product 28.....	44
Product 29.....	45
Test methods:	46
High Pressure, High Temperature, static Autoclave test.....	46
Kettle-test	46
Making of formulations and brines for both test methods	48
References	49
Attachment	A
High pressure, high temperature, static Autoclave Test	A

Kettle-test results.....	I
Infrared (IR) Spectroscopy	O
NMR	S

Abbreviations

2-ME	2-mercaptoethanol
CI	Corrosion Inhibitor
CMC	Critical Micelle Concentration
DDQ	2,3-dichloro-5,6-dicyano-p-benzoquinone
Eq.	Equivalent
FFCI	Film-Forming Corrosion Inhibitor
GC	Gas Chromatography
GPC	Gel Permeation Chromatography
HPHT	High Pressure, High Temperature
IR	Infrared Spectroscopy
LCMS	Liquid Chromatography Mass Spectrometry
LPR	Linear polarization resistance
MIC	Microbial Influenced Corrosion
mpy	mils per year
NMR	Nuclear Magnetic Resonance
p-TsOH	para-Toluenesulfonic acid
RCE	Rotating Cylinder Electrode
REACH	Registration, Evaluation, Authorisation and Restriction of Chemicals
SEM	Scanning Electron Microscopy
w/	with
w/o	without
wt%	weight percentage

List of Figures

FIGURE 1: CORROSION CYCLE OF STEEL (DAVIS, 2000).....	1
FIGURE 2: CORROSION CELL REACTION(KELLAND, 2014)	2
FIGURE 3: EXAMPLE OF CREVICE CORROSION (STEEFAB, 2017A)	3
FIGURE 4: EXAMPLE OF PITTING CORROSION(STEEFAB, 2017D)	3
FIGURE 5: EXAMPLE OF INTERGRANULAR CORROSION(STEEFAB, 2017C).....	3
FIGURE 6: EXAMPLE OF GALVANIC CORROSION(STEEFAB, 2017B)	4
FIGURE 7: EXAMPLE OF EROSION-CORROSION(INSA, 2013A).....	4
FIGURE 8: EXAMPLE OF STRESS-CORROSION-CRACKING(INSA, 2013B)	4
FIGURE 9: EXAMPLE OF MICROBIAL INFLUENCED CORROSION(TANKS, 2017)	5
FIGURE 10: THREE BEHAVIORS OF METAL IN A CORROSIVE ENVIRONMENT (DAVIS, 2000)	5
FIGURE 11: FACTORS WHICH INCREASE OF DECREASE THE COSTS OF CORROSION (DAVIS, 2000)	7
FIGURE 12: THE EFFECT OF AN FFCI SURFACTANT (KELLAND, 2014).....	14
FIGURE 13: STRUCTURES OF TYPICAL PHOSPHATE ESTER FFCIS (KELLAND, 2014)	15
FIGURE 14: QUATERNARY AMMONIUM, ALKYL PYRIDINE QUATERNARY, AND ZWITTERIONIC BETAINES FFCIS (KELLAND, 2014)	16
FIGURE 15: AMIDOETHYL IMIDAZOLINES (KELLAND, 2014)	16
FIGURE 16: EXAMPLE OF A POLYMETHYLENEPOLYAMINEDIPROPIONAMIDE FFCI (KELLAND, 2014)	16
FIGURE 17: N',N'-DIOCTYL-N,N'-BIS(1-DEOXYGKYCITYL)ETHYLENEDIAMINE (KELLAND, 2014)	17
FIGURE 18: THIOGLYCOLIC ACID, 3,3'-DITHIODIPROPIONIC ACID, AND POTASSIUM DIMETHYL DITHIOCARBAMATE (KELLAND, 2014).....	17
FIGURE 19: SODIUM POLYASPARTATE (KELLAND, 2014).....	17
FIGURE 20: REACTION EQUATION FOR POLAR ADDITION OF HBR TO ETHENE. (H. HART, HADAD, CRAINE, & HART, 2011)	20
FIGURE 21: REACTION ENERGY DIAGRAM FOR THE ADDITION OF HBR TO AN ALKENE (ETHENE)(D. J. HART, 2012; H. HART ET AL., 2011)	20
FIGURE 22: REACTION SCHEME FOR THE EXPECTED PRODUCTS FOR THE DIFFERENT ALDEHYDES USED IN SYNTHESIS.	23
FIGURE 23: REACTION MECHANISM FOR THE SYNTHESIS, WHERE R IS THE ALKYL CHAIN AND R2 ARE CONNECTED TO THE ALDEHYDES AND DIFFERS DEPENDING ON THE ALDEHYDE USED IN THE REACTION.	23
FIGURE 24: REACTION MECHANISM FOR THE FORMATION OF THE IMINE.....	26
FIGURE 25: STRUCTURE V - IMINE	26
FIGURE 26: REACTION MECHANISM FOR THE BIS ADDUCT	27
FIGURE 27: STRUCTURE IV - BIS ADDUCT	27
FIGURE 28: AVERAGE CORROSION RATE FROM HPHT STATIC AUTOCLAVE TESTS	29
FIGURE 29: PRODUCT 12.....	30
FIGURE 30: PRODUCT 20.....	30
FIGURE 31: PRODUCT 24.....	30
FIGURE 32: LPR GRAPH FOR PRODUCT 12, PRODUCT 20, AND PRODUCT 24	31
FIGURE 33: SET-UP FOR VACUUM SYNTHESIS	38
FIGURE 34: SET-UP FOR DEAN-STARK SYNTHESIS.....	39
FIGURE 35: HPHT STATIC AUTOCLAVE TEST EQUIPMENT	46
FIGURE 36: ASSEMBLED HPHT STATIC AUTOCLAVE TEST EQUIPMENT.....	46
FIGURE 37: KETTLE-TEST SET-UP FOR ONE TEST CELL.....	47
FIGURE 38: CORROSION RATES FOR EACH COUPON FROM THE HPHT STATIC AUTOCLAVE TEST	A
FIGURE 39: PRODUCT 1.....	B
FIGURE 40: PRODUCT 2.....	B
FIGURE 41: PRODUCT 3.....	B
FIGURE 42: PRODUCT 4.....	B
FIGURE 43: PRODUCT 5.....	B
FIGURE 44: PRODUCT 6.....	B
FIGURE 45: PRODUCT 7.....	C
FIGURE 46: PRODUCT 8.....	C
FIGURE 47: PRODUCT 9.....	C
FIGURE 48: PRODUCT 10.....	C
FIGURE 49: PRODUCT 11.....	C

FIGURE 50: PRODUCT 13.....	C
FIGURE 51: PRODUCT 14.....	D
FIGURE 52: PRODUCT 15.....	D
FIGURE 53: PRODUCT 18.....	D
FIGURE 54: PRODUCT 19.....	D
FIGURE 55: PRODUCT 21.....	D
FIGURE 56: PRODUCT 16.....	D
FIGURE 57: PRODUCT 25.....	E
FIGURE 58: PRODUCT 22.....	E
FIGURE 59: PRODUCT 17.....	E
FIGURE 60: PRODUCT 26.....	E
FIGURE 61: PRODUCT 23.....	E
FIGURE 62: PRODUCT 27.....	E
FIGURE 63: PRODUCT 28.....	F
FIGURE 64: PRODUCT 29.....	F
FIGURE 65: LPR GRAPH INCLUDING RESULTS FROM CELLS WITH 100% BRINE.....	I
FIGURE 66: LPR GRAPH INCLUDING RESULTS FROM CELLS WITH 80% BRINE, 20% KEROSENE.....	J
FIGURE 67: LPR GRAPH INCLUDING RESULTS OF PRODUCT 12.....	K
FIGURE 68: LPR GRAPH INCLUDING RESULTS OF PRODUCT 20.....	L
FIGURE 69: LPR GRAPH INCLUDING RESULTS OF PRODUCT 24.....	M
FIGURE 70: FULL KETTLE-TEST SET-UP WITH 5 TEST-CELLS.....	N
FIGURE 71: PRODUCT 24 IN 80% BRINE W/2-ME.....	N
FIGURE 72: IR OF PRODUCT 12.....	O
FIGURE 73: IR OF PRODUCT 20.....	P
FIGURE 74: IR OF PRODUCT 24.....	Q
FIGURE 75: IR OF PRODUCT 24 AND PRODUCT 24 REHEATED.....	R
FIGURE 76: ¹ H-NMR OF PRODUCT 12.....	S
FIGURE 77: ¹ H-NMR OF PRODUCT 12.....	T
FIGURE 78: ¹ H-NMR OF PRODUCT 12.....	U
FIGURE 79: ¹³ C-NMR OF PRODUCT 12.....	V
FIGURE 80: ¹³ C-NMR OF PRODUCT 12.....	W
FIGURE 81: ¹³ C-NMR OF PRODUCT 12.....	X
FIGURE 82: 2D-NMR COSY OF PRODUCT 12.....	Y
FIGURE 83: 2D-NMR HSQC OF PRODUCT 12.....	Z
FIGURE 84: ¹ H-NMR OF PRODUCT 20.....	Æ
FIGURE 85: ¹ H-NMR OF PRODUCT 20.....	∅
FIGURE 86: ¹ H -NMR OF PRODUCT 20.....	Å
FIGURE 87: ¹³ C -NMR OF PRODUCT 20.....	AA
FIGURE 88: ¹³ C -NMR OF PRODUCT 20.....	BB
FIGURE 89: ¹³ C -NMR OF PRODUCT 20.....	CC
FIGURE 90: 2D-NMR COSY OF PRODUCT 20.....	DD
FIGURE 91: 2D-NMR HSQC OF PRODUCT 20.....	EE
FIGURE 92: ¹ H -NMR OF PRODUCT 24.....	FF
FIGURE 93: ¹ H -NMR OF PRODUCT 24.....	GG
FIGURE 94: ¹ H -NMR OF PRODUCT 24.....	HH
FIGURE 95: ¹³ C -NMR OF PRODUCT 24.....	II
FIGURE 96: ¹³ C -NMR OF PRODUCT 24.....	JJ
FIGURE 97: ¹³ C-NMR OF PRODUCT 24.....	KK
FIGURE 98: 2D-NMR COSY OF PRODUCT 24.....	LL

List of Tables

TABLE 1: LIST OF EXAMPLES FOR EACH ELEMENT OF COST	8
TABLE 2: OVERVIEW OF COMPONENTS AND METHOD USED IN THE DIFFERENT PRODUCTS, WHERE PRODUCT 1-11 ARE FROM THE SCREENING PROJECT, AND PRODUCT 12-29 ARE FROM THE EXPERIMENTAL DESIGN PROJECT. FURTHER DETAILS FOR EACH PRODUCT ARE DESCRIBED IN CHAPTER 9 - EXPERIMENTAL	24
TABLE 3: INHIBITION EFFICIENCY RESULTS FROM KETTLE-TEST. THE NUMBERS ARE USED IN THE DISCUSSION.	32
TABLE 4: OVERVIEW OF CORROSION RATES AND COMMENTS REGARDING SURFACE CONDITIONS FOR HPHT, STATIC AUTOCLAVE TESTS	G
TABLE 5: OVERVIEW OF CORROSION RATES AND COMMENTS REGARDING SURFACE CONDITIONS FOR HPHT, STATIC AUTOCLAVE TESTS	H

Chapter 1 - Introduction to Corrosion

What is corrosion?

Corrosion is a natural process. Just like water flows to the lowest level, all natural processes tend towards the lowest possible energy state. A general definition of corrosion is degradation of material through environmental degradation. This includes all materials both naturally occurring and man-made such as metals, plastics, and ceramics (Peabody, Bianchetti, National Association of Corrosion, & International, 2001). From a practical view, the term materials refers to the substances used in the construction of machines, process equipment, and other manufactured products (Stansbury & Buchanan, 2000). A simplified definition of corrosion is to eat or into or wear away material gradually, like gnawing. In this article, corrosion will be defined as a chemical or electrochemical reaction between material, usually a metal, and the environment which causes deterioration of the metal and its properties. The environment consists of the entire surroundings in contact with the material. The primary factors to describe the environment are as follow: a) physical state – liquid, gas or solid, b) chemical composition – constituents and concentration, and c) temperature.

To summarize corrosion is the deterioration of a metal and is caused by the reaction between the metal and the environment (Davis, 2000).

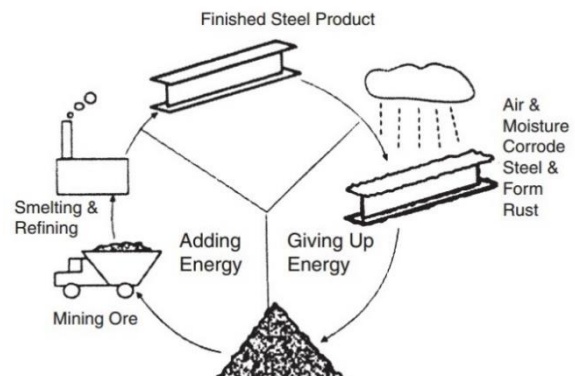


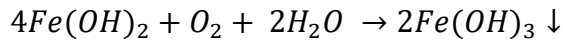
Figure 1: Corrosion Cycle of steel (Davis, 2000)

Internal and external corrosion of downhole tubing and equipment, either subsea or surface pipelines, in pressure vessels and storage tanks is a major issue in the oil and gas industry. As well as basic wastage of metal, local or general, the consequences of electrochemical corrosion can also be embrittlement and cracking. All of this can lead to equipment failure (Kelland, 2014).

For corrosion to occur of iron on steel, the presence of water and aqueous species which can be reduced while iron is oxidized, are required. Natural organic acids, oxygen and acidic gases such as CO₂ and H₂S in the produced fluids all contributes to corrosion(Kelland, 2014).

Corrosion involves redox-reactions, with removal of electrons of the metal – oxidation – and the consumption of the same electrons by some reduction reaction, for example oxygen or water reduction. The reduction reaction is often called the cathodic reaction while the oxidation reaction often is called anodic reaction. For corrosion to occur, both reactions are necessary. The oxidation reaction causes the actual metal loss, but the reduction reaction must be present to consume the electrons from the oxidation reaction, to maintain a neutral charge. Otherwise, there would rapidly develop a large negatively charge between the metal and electrolyte leaving the corrosion process to cease (Peabody et al., 2001).

One common corrosion process is the formation of ferric hydroxide, Fe(OH)₃:



Where equation (1) is the oxidation reaction and (2) is the reduction reaction (Peabody et al., 2001; Perez, 2004).

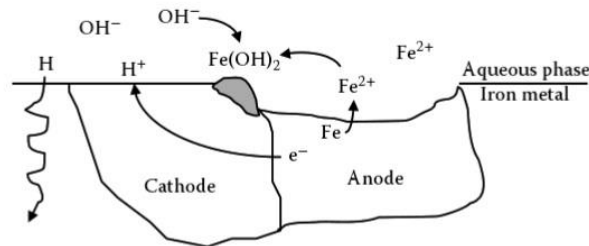


Figure 2: Corrosion cell reaction (Kelland, 2014)

There are four necessary components for corrosion to occur. There must be an anode and a cathode, a metallic path electrically connecting the anode and cathode, normally the pipeline itself, and the cathode and the anode must be immersed in an electrically conductive electrolyte. These four components constitute a differential corrosion cell (Peabody et al., 2001). The corrosion process stops if any of these four components are eliminated. The metal cannot dissolve if the anode is removed or made passive. Removing the cathode has been shown to be an effective way to control corrosion, because this results in no consumption of the electrons generated at the anode. Similarly, if the ionic current path, the electrolyte, is removed there is no means for the transfer of ionic electrical charge from the anode to the cathodes. Elimination of the electric path between the cathode and anode also eliminates corrosion, because the electrons are not able to move from the anode to the cathode, making it hard for the cathode to neutralize the large negative charge that builds up (Davis, 2000).

Types of corrosion

Corrosion occurs in several widely differing forms. These three factors are used as base when classifying corrosion (Davis, 2000):

- Nature of the corrodent: can be classified as “wet” or “dry”. Wet corrosion requires a liquid or moisture, while dry corrosion often involves reactions with high-temperature gases.
- Mechanism of corrosion: involves electrochemical or direct chemical reaction.
- Appearance of the corroded metal: there is either uniform corrosion with the same corrosion rate over the entire surface, or localized where only small areas are affected.

In an oilfield, there are many types of corrosion that can occur. This includes general/uniform corrosion, localized corrosion, pitting and crevice corrosion, intergranular corrosion, galvanic corrosion, erosion corrosion, corrosion due to variation in fluid flows, stress corrosion, cracking corrosion, and microbial influenced corrosion (MIC) (Chilingar, Mourhatch, & Al-

Qahtani, 2013; Davis, 2000; Kelland, 2014). These types of corrosion are described shortly below.

General corrosion

General corrosion is also called uniform corrosion, is the easiest type of corrosion to manage. General corrosion is uniform wastage of metal along the flowline or the whole tubing without any localized attack. This type of corrosion does not penetrate deep inside. The most common and familiar example is rusting of metal/steel in air.

Localized corrosion

Localized corrosion occurs at specific points and takes place more often than general corrosion. Examples of localized corrosion are crevice corrosion, pitting corrosion.

Crevice corrosion

Crevice corrosion is an example of localized attack in the shielded areas of metal constructions like pipes and collars, nails and boxes, tubing and drill pipe joints. Crevice corrosion is caused by concentration differences of corrodents over a metal surface. Electrochemical potential differences result in selective crevice or pitting corrosion attack. Oxygen dissolved in drilling fluids promotes crevice and pitting attacks of metal in the shielded areas of drill string and is the most common cause to outwash and destruction under rubber pipe protectors (Chilingar et al., 2013).



Figure 3: Example of Crevice Corrosion (Steelfab, 2017a)

Pitting corrosion

Pitting is mostly localized in a crevice, but can also occur on clean metal surfaces in a corrosive environment. An example of this type of corrosion attack is corrosion of steel in high-velocity seawater, low-pH aerated brines, or drilling fluids. By pit formation, corrosion continues as a crevice but at an accelerated rate (Chilingar et al., 2013).

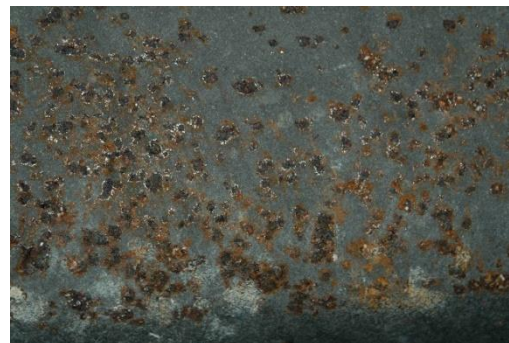


Figure 4: Example of Pitting Corrosion (Steelfab, 2017d)



Figure 5: Example of Intergranular Corrosion (Steelfab, 2017c)

Intergranular corrosion

Metal is preferentially attacked along the grain boundaries. Improper heat treatment of alloys or high-temperature exposure can lead to precipitation of materials or non-homogeneity of metal structure by the grain boundaries, which results in preferential attack. Weld decay is a form for intergranular attack (Chilingar et al., 2013).

Galvanic corrosion

Galvanic corrosion occurs when two metals are in metal-to-metal contact in a corrosive electrolyte, where the metals have different electrochemical potentials or with different tendencies to corrode (Chilingar et al., 2013).

Erosion-corrosion

Erosion corrosion is also called flow-induced localized corrosion. Erosion corrosion is a complex materials degradation mechanism involving the combined effects of mechanical erosion and electrochemical corrosion. The combination of erosion and corrosion result in severe localized attack of metal. Damage appears as smooth groove or hole in the metal, such as in a washout of the drill pipe, tubing, or casing. The outwash is initiated by pitting in a crevice which penetrates the steel. The erosion-corrosion process completes the destruction of metal. The erosion process removes the protective film layer from the metal surface, leaving the clean metal surface to the corrosive environment. This accelerates the corrosion process (Chilingar et al., 2013).



Figure 6: Example of Galvanic Corrosion(Steelfab, 2017b)



Figure 7: Example of Erosion-Corrosion(INSA, 2013a)

Corrosion due to variation in fluid flows

Turbulence of fluid flow along with differences in velocity over the metal surface cause localized corrosion. Variation in flow can, in addition to the combined effects of erosion and corrosion, cause differences in concentration of the corrodents and depolarizes, which may result in a selective attack of metals (Chilingar et al., 2013).

Stress corrosion

The combined effects of stress and corrosion on metals make up stress corrosion. Local action cells developed due to the residual stresses induced in the metal and adjacent unstressed metal in the pipe is an example of stress corrosion. Stressed metal is anodic while unstressed metal is cathodic. The degree to which these stresses are induced in pipes varies with

1. The metallurgical properties
2. Cold work
3. Weight of pipe
4. Effects of slips, notch effects at tool joints
5. Presence of H₂S gas.

In oil fields, H₂S-induces stress corrosion has been instrumental in bringing about sudden failure of drill pipes (Chilingar et al., 2013).



Figure 8: Example of Stress-Corrosion-Cracking(INSA, 2013b)

Cracking corrosion

Cracking corrosion is characterised by fine cracks which lead to failure due to a combination of tensile stress, the environment and in some systems, a metallurgical condition (Chilingar et al., 2013).

Microbial influenced corrosion (MIC)

MIC is a very widespread corrosion caused by chemical processes initiated by the metabolism of anaerobic microorganisms in the produced fluids. Most MIC takes the form of pits that form underneath colonies of bacteria, known as biofilms. These are frequently developed within minerals and bio deposits. Biofilms creates a protective environment where conditions can become corrosive and corrosion is accelerated (Kelland, 2014).



Figure 9: Example of Microbial Influenced Corrosion (Tanks, 2017)

Corrosive behaviour

When metal is immersed into a corrosive environment, it can behave in one of three ways. It can have an immune, active or passive behavior, and is shown in figure 10.

Immune behavior

Metals known to display immune behavior are often called noble metals and include metals like gold, silver, and platinum. For a combination of metal and environment resulting in immune behavior, there is no reaction of the metal, and there is no corrosion of the metal. Immune behavior results from the metal being thermodynamically stable in the particular environment; that is, the corrosion reaction does not occur spontaneously (Davis, 2000).

Active behavior

When the metal corrodes, there is an active behavior, and the metal dissolves in solution and forms, nonprotective corrosion products. The corrosion process continues in this solution because the corrosion product does not prevent further corrosion (Davis, 2000).

Passive behavior

Passive behavior is when a metal corrodes, but it does not dissolve in solution. Instead, a protective film form onto the metal. This protection film, also called a passive film, slows down the reaction to very low levels. The corrosion resistance when dealing with passive behavior depends on the integrity of the protective film. If this film is broken or

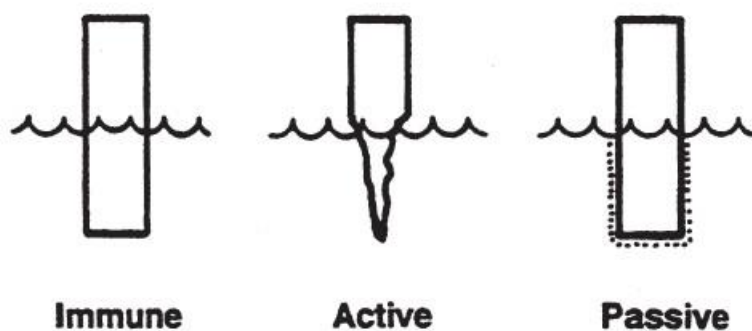


Figure 10: Three behaviors of metal in a corrosive environment (Davis, 2000)

dissolves, then the metal can convert to active behavior and rapid dissolution can occur. It is important to acknowledge that a passive film is unlike a coat of paint – even though for many practical purposes it can appear to behave as such. If one looks from a corrosion control perspective, immune behavior is the most desirable because corrosion protection is independent from the stability of the protective films. Engineering alloys, however, are passive in their application and therefore depending of the integrity of the passive film. Where the environment becomes more corrosive, metals tend to display local forms of corrosion, for example pitting, stress corrosion, cracking and crevice corrosion. This result because the bulk of the alloy surface remains protected by the passive film, but rapid corrosion occurs in those areas where the film has broken down. Only the most noble metals exhibit immune behavior in a wide variety of corrosive environments. In most cases, it is not practical to use these materials for engineering applications because of their excessive costs and strength limitations (Davis, 2000).

Effects of corrosion

The effects of corrosion in the daily life are both direct and indirect. Service lives of our possessions are affected directly by corrosion, while producers and suppliers are affected with corrosion costs which they pass on to consumers and we are therefore affected in an indirect way. In a household, corrosion is often recognized as rust on cars, charcoal grills, tools made of metal, and outdoor furniture. In order to maintain, and extend, the lifetime of the items, preventative methods such as applying a coat of paint protects them towards corrosion. Other household appliances such as water heaters, washers, dryers, furnaces and ranges, have built in corrosion protection (Davis, 2000).

Corrosion can have more severe consequences in how it affects the transportation forth and back from work and school. Corrosion does not only occur in plain sight, but also in places where it is hard to detect it. For example, the corrosion of steel reinforcing bar in concrete can occur out of sight and can suddenly (or seemingly so) result in the collapse of electrical towers, bridges, cause damage on buildings, parking structures, failure of a section of the highway, etc. resulting in high repair costs and endangering public safety. Most dangerous of all corrosion is perhaps the corrosion which takes place in major industrial plants like chemical processing plants or electrical power plants. Shutdowns of plants due to corrosion can and do happen.

The Economic impact of Corrosion

Figure 11 shows some of the factors which influence the costs related to corrosion. Corrosion costs are reduced by the application of available corrosion technology, together with technology transfer. New and improved corrosion technology is a result of research and development. Corrosion costs decrease even more with proper application of corrosion control methods (e.g. coatings, inhibitors and cathodic protection). Factors like deferred maintenance and extended lifetime and useful lives of buildings and equipment, tend to increase the corrosion costs. These costs are often realized when higher performance specification and more hostile environments are encountered. Finally, corrosion costs also increase as a result of government regulations which limits and prohibit the use of time-honored methods for protection due to safety or environmental damage (Davis, 2000).

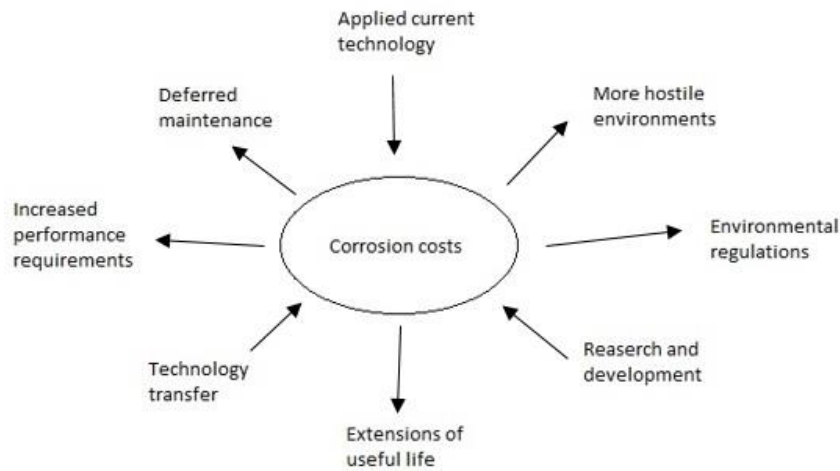


Figure 11: Factors which increase or decrease the costs of corrosion (Davis, 2000)

Even though the costs vary in relative significance from industry to industry, several generalized elements combine to make up the total costs of corrosion. Some of them are easily recognized, others are not. During production, corrosion costs are incurred in the product development cycle in many ways, based on materials, energy, labor, and technical expertise required to produce a product. Other operating costs are affected by corrosion. Corrosion inhibitors, for example, must often be applied to water treatment systems. Parts of maintenance and repair can be attributed to corrosion, and corrosion experts are therefore employed to implement corrosion control programs. Capital costs also are incurred due to corrosion. The useful lifetime of manufacturing equipment decreases due to corrosion. For an operation that is expected to run continuously, excess capacity is required to allow planned downtime and corrosion related maintenance. In other cases, redundant equipment is installed to enable maintenance on one unit while processing continues with another unit. For the end user or consumer, corrosion costs are incurred for purchases of corrosion prevention and control products, maintenance and repair, and premature replacement (Davis, 2000).

The original Battelle/NIST study (Standards, Bennett, & Laboratories, 1978) identified ten elements of the cost of corrosion:

- Replacement of equipment or buildings
- Loss of product
- Maintenance and repair
- Excess capacity
- Redundant equipment
- Corrosion control
- Technical support
- Design
- Insurance
- Parts and equipment inventory

Replacement of equipment or buildings, loss of product, and maintenance and repair are quite straight forward. Excess capacity is a corrosion cost if downtime for a plant which

operate continuously, could be reduced were corrosion is not a factor. This element accounts for extra plant capacity (capital stock) maintained because of corrosion. Redundant equipment accounts for extra equipment (capital stock) required because of corrosion. Specific critical components like large fans and pumps, has an extra component backed up to allow continuous operation during maintenance for corrosion control. Corrosion costs related to corrosion control and technical support (engineering, research and development, and testing) are fairly straight forward. Corrosion costs related to design are not always as obvious. The last two elements, insurance and parts and equipment inventory, can be significant in certain cases.

In addition to these ten elements, other less quantifiable cost factors, like loss of life or loss of goodwill due to corrosion, can have a major impact (Davis, 2000).

Table 1: List of examples for each element of cost

Element of cost	Example
Replacement of equipment or buildings	Corroded pressure vessel
Loss of product	Corrosion leak Corrosion contamination of product Corrosion during storage
Maintenance and repair	Repair corroded corrugated metal roof Weld overlay of chemical reaction tank Repair pump handling corrosive slurry – erosion and corrosion Scheduled downtime for plant in continuous operation, for example, petroleum refinery
Redundant equipment	Installation of three large fans where two are required during operation
Corrosion control Inhibitors Organic coatings Metallic coatings Cathodic protection	Injection of oil wells Coal tar on exterior of underground pipeline Paint on wooden furniture Topcoat on automobile – aesthetics and corrosion Zinc-rich paint on automobile Galvanized steel sidings Chrome-plated faucets – aesthetics and corrosion Cathodic protection of underground pipelines
Technical support	Material selection Corrosion monitoring and control
Design Material of construction for structural integrity Material of construction Corrosion allowance	Stainless steel for corrosive applications Stainless steel for high-temperature mechanical properties High alloy to prevent corrosion products contamination, for example drug industry Thicker wall for corrosion

Special processing for corrosion resistance	Stress relief, shot peening, special heat treatment (e.g., Al alloys) for corrosion
Insurance	Portion of premiums on policy to protect against loss because of corrosion (to cover charge of writing and administering policy, not protection amount)
Parts and equipment inventory	Pumps kept on hand for maintenance, for example, chemical plant inventory.

Corrosion control

Management of corrosion often requires a combination of monitoring, inspection, and modelling of a system along with various control strategies. By setting key performance indicators, such as the number of leakages per year, and reviewing inspection data and making improvements, the number of corrosion failures ought to decrease (Kelland, 2014). There are five primary methods of corrosion control. Each is described briefly underneath (Davis, 2000). In addition to these five primary ways to control corrosion, other methods such as water removal, biocides for preventing MIC, pH stabilization and drag reduction, are used to reduce corrosion.

Materials

Every metal and alloy has a unique and inherent corrosion behavior which varies from high resistance in noble metals like gold and platinum, to low resistance in active metals like sodium and magnesium. Furthermore, corrosion resistance of a metal strongly depends on the environment which it is exposed, meaning chemical composition, velocity, temperature, etc. The general relation between the rate of corrosion, the corrosivity of the environment, and the corrosion resistance of the material is:

$$\frac{\text{corrosivity of environment}}{\text{corrosion resistance of metal}} \approx \text{rate of corrosive attack}$$

For a given corrosion resistance of the material, as the corrosivity increases in the environment, the corrosion rate increases. For a given corrosivity of the environment, as the corrosion resistance of the material increases, the corrosion rate decreases. An acceptable rate of corrosion is often fixed, and the challenge is to match the corrosion resistance of the material with the corrosivity of the environment to be beneath or at the same level as the specified rate. Usually, there are multiple materials which meet the requirement, and the selection of material becomes one of determining which of the materials provides the most economical solution for the particular service.

Consideration of corrosion resistance is often as important in the selection process as the mechanical properties of the alloy. A common solution to a corrosion problem, is to substitute an alloy with greater corrosion resistance for the alloy that has corroded (Davis, 2000).

Coatings

Coatings for corrosion protection can be divided into two groups – metallic and non-metallic (organic and inorganic). The purpose of both types of coating is to isolate the underlying metal from the corrosive media.

Metallic Coating: The concept of applying a more noble metal coating takes advantage of the higher corrosion resistance of the noble metal. An example of this application is tin-plated steel. Alternatively, a more active metal can be applied, and in this case the coating corrodes preferentially, or sacrificial, to the substrate. An example of this system is galvanized steel, where the sacrificial zinc coating corrodes preferentially and protects the steel.

Organic Coating: The primary function of the organic coating as corrosion protection is to isolate the metal from the corrosive environment. In addition to create a barrier layer to choke corrosion, the organic coating can also contain corrosion inhibitors. There are several formulas for organic coatings that already exist, as do a variety of application processes to choose from for a given product or service condition.

Inorganic Coating include porcelain enamels, chemical-setting silicate cement linings, glaze coatings and linings, and other corrosion resistant ceramics. Like organic coatings, inorganic coatings for corrosion application functions as a barrier coating (Davis, 2000).

Inhibitors

Just like some chemical species, like salt, promote corrosion, other chemical species prevent corrosion. Silicates, organic amines and chromates are common inhibitors. The inhibition mechanism can be quite complex. For organic amines, the inhibitor adsorbs on the anodic and cathodic sites and stifles the corrosion current. Other inhibitors affect either the anodic or cathodic process specifically, while other inhibitors promote the formation of protective films on the metal surface.

The use of inhibitor is favored in closed systems where the necessary concentration of inhibitor is more readily maintained. The increased use of cooling towers stimulated the development of new inhibitor/water-treatment packages to control corrosion and biofouling. Inhibitors can be incorporated in a protective coating or in a primer for the coating. At a defect in the coating, the inhibitor leaches from the coating and controls the corrosion (Davis, 2000).

Cathodic protection

Cathodic protection suppresses the corrosion current that causes damage in a corrosion cell and forces the current to flow to the metal structure to be protected. This way corrosion or metal dissolution is prevented. In practice, cathodic protection can be applied two ways that varies based on the source of protective current. An impressed current-system uses a power source to force the current from inert anodes to the structure to be protected. A sacrificial-anode system uses active metal anodes, for example zinc or magnesium, which are connected to the structure to provide the cathodic protection current (Davis, 2000).

Design

The application of rational design principles can eliminate many corrosion problems and reduce time and costs related to corrosion maintenance and repair. Corrosion often occurs in dead spaces or crevices where the corrosive medium becomes more corrosive. These areas can be eliminated or minimized in the design process. When stress-corrosion is possible, components can be designed to operate at stress-levels below the threshold stress for cracking.

Where corrosion damage is anticipated, design can provide maximum interchangeability and partial standardization of critical components. Interchangeability and partial standardization reduce the inventory of parts required. Maintenance and repair can be anticipated, and easy access can be provided. Furthermore, redundant equipment is installed for items, like primary pumps or fans, which are critical to the entire operation. This way maintenance is permitted on one unit while the other unit is operating (Davis, 2000).

Chapter 2 - Corrosion inhibitors

The history of corrosion inhibitors and neutralizers and their invention, development and application in the petroleum industry is documented briefly by Fisher (Fisher, 1993). He reviews early corrosion inhibitor application in each of the different segments of the industry, including oil wells, natural gas plants, refineries, and product pipelines (Fink, 2003).

Corrosion and scale deposition are the two most expensive problems in the oil industry. Corroding surfaces are found in production-, transport- and refining equipment. An overview of corrosion problems and methods to prevent corrosion is given in *Corrosion and scale handbook* (Becker, 1998).

Classification

Corrosion inhibitors can be categorized as passivating (anodic), cathodic, vapor phase or volatile, and film-forming. Passive inhibitors are not used in the oil and gas production, as they are in closed circuit heating/cooling systems. Cathodic inhibitors are not used in production operations, but they can be used in drilling fluids. Vapor-phase corrosion inhibitors are organic compounds that have sufficient vapor pressure under ambient atmospheric conditions to essentially travel to the surface of the metal by gas diffusion and physically adsorbing onto the surface (Kelland, 2014). Film-forming corrosion inhibitors are described more detailed later.

Corrosion inhibitors, which are used for protection in oil field pipelines, are often complex mixtures. The majority of corrosion inhibitors which are used in the oil systems are nitrogenous and have been classified into the following broad groupings (Fink, 2003):

- Amides and imidazolines
- Salts of nitrogenous molecules with carboxylic acids (fatty acids, naphthenic acids)
- Nitrogen quaternaries
- Polyoxylated amines, amides, and imidazolines
- Nitrogen heterocyclics

Fields of application

Corrosion problems can occur in several systems within the petroleum industry. These include

- Acid stimulation jobs
- Cooling systems
- Drilling muds
- Oil production units
- Oil storage tanks
- Oil well
- Protection of pipelines
- Refinery units
- Scale removal treatments using acids
- Steam generators
- Technologic vessel

Many components involve environmentally dangerous products, like chromates, fatty amines of high molecular weights, imidazolines, etc. The use of some of the alternatives, for example polyphosphate or polyphosphonate, are limited because they precipitate in the presence of salts of alkaline earth metals or because of their high costs (Fink, 2003).

Application of Corrosion Inhibitors

Batch application vs. Continuous Application

Batch treatment of pipelines with liquid or gel slugs of inhibitor, with continuous injection as backup (or vice versa), are accepted methods for corrosion prevention (Kennard & McNulty, 1992). Batching fluids or gel inhibitors using pigs is more likely to achieve full coverage of the inner surface of the pipe wall by continuous injection. The film laid down is quite resilient and of long duration. Important factors to optimize the application include to determine

the film thickness and selecting an appropriate pigging system and program. Cleaning of pipeline before inhibitor pigging is recommended (Fink, 2003).

Emulsions

Corrosion inhibitors are often emulsions which are capable of forming an organic film on the parts to be protected.

Application in Solid Form

The preparation of corrosion inhibitor in the solid form allows the development of a new technique for continuous intensive corrosion protection for gas and oil pipelines, as well as acidizing operations of oil wells (Guimaraes, Monterio, & Mainier, 1994). The controlled dissolvment of the solid inhibitor creates a thin protective layer on the metal surface which prevent or minimize unwanted corrosion reactions (Fink, 2003).

Film-Forming Corrosion Inhibitors

Film-forming Corrosion Inhibitors (FFCIs), sometimes together with synergists, are mostly used for protection of oil, condensate, and gas production lines, which are essentially anaerobic. FFCIs are especially useful in prevention of chloride, CO, and H₂S corrosion. They can be distributed either by continuous injection or by batch treatment downhole or at the wellhead (Kelland, 2014).

How does FFCIs work?

FFCIs generates a protective layer on the metal surface which prevents corrosive chemicals, like water and chloride ions, from penetrating to the metal surface (Wong & Park, 2009). The effectiveness of the FFCIs are partially depending on the strength of the adsorption to the metal surface (or a ferrous scale surface such as siderite, iron carbonate). Both small molecules and polymers can make up FFCIs. However, many FFCIs are organic amphiphiles, also known as surfactants. Amphiphiles have a hydrophilic head, and a polar (hydrophobic) tail. The headgroup is designed to interact with iron atoms on the surface, and the tail attracts liquid hydrocarbons, forming an oily film. This oily film physically prevents the corrosive aqueous phase from penetrating to the metal phase (Pähler, Santana, Schuhmann, & Souto, 2011; Wylde, Reid, Kirkpatrick, Obeyesekere, & Glasgow, 2013). A protective double layer (bilayer) of surfactant FFCIs with or without a cosurfactant or solvent, can also be formed if

the tail is long. Under some multiphase flow conditions, parts of the pipe wall are left unprotected by surfactant FFCIs, giving the possibility of localized corrosion (Wang, Jepson, Wang, & Shi, 2002). An example of this corrosion on the top part of a pipeline due to the mixture of condensed water, CO₂, H₂S and organic acids. This corrosion challenge occurs since the inhibitor is injected into the liquid phase, and therefore might not cover these parts (Martin, 2009). To help improve design and development of more environmental-friendly FFCIs, computer modelling and quantitative structure-activity relationship (QSAR) have been used (Kelland, 2014).

For more than 40 years, corrosion inhibitors have been successfully applied in sour oil and gas systems. Even though they work effectively, little is understood about their interaction with sour corrosion product layers and their inhibitive mechanisms. The FFCI performance is not determined by adsorption strength alone, but also by its ability to bind into the product layer providing protection and by changing the morphology of the future scale growth (Park, Morello, & Abriam, 2009; Stewart, Menendez, Jovancicevic, & Moloney, 2009).

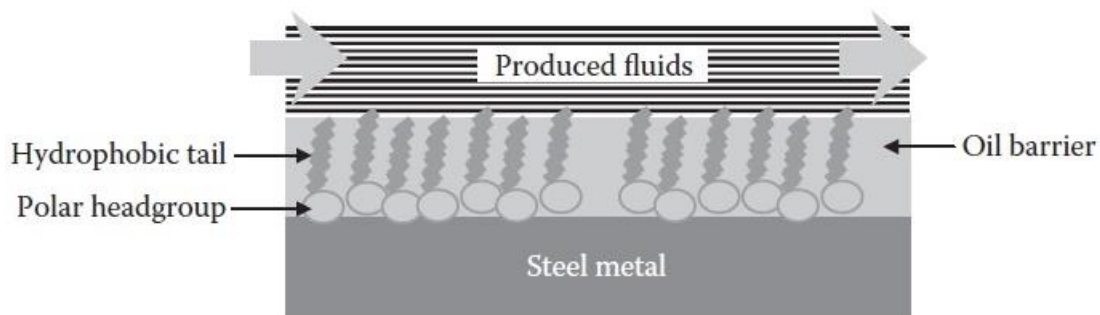


Figure 12: The effect of an FFCI surfactant (Kelland, 2014)

Classes of FFCIs

When it comes to the structure of FFCIs, most of them contains heteroatoms in one or more of the head groups, which bind via lone electron pairs to iron atoms on the metal surface. Normally, you find nitrogen, phosphor, sulphur and oxygen atoms in the headgroup. The most common categories of surface active FFCIs are:

- Phosphate esters
- Various nitrogenous compounds
- Sulphur compounds often with other heteroatoms such as nitrogen

Biodegradable and low-toxicity polyamino acids used in environmentally sensitive areas. The various nitrogenous compounds include:

- Amine salts of (poly)carboxylic acids
- Quaternary ammonium salts and betaines (zwitterionics)
- Amidoamines and imidazolines
- Polyhydroxy and ethoxylated amines/amidoamines
- Amides
- Other heterocyclics

Amines like fatty alkyldiamines and polyamines with hydrophobic tails have also been claimed as FFCIs. In addition to film-forming properties, amines will help neutralize corrosive carbonic acids (H_2CO_3) and hydrogen sulphide (H_2S) in the aqueous phase. In older patents, oxazolines, pyrrolinediones, and rosin amines were claimed as FFCIs, but they are not used in general today (Okafor, Liu, Zhu, & Zheng, 2011). Some FFCIs work synergistically together, like imidazolines and phosphate esters. There are many other possible corrosion inhibitor formulations, including one or more classes of FFCIs. This is because one FFCIs may be best at protecting the anode, while the other protects the cathode on the ferrous metal surface best. It can also be that a mixture of the classes produces a better film (Kelland, 2014).

Phosphate Esters

Both phosphate monoesters and phosphate diesters are good FFCIs. They are often blends with other classes of FFCIs. In figure 13, a mixture of both monoesters and diester is formed, which, having different hydrophilicities, will partition between the liquid hydrocarbon and water phases. Phosphate esters containing hydrophobic nonylphenol group have been shown to be considerably more effective FFCIs the linear or branched aliphatic phosphate esters (Kelland, 2014).

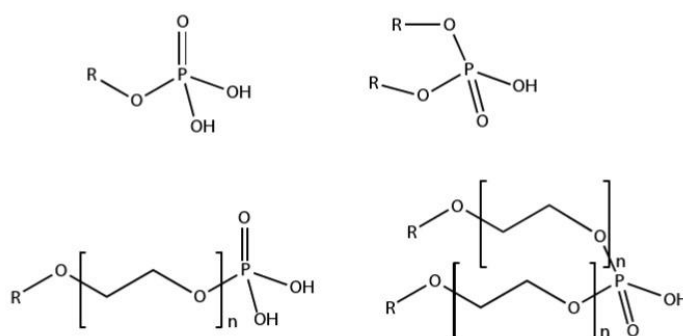


Figure 13: Structures of typical phosphate ester FFCIs (Kelland, 2014)

Amine Salts of (Poly)carboxylic Acids

Amine salts of fatty carboxylic acids have long been used in FFCI formulations. Typically, is the amine a trialkylamine, alkylpyridine, alkylquinoline, or imidazoline. Blends with mercatocarboxylic acid amine salts have been claimed to give improved performance” (Kelland, 2014).

Quaternary Ammonium and Iminium Salts and Zwitterionics

Also, Quaternary ammonium surfactants have long been known FFCIs. They are however, rarely used alone, but in combination with other FFCI classes. Quaternary ammonium surfactants are usually quite toxic, but many of them are also useful as biocides, which can help prevent biofilm formation and thus underdeposit corrosion.

Zwitterionics such as betaines can also function as FFCIs and are generally significantly less toxic than ordinary quaternary surfactants (Kelland, 2014).

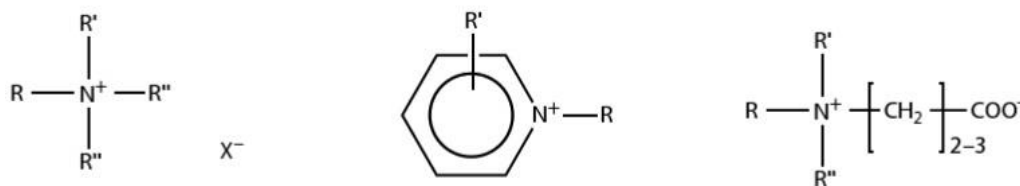


Figure 14: Quaternary ammonium, alkyl pyridine quaternary, and zwitterionic betaine FFCIs (Kelland, 2014)

Amidoamines and Imidazolines

Imidazolines are possibly the most common class of general corrosion FFCI used in the oil and gas industry, and the class which is most studied. Certain imidazoline-based FFCIs appear to perform well even in HPHT conditions (Ramachandran, Ahn, Greaves, Jovancicevic, & Bassett, 2006). Although the basic imidazolines only offer poor to moderate performance at these conditions (Chen, Jepson, & Hong, 2000), other HPHT FFCIs have been reported (Obeyesekere, Naraghi, Chen, Zhou, & Wang, 2005). Using a molar excess of polyamine, the imidazoline products are claimed to perform better than monomeric imidazolines. Thereof, tetrahydropyridines, six-rings analogues of imidazolines, and methylol derivatives are also useful FFCIs (Kelland, 2014).

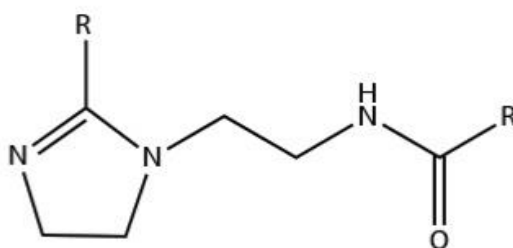


Figure 15: Amidoethyl imidazolines (Kelland, 2014)

Amides

Amides derivatives of long-chain amines have been proposed as environmentally acceptable FFCIs in oil production applications (Darling & Rakshpal, 1998). Unfortunately, such materials can be difficult to formulate and adversely affect the oil-water separation process.

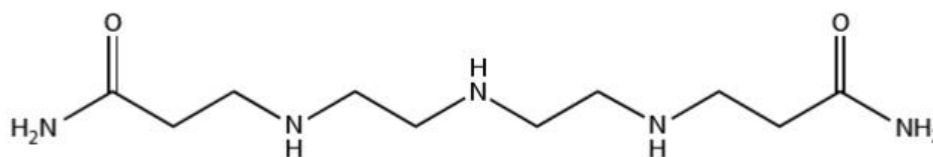


Figure 16: Example of a polymethylenepolyaminedipropionamide FFCI (Kelland, 2014)

Polyhydroxy and Ethoxylated Amines/Amides

A commonly used FFCI formulation are ethoxylation of fatty amines or diamines with ethylene oxide gives ethoxylated amines. A biodegradable link, such as an amide group between the hydrophobic tail and the ethoxylated nitrogen atom can make the product more environmentally attractive. Examples claimed to be good FFCIs are deoxyglucityl derivatives of alkylamines (Figure 17) (Kelland, 2014).

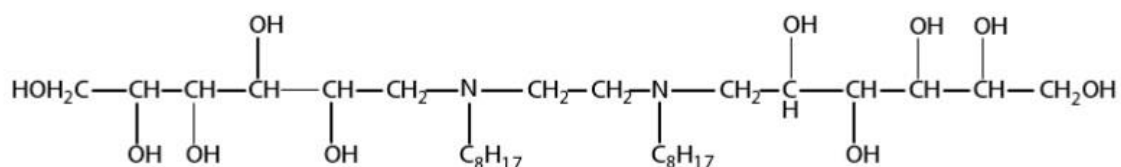


Figure 17: *N',N'*-dioctyl-*N,N'*-bis(1-deoxyglycyl)ethylenediamine (Kelland, 2014)

Sulfur Compounds

Both thiosulfate ions and mercaptocarboxylic acids work as synergists for nitrogenous FFCIs. In fact, a number of sulfur compounds are particularly good at preventing cracking corrosion. FFCIs containing water-soluble mercaptocarboxylic acids have been used successfully in high-shear applications; however, used alone, they are only partially effective at inhibiting corrosion in a CO₂-saturated environment (Figure 18) (Kelland, 2014).

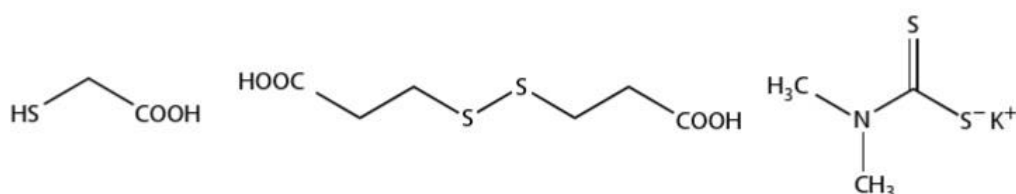


Figure 18: Thioglycolic acid, 3,3'-dithiodipropionic acid, and potassium dimethyl dithiocarbamate (Kelland, 2014)

Polyamino Acids and Other Polymeric Water-Soluble Corrosion Inhibitors

Phosphates and organic phosphonates have long been used as scale inhibitors and are also regularly used for corrosion protection in water treatment systems. It has been found that polyamino acids with pendant carboxylate groups function very well as scale inhibitors, but they also gave fairly good CO₂ corrosion protection although not as good as the best FFCIs at the time. The best known and cheapest examples of polyamino acids are salts of polyaspartic acid, although glutamic acid can be used (Figure 19) (Kelland, 2014).

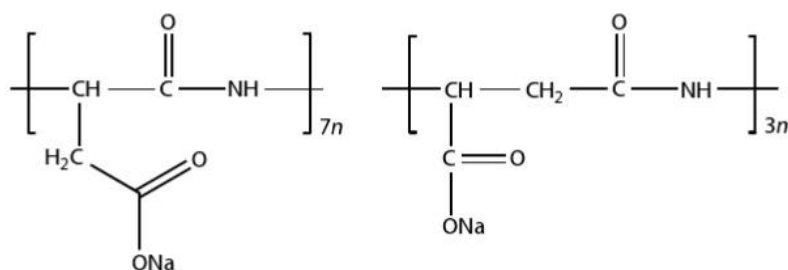


Figure 19: Sodium polyaspartate (Kelland, 2014)

Chapter 3 – Testing of Corrosion Inhibitors

There are several methods for testing of corrosion inhibitors in the oil industry. These include the following:

- Bubble or kettle test
- Rotating cylinder electrode (RCE) test
- Rotating disc electrode (RDE) test
- Jet impingement test
- High-shear autoclave
- Rotating cage test
- Flow loop test
- Wheel test
- Static Autoclave test

The objective with corrosion testing is to measure weight loss over time, observe surface changes, or measure current flow and interpret that as a corrosion current. In many of the test methods mentioned above, a metal coupon with the same composition as the pipe is placed in the apparatus. The corrosion rates are usually monitored using LPR or electrochemical impedance spectroscopy. From this, the corrosion rate as the number of millimeters of metal loss per year can be calculated. Pitting corrosion can be observed using optical microscopy, surface profilometry or scanning electron microscopy (SEM). In reality, film-forming corrosion inhibitors are exposed of turbulent fluid flow, which may result in removal of the inhibitor from the pipe wall unless it adsorbs well. Therefore, at some point, a test with turbulent flow must be performed to qualify an inhibitor. The pipe wall shear stress is often blamed for removal of protective surface layers, such as iron carbonate or inhibitor films (Kelland, 2014).

For low-cost, initial chemical screening under low-shear conditions, bubble test is often used. The RCE and RDE test are tests of corrosion inhibitors under medium shear-stress or turbulent regimes that are quite simple, low-cost methods. More expensive, but also more realistic tests, can be carried out in flow loops or jet impingement tests. The use of high-shear autoclave is useful for very high shear conditions that lead to flow-induced localized corrosion such as slug flow. Flow loops test procedures for investigating erosion corrosion have also been reported (Ramachandran, Ahn, Jovancicevic, & Bassett, 2005; Tandon et al., 2006).

For FFCIs there is often need of compatibility testing with other production chemicals. This is because many FFCIs adversely affect the performance of kinetic hydrate inhibitors and scale inhibitors. Compatibility tests for FFCIs can also include solvent flashing, foaming, thermal stability, and compatibility with materials such as elastomeric seals. It is for example frequently required that FFCIs possess low foaming properties. Further, an FFCIS should not exacerbate the formation of emulsions, making oil-water separation more difficult. Changes in water cuts can drastically alter emulsion stability in the presence of FFCIs (Kelland, 2014).

High Pressure, High Temperature Static Autoclave Test

The HPHT static autoclave is a method for evaluating corrosion inhibitor performance under static (non-shear) conditions at elevated temperatures and pressures. These tests were performed by Paul Barnes at Schlumberger in Aberdeen.

Corrosion testing by LPR – Kettle test

Purpose

The bubble (or kettle) test is widely used and accepted test method for the evaluation of oil field corrosion inhibitors. It is based on the principle of linear polarization resistance (LPR). In essence, the test involves an electrochemical evaluation of inhibitor performance in a vessel of fluids that is constantly being sparged with corrosive gas. This test is ideal for rapidly carrying out a large number of tests, for example as the first stage of corrosion inhibitor selection, or for screening a wide range of field conditions.

The performance of corrosion inhibitors can be evaluated with respect to corrosion protection performance and oil/water partitioning ability. Field conditions are simulated as closely as possible using natural or synthetic brines and crude oils, however, tests are limited to ambient pressure (1 bar), and temperatures between ambient and 90 °C. Field shear stresses are not reproduced in this test. Evaluation of corrosion inhibitors under shear conditions should be conducted by other methods (RCE, Rotating Cage Autoclave, Flow Loop or Jet Impingement). Some of these methods also allow an evaluation to be conducted at elevated pressures and temperatures.

Calculation

Corrosion rate in the software are given as mm/year while in the LPR graph it is given as mils/year. One mil is equal to one thousandth of an inch. In metric expression one mil equals to 0.0254 mm. Time is also given in seconds and needs to be converted to hours for the graph. The formula is given:

$$mm/year \cdot 1/39.3700787 = mils/year$$

The efficiency of the inhibitor is calculated as follow:

$$\%Eff = \frac{(C1 - C2)}{C1} \cdot 100$$

C1 = Uninhibited corrosion rate (corrosion rate just before injection of formulation)

C2 = Inhibited corrosion rate (corrosion rate 6h after injection of formulation)

Chapter 4 – Catalysts

Reaction rates: How fast does a Reaction go?

The equilibrium constant for a reaction indicates whether or not products are more stable than reactants. However, the equilibrium constant does not tell anything about the *reaction rate*. For example, the equilibrium constant for the reaction of gasoline with oxygen is very large, but gasoline can be safely handled in air because the reaction is very slow unless a spark is used to initiate it. The rate of addition of HBr to ethene is also very slow, although the reaction is exothermic.

Molecules must collide with each other with enough energy in order to react. In addition, the molecules must collide in the right orientation so that the breaking and making of bonds can occur. The energy required for the reaction process, is an energy barrier, and the higher the required energy, the slower the reaction.

Reaction energy diagrams are often used by chemists to show the changes in energy that occur in the course of a reaction. Figure 21 shows the reaction energy diagram for the polar addition of the acid HBr to ethene (figure 20) (H. Hart et al., 2011).

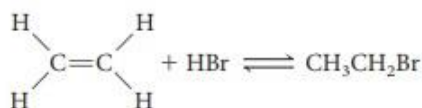


Figure 20: Reaction equation for polar addition of HBr to ethene. (H. Hart, Hadad, Craine, & Hart, 2011)

The reactants start with the energy shown at the left of the diagram. The reaction occurs in two steps. The first step is when the π bond breaks and a C – H σ bond is formed, giving a carbocation intermediate product. As the π bond begins to break and the new σ bond begins to form, the structure formed by the reactants reaches a maximum energy. The structure with maximum is called the **transition state** for the first step. The energy difference between the reactants and the transition state is called the **activation energy, E_a** . The activation energy determines the reaction rate, and if E_a is large the reaction rate is slow, while a small E_a give a rapid reaction rate. Figure 21 shows that the final product has a lower energy (ΔH) than the reactants. The overall reaction is **exothermic** because the product is lower in energy than the reactions. However, the reaction rate is determined by the highest energy barrier, in this case the first activation energy (H. Hart et al., 2011).

Factors that affect reaction rates are **temperature** and **catalysts**. Heating a reaction generally increases the rate at which the reaction occurs by providing the reactant molecules with more

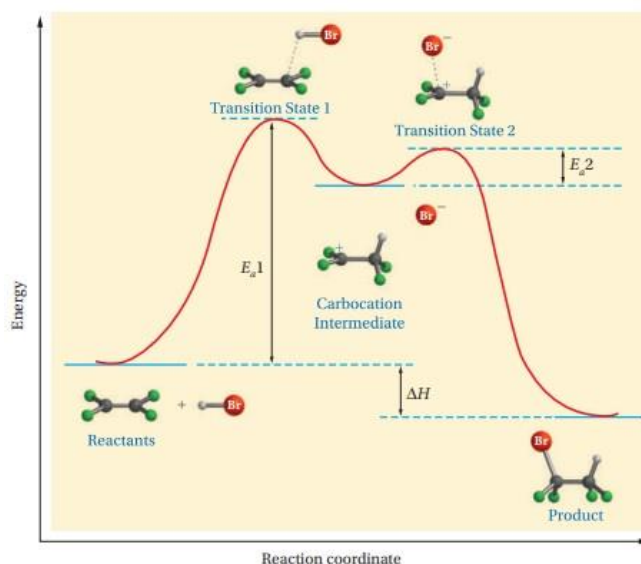


Figure 21: Reaction energy diagram for the addition of HBr to an alkene (ethene)(D. J. Hart, 2012; H. Hart et al., 2011)

energy to surmount activation energy barriers. Catalyst speed up a reaction by providing an alternative pathway or mechanism for the reaction, one which the activation energy is lower (H. Hart et al., 2011).

Catalysts

A catalyst is a chemical substance which affect the reaction rate by altering the activation energy required for the reaction to proceed. The catalyst is not consumed during the reaction, and it may contribute in multiple reactions at a time. The only difference between a reaction with and without a catalyst is the activation energy for the reaction. Therefore, the catalyst does not change the reactants energy, or the energy of the final product, giving the same ΔH .

A catalyst may allow a reaction to proceed at a lower temperature or increase the reaction rate. Catalysts often react with reactants to form intermediates that eventually yield the same reaction products and regenerate the catalyst. Note that the catalyst may be consumed during one of the intermediate steps, but it will be regenerated before the reaction is completed.

The use of catalyst in this thesis

Previously, commercial available mono-, di-, tri-, and tetra amines were tested and not found to be effective towards corrosion (Barnes, 2018). By ring closure of amines into heterocycles, it is well known that these head groups will have an affinity to metal surfaces (Kelland, 2014) and hence, be a good starting point to develop a corrosion inhibitor. With this as a starting point, the syntheses were based on forming heterocycles including nitrogen. Traditionally, imidazolines are utilized as CIs. When imidazolines were tested under high temperature conditions, their performance seems to deteriorate, probably due to hydrolysis. Hence, attention was paid to readily available heterocycles that didn't easily undergo hydrolysis. These heterocycles include hexahydropyrimidines, as reaction products from commercial diamines and aldehydes. Traditionally, these six-membered rings have been made at temperatures above 100 °C (Hoffmann & Kremer, 1996). It was therefore desirable to investigate whether the ring closure step was could take place at a lower temperature or not, and therefore avoiding unwanted by-products. Hence, we initiated a study involving catalysts typically used in the chemical industry.

The choice of catalysts were based on them being commercially available materials and on literature found (Lanigan, Starkov, & Sheppard, 2013; Molander, Katritzky, & Taylor, 2005).

B(OCH₂CF₃)₃ – Tris(2,2,2-trifluoroethyl) borate

This catalyst was chosen based on the article *Direct Synthesis of Amides from Carboxylic Acids and Amines using B(OCH₂CF₃)₃* (Lanigan et al., 2013). The article describes the use of B(OCH₂CF₃)₃ as a catalyst in reactions for ring closure of both five-membered and six-membered rings including nitrogen. Tris(2,2,2-trifluoroethyl) borate is commercially available, but is quite expensive. However, based on the article, it was decided to move forward with this as one of the catalysts to be tested.

DDQ – 2,3-dichloro-5,6-dicyano-p-benzoquinone

For imidazolidine formation from aliphatic and aromatic aldehydes, DDQ has been used earlier. For the uncatalyzed reaction, it was reported increased reaction time and inferior yields (Eynde, Delfosse, Lor, & Haverbeke, 1995; Molander et al., 2005). Based on this, DDQ was also chosen to be tested in our syntheses.

p-TsOH – p-Toluenesulfonic acid

p-Toluenesulfonic acid was considered to be used as a catalyst because it is a widely used material in the chemical industry and is also quite cheap. It was also chosen to see whether protonation of the aldehyde could promote reaction of nitrogen to the carbonyl group and provide the six-membered ring. Protonation of the carbonyl increases its electrophilicity and should therefore be more reactive. A proton source will also assist in the dehydration step to the imine.

Chapter 5 – Synthesis of Hexahydropyrimidine

In figure 22 there is an overview of the three expected products to achieve from synthesis of N-oleyl-1,3-diaminopropane with Cinnamaldehyde (left), Citral (centre), and α -Hexylcinnamaldehyde (right). The Citral used in this study was a mixture of E- and Z-isomers. In the figure below, only the Z-isomer has been drawn in. The reaction equation is the same for both vacuum-synthesis set-up and Dean-Stark synthesis set-up.

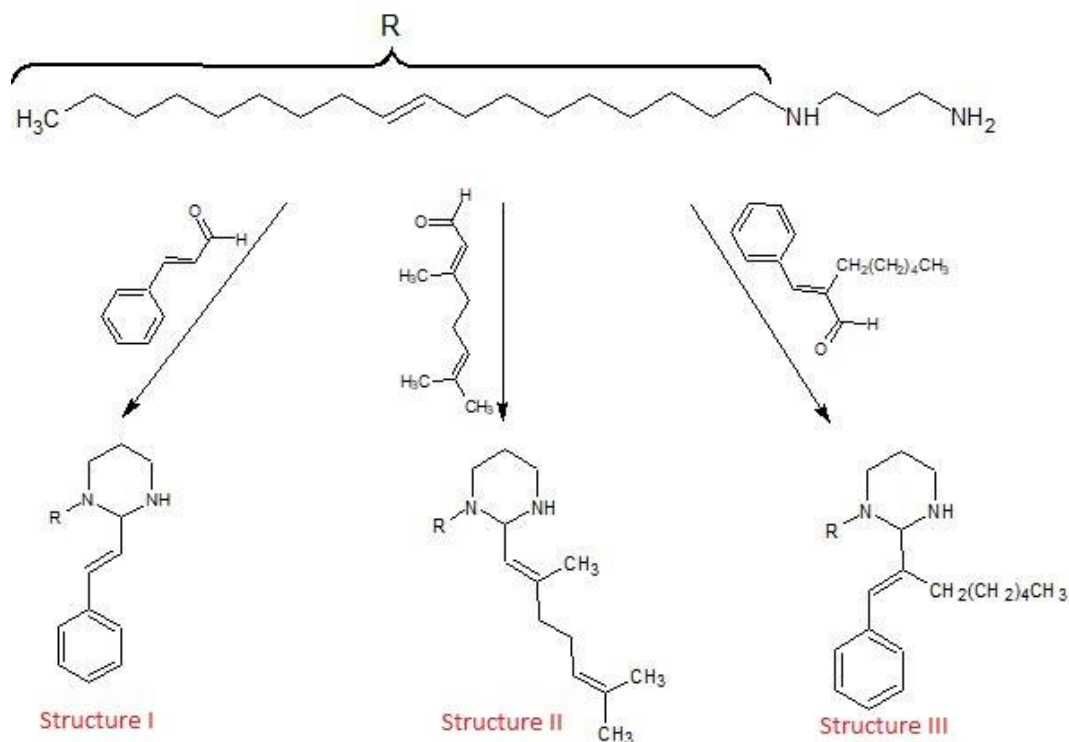


Figure 22: Reaction scheme for the expected products for the different aldehydes used in synthesis.

Figure 23 (below) shows the reaction mechanism for the reactions performed in both types of synthesis. The R-group is the alkyl chain and R₂-group differs dependent on the aldehyde used in the reaction.

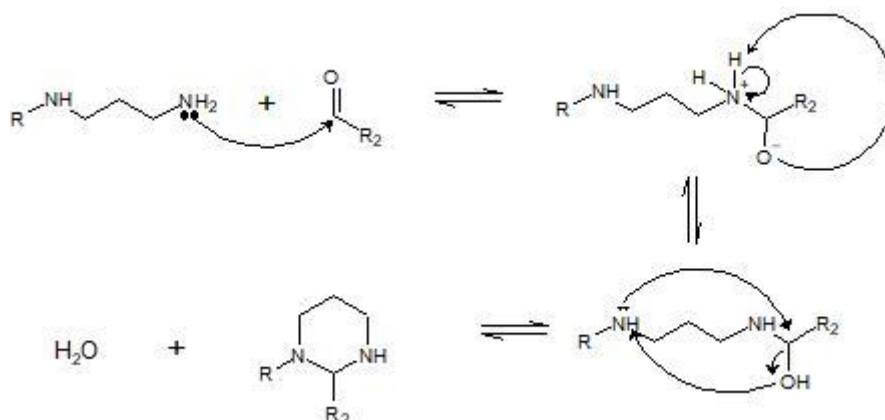


Figure 23: Reaction mechanism for the synthesis, where R is the alkyl chain and R₂ are connected to the aldehydes and differs depending on the aldehyde used in the reaction.

Table 2: Overview of components and method used in the different products, where product 1-11 are from the screening project, and product 12-29 are from the experimental design project. Further details for each product are described in Chapter 9 - Experimental

Product #	N-alkyl-1,3-Diaminopropane	Aldehyde	Catalyst	Method
1	N-Tallow-1,3-diaminopropane	Cinnamaldehyde	-	Vacuum
2	N-Tallow-1,3-diaminopropane	Cinnamaldehyde	-	Dean-Stark
3	N-Tallow-1,3-diaminopropane	Cinnamaldehyde	p-TsOH	Vacuum
4	N-Tallow-1,3-diaminopropane	Cinnamaldehyde	p-TsOH	Vacuum
5	N-Tallow-1,3-diaminopropane	Cinnamaldehyde	-	Vacuum
6	N-Tallow-1,3-diaminopropane	Cinnamaldehyde	p-TsOH	Vacuum
7	N-Tallow-1,3-diaminopropane	Cinnamaldehyde	DDQ	Vacuum
8	N-Tallow-1,3-diaminopropane	Cinnamaldehyde	DDQ	Dean-Stark
9	N-Tallow-1,3-diaminopropane	Cinnamaldehyde	B(OCH ₂ CF ₃) ₃	Vacuum
10	N-Tallow-1,3-diaminopropane	Cinnamaldehyde	B(OCH ₂ CF ₃) ₃	Dean-Stark
11	N-Tallow-1,3-diaminopropane	Cinnamaldehyde	B(OCH ₂ CF ₃) ₃	Dean-Stark
12	N-Oleyl-1,3-diaminopropane	Cinnamaldehyde	p-TsOH	Vacuum
13	N-Oleyl-1,3-diaminopropane	Cinnamaldehyde	p-TsOH	Dean-Stark
14	N-Oleyl-1,3-diaminopropane	Cinnamaldehyde	DDQ	Vacuum
15	N-Oleyl-1,3-diaminopropane	Cinnamaldehyde	DDQ	Dean-Stark
16	N-Oleyl-1,3-diaminopropane	Cinnamaldehyde	B(OCH ₂ CF ₃) ₃	Dean-Stark
17	N-Oleyl-1,3-diaminopropane	Cinnamaldehyde	B(OCH ₂ CF ₃) ₃	Vacuum
18	N-Oleyl-1,3-diaminopropane	Citral	p-TsOH	Vacuum
19	N-Oleyl-1,3-diaminopropane	Citral	p-TsOH	Dean-Stark
20	N-Oleyl-1,3-diaminopropane	Citral	DDQ	Vacuum
21	N-Oleyl-1,3-diaminopropane	Citral	DDQ	Dean-Stark
22	N-Oleyl-1,3-diaminopropane	Citral	B(OCH ₂ CF ₃) ₃	Dean-Stark
23	N-Oleyl-1,3-diaminopropane	Citral	B(OCH ₂ CF ₃) ₃	Vacuum
24	N-Oleyl-1,3-diaminopropane	α -hexyl cinnamaldehyde	p-TsOH	Vacuum
25	N-Oleyl-1,3-diaminopropane	α -hexyl cinnamaldehyde	p-TsOH	Vacuum
26	N-Oleyl-1,3-diaminopropane	α -hexyl cinnamaldehyde	DDQ	Dean-Stark
27	N-Oleyl-1,3-diaminopropane	α -hexyl cinnamaldehyde	DDQ	Dean-Stark
28	N-Oleyl-1,3-diaminopropane	α -hexyl cinnamaldehyde	B(OCH ₂ CF ₃) ₃	Vacuum
29	N-Oleyl-1,3-diaminopropane	α -hexyl cinnamaldehyde	B(OCH ₂ CF ₃) ₃	Dean-Stark

Selection of starting materials

For starting materials there were three different diaminopropanes to choose from, including:

- N-Coco-1,3-diaminopropane
- N-Tallow-1,3-diaminopropane
- N-Oleyl-1,3-diaminopropane

N-Coco-1,3-diaminopropane consists mainly of a C14 alkyl chain, and is the least pure compound out of the three. It has also shown to be less effective regarding performance (Barnes, 2018) and was therefore not considered for these projects. Both N-Tallow-1,3-diaminopropane and N-Oleyl-1,3-diaminopropane consists of a C18 alkyl chain which are effective against corrosion, but N-Oleyl-1,3-diaminopropane is purer hence more expensive. Therefore N-Tallow -1,3-diaminopropane was chosen to use during the screening project, while N-Oleyl-1,3-diaminopropane was preferred during the experimental design project in expectation to end up with a purer product.

The different aldehydes were chosen on an ongoing Schlumberger project in order to investigate different groups attached to hexahydropyrimidines. In addition, the aldehydes chosen were all commercial available in large quantities for the purpose to develop a new commercial corrosion inhibitor.

Characterization of products

NMR spectra was difficult to interpret due to same signals for several groups- The reported results might be regarded as suggestions rather than definite proof and might be subjected to change if the products were purified and analyzed on a stronger magnetic field NMR. It was expected that E- and Z-isomers of the N-alkenyl-1,3-diamine would give doublets in the spectra for the alkene carbons.

All NMR-specters of Structure I shows that the desired ring-closing step have taken place. This is confirmed by 2D-NMR HSQC (Figure 83 in attachments) of product 12 where there is a connection between the aminal carbon and its proton (δ 81.93 and δ 3.90). For structure III NMR shows that there are no signal for the aminal carbon around 80 ppm where it is expected to be. This is proven in ^{13}C -NMR (figure 95 in attachments) for product 24 where the signal is missing. Moreover, a strong signal at 165.21 in C-NMR suggest formation of imine. This is supported by the presence of a small signal at 160.59 indicating E/Z-isomerism. To make sure temperature was not a limiting factor, a sample of product 24 was reheated to 200°C (external) for 4h. After this IR was taken and compared to the original sample. This comparison shows none/small changes (figure 75 in attachments). IR also suggest the presence of an imine with a stretch at 1629 cm^{-1} . This stretch is not observed in products derived from Cinnamaldehyde or Citral. From this it was concluded that the formation of the six-membered ring had not taken place. The expected hexahydropyrimidines formation did not take place, probably due to steric hindrance. Based on both NMR and IR it is currently believed that the reaction stopped at formation of the imine. In addition, the imine structure retains conjugation of double bonds into the phenyl group indication a more kinetic stable product than the corresponding hexahydropyrimidines, providing the following reaction mechanism where R is the alkyl chain and R2 being the aldehyde body:

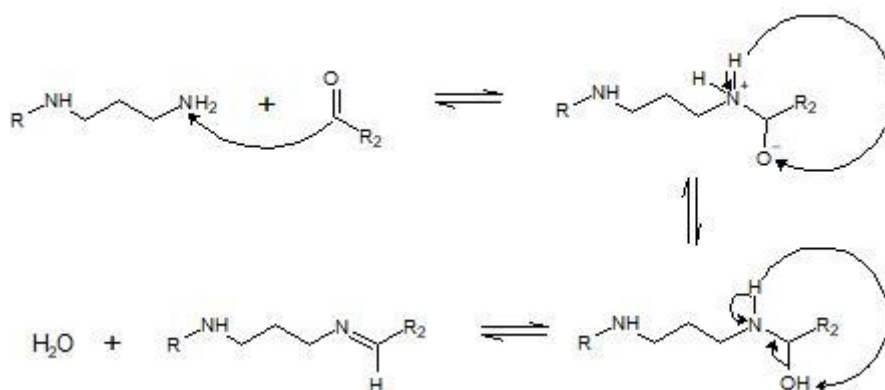


Figure 24: Reaction mechanism for the formation of the imine

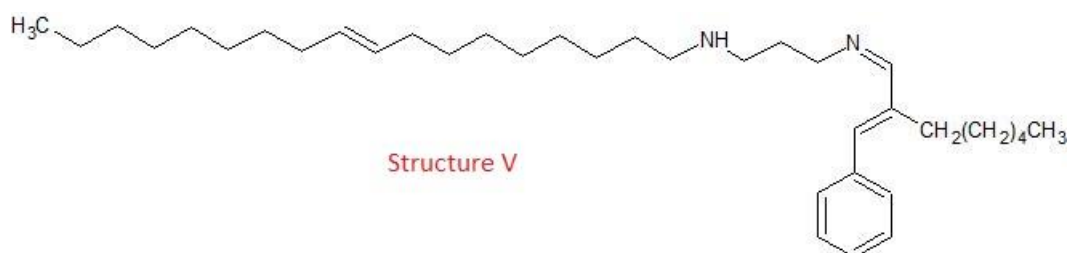


Figure 25: Structure V - Imine

Regarding structure II it is believed to consist of bis adduct (Structure IV in figure 27). The rationale for this is that the signal at 72.18 ppm in ^{13}C -NMR (figure 87 in attachments) can be a signal for the aminal carbon in the bis adduct, almost 10 ppm in difference from the aminal carbon in Structure I, suggesting that annulation to the six-membered ring has not taken place. In 2D-NMR HSQC for product 20 (figure 91 in attachments), it is observed a correlation between the carbon at 72.18 ppm and proton at 3.01 and 3.05 ppm. The two signals are probably due to the E- and Z-isomers of Citral. An in-depth analysis of proton integration could reveal if structure IV has been formed.

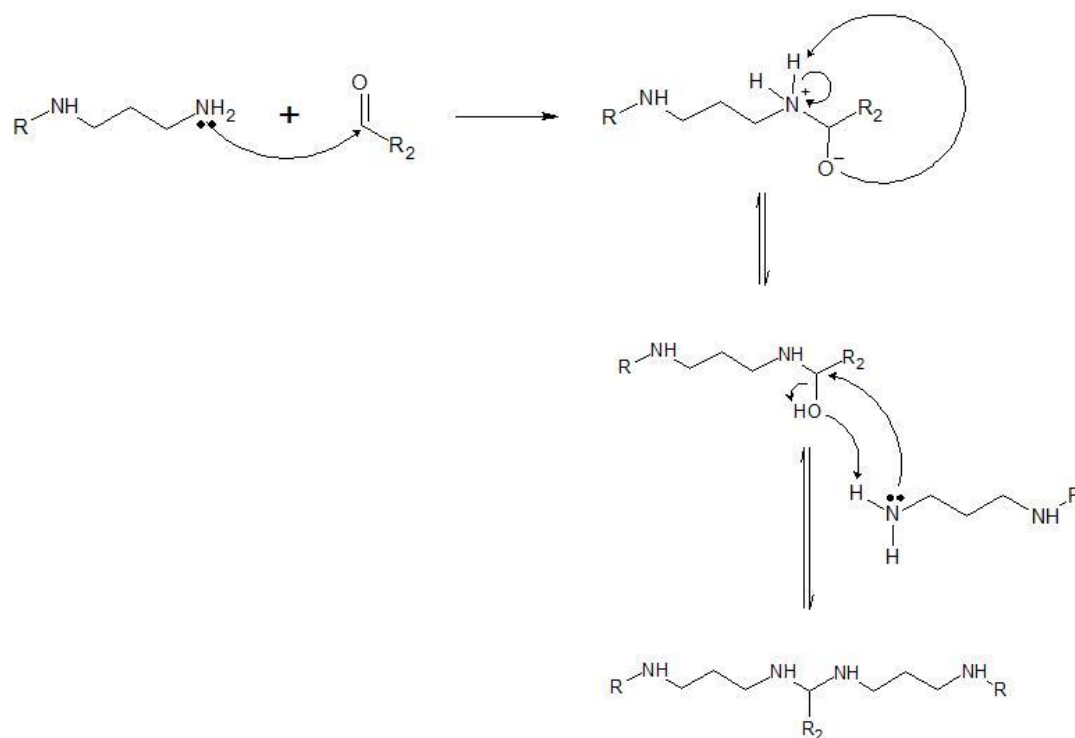


Figure 26: Reaction mechanism for the bis adduct

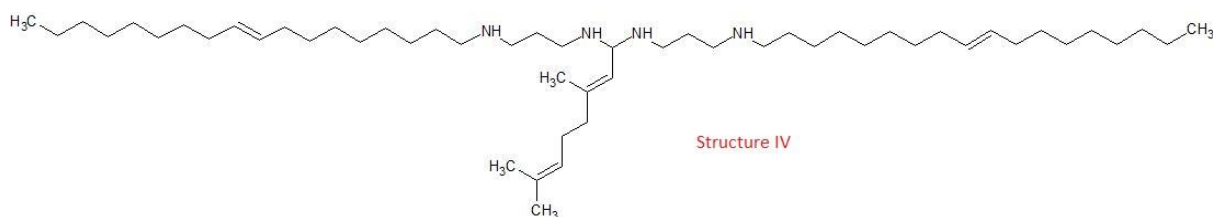


Figure 27: Structure IV - Bis adduct

Other methods for characterizing the products have also been tried without any success. The challenges for Gel permeation chromatography (GPC) was that the products are outside calibration range and not different enough to be separated on the column. Gas Chromatography (GC) and Liquid Chromatography Mass Spectrometry (LCMS) was not performed in these projects because previously these method have not worked for products correspondingly to the ones synthesized during the master thesis projects (Strenitz, 2018). The issue with LCMS is that the functional groups is splitted off, and only the alkyl chain is visible in the graph post run. For GC there is a different, but related problem. The product sticks to the column, hence no or little separation. In order to use both of these methods, derivation of the products is necessary. However, this derivation process is complicated, and also includes some highly dangerous chemicals which requires special facilities when handled.

Purification

During the first period where we did some reactions in order to figure out the catalysts to use, temperature, time, and solvents, time was also spent on different methods to purify our products. In the effort to find a purification method, both TLC and column chromatography was performed. Unfortunately, none of the methods succeeded. After many attempts, using different systems for the TLC, it was concluded that the products probably hydrolyzed on the

silica. Therefore, we had the same problem for the column chromatography since the top layer is silica gel. For both methods, reverse TLC and reverse column chromatography was then tried out to see if the hydrolysis issue was resolved. But here we also had trouble separating the different material segments in the products from each other.

As it turns out, literature (Moke & Leathers, 1967; Muhlbauer & Cour, 1964) shows that amines are very difficult to purify, and it was decided to direct time and energy to other aspects of the master project. This decision was based on the fact that it was not known if it was expedient for the performance to have a 100% pure product. An experimental design project (period 2) was therefore established to find the optimal composition of diamine, aldehyde and catalyst.

Chapter 6 – Results

High Pressure, High Temperature Static Autoclave Test

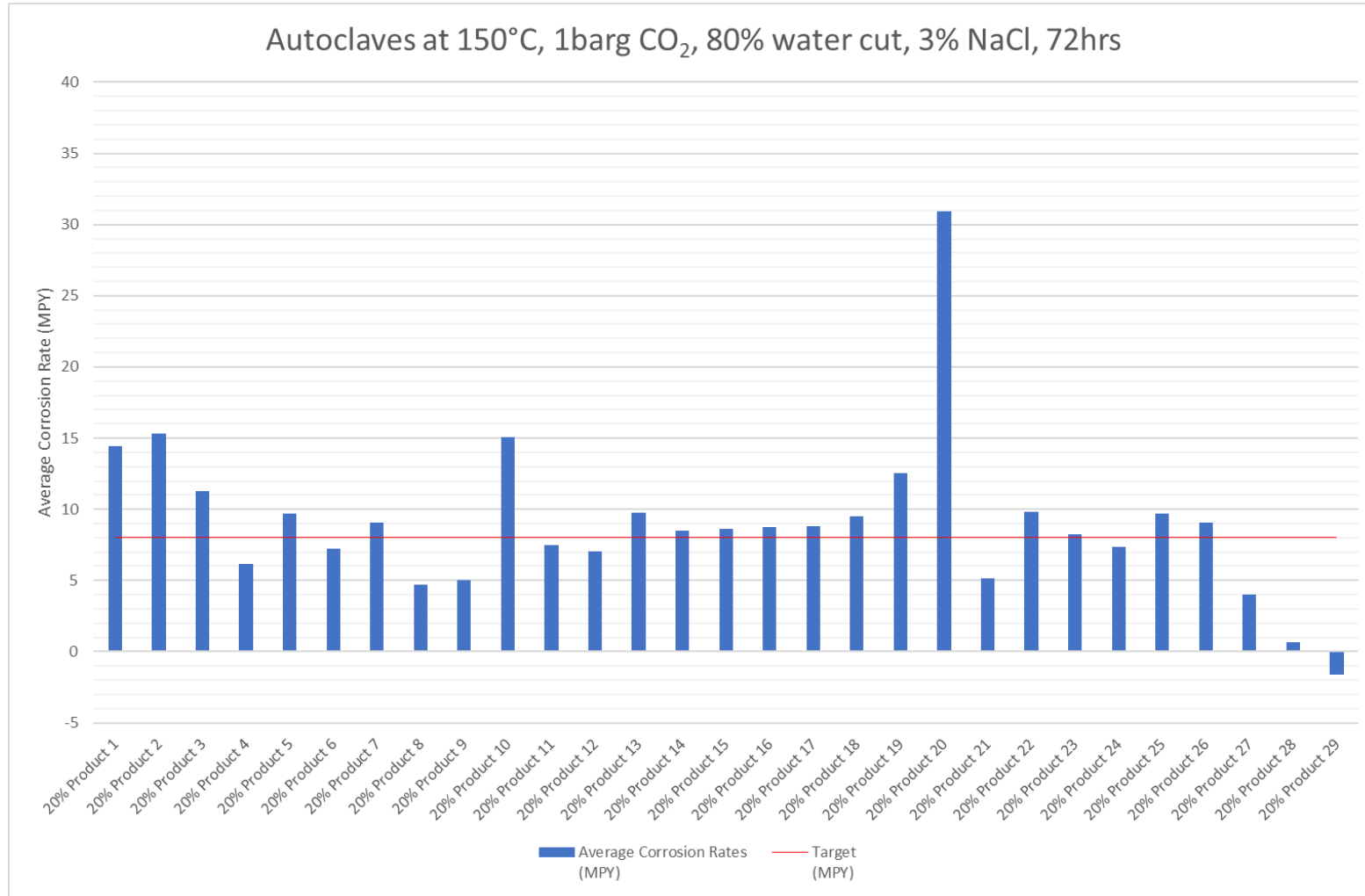


Figure 28: Average corrosion rate from HPHT static autoclave tests

In figure 29, 30 and 31, the coupons from testing of product 12, product 20 and product 24 are pictured. These are also the products which were tested during the Kettle-test.



Figure 29: Product 12



Figure 30: Product 20



Figure 31: Product 24

Kettle-test

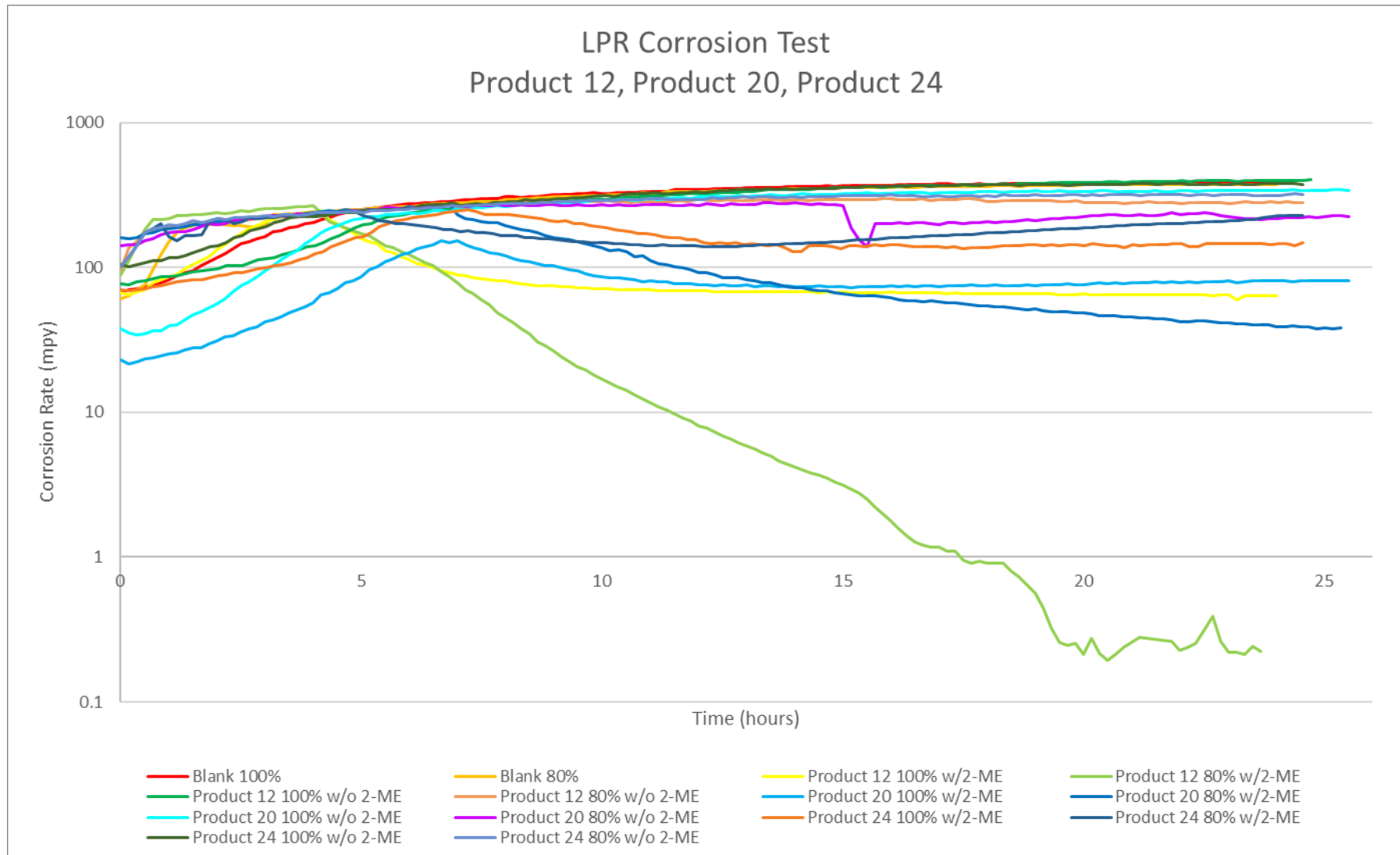


Figure 32: LPR graph for Product 12, Product 20, and Product 24

Table 3: Inhibition efficiency results from Kettle-test. The numbers are used in the discussion.

	#	Free corrosion rate (mpy)	Inhibited corrosion rate (after 6h) (mpy)	%Inhibition after 6h
Blank 100% brine	A	n/a	n/a	n/a
Blank 80% brine	B	n/a	n/a	n/a
Product 12 in 100% brine w/2-ME	C	246.3	71.2	71.1
Prduct 12 in 80% brine w/2-ME	D	265.1	16.9	93.6
Product 12 in 100% brine w/o 2-ME	E	254.0	336.1	-32.3
Product 12 in 80% brine w/o 2-ME	F	264.5	287.8	-8.8
Product 20 in 100% brine w/2-ME	G	143.9	75.4	47.6
Product 20 in 80% brine w/2-ME	H	231.7	85.2	63.2
Product 20 in 100% brine w/o 2-ME	I	245.1	308.1	-25.7
Product 20 in 80% brine w/o 2-ME	J	270.9	268.1	1.0
Product 24 in 100% brine w/2-ME	K	248.2	144.0	42.0
Product 24 in 80% brine w/2-ME	L	227.9	142.0	37.7
Product 24 in 100% brine w/o 2-ME	M	264.9	342.0	-29.1
Product 24 in 80% brine w/o 2-ME	N	240.4	296.7	-23.4

Chapter 7 - Discussion

High Pressure, High Temperature Static Autoclave Test

When analyzing the results from the Autoclave test, we consider the surface conditions of the coupons first for localized corrosion, and then consider the corrosion rate. When looking at the corrosion rate, I have also taken to consideration which of the products have the lowest difference between corrosion rate 1 and 2 the rationale behind this is that the smaller the difference the more reproducible the results given the competing scaling reaction. The products giving the best surface conditions are product 6, product 11, product 14, product 18, product 19, product 20, product 22 and product 23, where the first two mentioned are synthesized during the screening process.

From the group of products having the best surface conditions, product 6 have the overall lowest average corrosion rate, as well as the lowest difference between corrosion rate 1 and 2. This is very interesting considering product 6 is made from 50% starting materials and 50% 2-butoxyethanol which is also the solvent used in the formulations used. This means in theory that out of the 20% of active product injected, there are now only 10% active product since half of it is the already used solvent. This is very interesting results compared to the other products tested, which does not necessarily give as good results. This observation can be rationalized based on the nature of the micelles formed at a given concentration i.e. at one concentration the polar groups are on the exterior thus promoting partition behavior, however and another concentration this situation is reserved leaving the polar head groups on the interior thus negatively affecting the partition of the inhibitor. This is over simplified but does address the reasoning behind the negative impact when over dosing surfactants.

Looking at figure 28, it might appear a bit peculiar why product 4, product 9, and product 16 is considered among the better corrosion inhibitors, and that is because of their respectively surface condition. Product 4 had some residual siderite present on the surface, product 9 have both siderite present and localized pitting corrosion in the coupons. Product 16 had some etching on the sides and on the bottom of the test coupons. Product 8 averaged 4.734 mpy although siderite is still present on the surface, however, the surface looks quite good. By just looking at the graph it would be natural to believe that also product 12 and product 17 makes good corrosion inhibitors. The surface condition on the other hand tells a different story (see Figure 29 in results and figure 59 in attachments). Product 17 experience poor surface conditions and still have siderite present on the surface (dark grey area). On the coupons to product 12 there appears to be some etching on the top half of the coupon which might be due to water in oil emulsions.

The negative corrosion rates indicate weight gain due to siderite deposition. Siderite can clearly be seen on all the coupons related to product 27, product 28 and product 29 (figure 62-64 in attachments) hence the artificially low corrosion rates. Siderite scale becomes a protective shield on the coupon against general corrosion, but local corrosion can become worse as this is generated underneath the siderite, hence the pitting on product 28 and product 29.

As expected, the tested products related to Structure V does not perform as good as the others. In addition to a terrible average corrosion rate of 30.955 mpy, product 24 have substantial siderite present on the coupon surfaces. Product 25 coupons have very different corrosion rates due to siderite deposition preferentially forming on one coupon over the other presumably due to emulsion effects, however, in either case the surface conditions are poor. Product 26 which have an average corrosion rate of 9.712 mpy, actually show good surface conditions with some emulsion markings on the surface. However, a large pit was present on the back of one of the coupons, which is a good example of localized corrosion.

Looking at figure 28, products which have the same chemistry and the same used materials, do not perform similarly. Product 1 and product 5 are good examples of this where product 1 have an average corrosion rate of 14.457 mpy while product 5 have an average corrosion rate of 9.688 mpy. A logical explanation for this is that the execution of the synthesis was not the same. In product 5, vacuum was applied to the system before Cinnamaldehyde was added. Also, the temperatures were different. Product 1 used 3h at 100°C and 3h at 120°C, while product 5 used 75°C for 5h. In the case of product 7 compared with product 14, the average corrosion rates are similar to each other, while the surface conditions are different. For product 7 there was corrosion occurring on the top halves of the coupons, while the surface condition for product 14 coupons were excellent. For these two products, only the order of execution which are different, however, for product 7 DDQ and Duomeen T was left in a flask from Friday to Tuesday which most likely caused the two materials to start reacting with each other in advance of the reaction.

Kettle-test

As we can see in figure 32, product 12 tested with 80% brine (3% NaCl) and 20% kerosene, injected with formulation including 2-ME gives the best result. This product has an efficiency of 93.6 % after 6 hours. Also, [C] and [H] show relatively good inhibition efficiency with 71.1% and 63.2% respectively. None except for [D] is close to the target of 8 mpy after 6h of inhibition. For product 12 and product 20 there is a visual difference whether the added inhibitor formulation contains 2-ME or not, and a distinct difference of whether the test was in a cell with 100% brine or 80% brine and 20% kerosene. For product 24 on the other hand, none of them gave any good results. [K] (41.9%) and [L] (37.7%) gave positive inhibition efficiency, but as we can see from the graph [L] starts to rise again, meaning that the inhibition effect wears off. With a slightly higher inhibition efficiency is [G] with 47.6%. For this there can also be observed a slight increase in the graph after 16 hours.

For all the tests we ran, a trend can be observed where cell injected with formulation containing 2-ME performs better than the cell injected with 2-ME free formulation. Except for [J] (1.0%), all of the test cells injected with formulations without 2-ME, had a negative inhibition efficiency. Meaning that the corrosion rate kept increasing by time after injection. In addition to this, both [E] and [M] end up with a corrosion rate on level with the blank test, while [I] is slightly below. This show us that [E] and [M] does not have any or minimal impact on the test cell as a corrosion inhibitor, while [I] might have slowed the corrosion rate down minimally. [F], [J] and [N] all fall below the blank test, and therefore probably have a small effect as an inhibitor. Also, there is a trend where the cells containing 80% brine and 20%

kerosene gives a better performance of the inhibitor compared to the cells containing 100% brine.

During the testing, [M] most likely had an oxygen leakage because the cell was completely orange (see figure 71 in attachments) after running over night. This have probably affected the test results since oxygen is more corrosive than CO₂. Another challenge during testing was that it took very long time for the baseline to stabilize, especially in the cells with 100% brine. Due to the workhours and time left on this project, it was decided to inject [C], [G] and [I] with the formulation despite the fact that the baseline was not stable. From the graph we still get a drop in the curve in both [C] and [G], while [I] continuous to increase. Even though it is not ideal to inject before the baseline had stabilized, it is possible to see an outcome where [C] and [G] have an impact on the corrosion rate. The outcome would most likely be similar if the baseline was stable in advanced.

Another source of error during the Kettle tests was the electrodes. They were not functioning optimal, and sometimes they lost contact with each other giving wrong values, and especially during the run of [L]. The problem occurred during the stabilization time, and to compensate for the wrong values, I had to insert number for the corrosion rate based on the numbers given for [N].

Comparing the Kettle test with the HPHT static autoclave tests there is a connection between which of the products that function as CIs. When comparing the results, we look at the tests where the conditions are the same, i.e. 80% brine, 20% kerosene, and formulations containing 1% 2-ME. Product 24 does not work at all, while product 20 is above the target and product 12 is below. However, the coupons from testing product 20 have better surface conditions than the coupons from testing product 12. Condition surface is weighed heavier, and product 20 is therefore considered giving better results in the HPHT static autoclave test. However, there are such a great difference in the test temperature, so it could also have been that one of the corrosion inhibitors had good performance at 70 °C but not at 150°C, and vice versa. Knowing this we can say that product 12 and product 20 are in some degree versatile regarding temperature.

The Kettle test was performed as additional testing as the HPHT autoclave testing was the primary test also giving more reliable and realistic results. The Kettle test ran at 70°C, which is not a realistic temperature considering the aim of these inhibitors is to function at a HPHT field.

Economic aspects

At the moment there are no commercial corrosion inhibitors which function well at 150°C. Therefore, there are no real prices to compare the costs of making these (in particular product 5) products on a greater scale, as well as the sales price. Compared to traditional, existing commercial CIs the price is at a reasonable level, especially since there are no alternatives at the time being. So, if the industry wants to protect for corrosion at higher temperatures, which they do, they must be willing to pay the price. Even if the price would be a bit higher than the already existing CIs, it would still be more beneficial to invest in the CI rather than having to replace damaged equipment due to corrosion damage.

Chapter 8 – Conclusions and further work

For the Kettle-test results there is a clear trend where the CIs perform poorly in 100% brine conditions. Also, there is a clear trend that the CIs perform better when the formulation contains 1% 2-ME. From the Kettle-test there are one combination that stands out, which is product 12 in 80% brine injected with formulation with 2-ME [D]. This combination has an effective inhibition percentage of 93.6% and shows a steep decrease in the graph after injection.

From the HPHT, static Autoclave tests there are no clear trend by first sight as there are multiple factors to take into consideration. However, product 5 stands out with an average corrosion rate 7.205 mpy and fairly good surface conditions. This is particularly interesting knowing that there is only half the amount of active product in this formulation compared to the other tests. For the products related to Structure III, none of them gave good performance as CIs. Even though product 28 and product 29 got an average negative mpy, this is due to upbuilt siderite on the surface. Pitting was also discovered on the coupons backing up the statement that these are no good.

From both tests it is observed that the products related to Structure I, perform the best among the three different aldehydes. Second best is the products related to Structure IV, while the products related to Structure V perform poorly. This support the theory and statement that the six-membered ring is important for the inhibition efficiency. Even though the purpose was to synthesize hexahydropyrimidines the main purpose of the study was to investigate the performance of the products made. Interestingly, the performance of the products where the aldehyde was Citral was similar to the products where the aldehyde was Cinnamaldehyde strongly indicating that the bis-adduct has corrosion inhibition properties similar to the corresponding hexahydropyrimidines.

Considering that the different orders of execution of the synthesis gives clear differences in performance, it would be interesting to do more research into which order gives the best performance results. Maybe another small experimental design project regarding optimization of material ratios could also be interesting as we in the screening phase, were inconsistent in the amounts of catalyst for example. It might also be clever to consider the economical aspect of production later in the process. Using 4wt% instead of 1wt% may or may not impact the performance, and it may or may not cause economical changes. Whether or not it is of interest to do these changes depends on the costs and performance.

Further characterization of the products related to Structure II and Structure III is work that needs to be done before the products can be commercialized. For now, there are theories regarding the structure of the (bi)products, but there are still work to be done for the product to reach the market. For Europe for instance, the products need to be approved by REACH and there are quite strict demands for product and identification of products before the approval is given.

There is also equipment available at Schlumberger to do further testing after the Kettle-test. After the Kettle-test it is possible to perform Rotating cylinder electrode test (RCE) and HPHT Autoclave tests as well. The Kettle-test are used as a screening of the corrosion inhibitors, and

then the ones that perform well are tested further in the RCE and HPHT autoclave tests. Since neither the Kettle-test nor the HPHT static autoclave test performed in Aberdeen apply any shear during testing, it could be interesting to test the best performing products after the HPHT static autoclave test in RCE since this test corrosion inhibitors under medium shear-stress or turbulent regimes.

As a new project related to this work, it could be interesting to do research on the dose response (in context of the HPHT static autoclave test) to find the cut off points in performance in terms of corrosion rate and surface conditions. As surfactants exhibit no linear solubility's, i.e. the amount of salt for instance, increase with increasing temperatures, etc. Surfactant polar head/non-polar tail above the CMC exist as micelles. However, the structure of the micelle at one point can have the polar groups outside and partition while at another point the hydrophobic groups are outside and the micelles remain in the oil phase. This will change with the ionic strength and composition of the brine, temperature, pH, etc. which will affect the performance of the CIs and the surface conditions of the metal (coupons in testing). This is an interesting aspect for future work. By optimizing dose rate, the performance could be improved, i.e. the amount of product in the brine phase.

This master thesis project was just part of a bigger picture project. I started when it was in the initial phase. This project will continue in Schlumberger researching on this chemistries functions towards different corrosion application as well.

Chapter 9 – Experimental

All chemicals, including solvents, were either supplied by Schlumberger or purchased by Sigma-Aldrich, and used without further purification.

Analysis

IR

Infrared spectra were recorded by adding a drop of the sample on Bruker ALPHA Platinum-ATR.

NMR

NMR spectra were recorded at 20°C in CDCl_3 or C_6D_6 with Bruker Ascend™ 400 spectrometer operating at 400 MHz. Chemical shifts are reported in parts per million (ppm), with internal reference: proton (Tetramethylsilane δ 0.00 ppm), carbon (Chloroform δ 77.31). Multiplicity was indicated as follows: s (singlet), d (doublet), t (triplet), q (quartet), m (multiplet).

Synthesis details

Method 1 – Vacuum synthesis

In a suitable, three-necked, round bottom flask, starting material A (N-alkyl-1,3-diaminopropane) was added together with a magnet. Starting material B (aldehyde) was charged to a dripping funnel, which was connected to the flask. To all reaction assembly joints, grease was applied to avoid damage to the glassware. Stirrer, heating block with thermometer, still-head, condenser, vacuum adapter and receiver flask was connected. See figure 33. Chill water was circulated through the condenser. Material A was melted, then starting material B was added. For some reactions, material B was added before vacuum was applied, and in other reactions, material B was added under vacuum. The reactions were ongoing for various lengths of time, and excess water was collected in the receiver flask. All temperatures listed are external temperatures. After the reactions had been running for the desired time, or until desired quantity of water is removed, the reaction was stopped and set to cool down to room temperature. The final products were transferred to a clean, suitable container. No further purification was performed, hence no total yield reported, except total mass of isolated crude mixture.



Figure 33: Set-up for vacuum synthesis

Method 2 – Dean Stark

In a suitable three-necked, round bottom flask, a magnet and starting material A (N-alkyl-1,3-diaminopropane) was added together with a solvent. Starting material B (aldehyde) was charged to a dripping funnel. The equipment was set up as shown in the figure 34, and grease was applied to all assembly joints to avoid damage to the glassware. Chill water was circulated through the condenser. Material A and the solvent was first melted while stirring and heating was on. When desired temperature (external temperatures listed) was reached, material B was added dropwise. The flask was covered with aluminum foil to avoid heat loss. The reaction was ongoing until desired quantity of water was removed. The amount of water in the Dean-Stark trap was recorded and the reaction was shut down, leaving the reaction to cool to room temperature. The solvent was then removed by rotary evaporation before the final product was transferred to a clean, suitable container. No further purification was performed, hence no total yield reported, except total mass of isolated crude mixture.



Figure 34: Set-up for Dean-Stark synthesis

Product 1

N-Tallow-1,3-diaminopropane (81.6 g, 0.24 mol, 1 eq.) melted at 80°C, then Cinnamaldehyde (32.8 g, 0.24 mol, 1 eq.) was added dropwise. When all Cinnamaldehyde was added, vacuum was applied to the reaction, and the temperature was raised to 100°C. After 3h a sample was collected, and the temperature was raised to 120°C for another 3h. The reaction was stopped and set to cool overnight. Water (3.61 g) was collected in a receiver flask. The final product (94.0 g) was a brown-black viscous liquid.

$^1\text{H-NMR}$ (400 MHz, CDCl_3): δ 0.88 (3H, t, $J = 7.0$ Hz), 1.00-1.50 (22H, m), 1.51-1.55 (2H, m), 1.55-1.70 (2H, m), 1.75-1.90 (2H, m), 1.90-2.15 (2H, m), 2.20-2.80 (2H, m), 3.10-3.40 (2H, m), 3.50-3.70 (2H, m), 3.90 (1H, s), 5.33-5.38 (2H, m), 7.20-7.35 (5H, m), 7.35-7.50 (2H, m); $^{13}\text{C-NMR}$ (100 MHz, CDCl_3): δ 14.14, 22.70, 27.30, 29.28-29.79 (12C), 31.91, 31.95, 32.63, 45.81, 52.15, 53.67, 81.94, 127.31, 127.81, 128.00, 128.48, 128.77, 129.87, 130.34, 142.68; IR (neat): ν 2920, 2851, 1738, 1636, 1455, 1374, 1126, 1071, 970, 747, 691 cm^{-1} .

Product 2

N-Tallow-1,3-diaminopropane (80.7 g, 0.23 mol, 1 eq.) was dissolved in Xylene (200 mL) at 150°C. When 150°C was reached, Cinnamaldehyde (32.2 g, 0.23 mol, 1 eq.) was added dropwise. The reaction was left at 150°C for 30 min. The temperature was then raised to 160°C for 1.5h, and then to 180°C until the reaction was finished. Water (4.25 mL) was

collected in the Dean-Stark trap. The final product (112.2 g) was a brown-black, viscous liquid. NMR and IR as for Product 1.

Product 3

N-Tallow-1,3-diaminopropane (40.5 g, 0.12 mol, 1 eq.) and p-toluenesulfonic acid (2.0 g, 2 wt%) was melted at 75°C. When everything was melted, vacuum was applied to the reaction, then Cinnamaldehyde (15.9 g, 0.12 mol, 1 eq.) was added drop wise – approximately 1 drop/s. Water (1.24 g) was collected on ice bath. After 2.5 h, a sample was collected, and the reaction was left on for another 2.5h. The final product (48.5 g) was a brown-black viscous liquid. NMR and IR as for Product 1.

Product 4

N-Tallow-1,3-diaminopropane (40.1 g, 0.121 mol, 1eq.) and p-toluenesulfonic acid (2.1 g, 2 wt%) was melted at 75°C. When all was melted, vacuum was applied and Cinnamaldehyde (15.6 g, 0.12 mol, 1 eq.) was added dropwise – 1 drop/sec. After 5h additional p-toluenesulfonic acid (2.1 g, 2 wt%) was added to the reaction. Water* was collected in a receiver flask. The final product (47.4 g) was a brown-black, viscous liquid. NMR and IR as for Product 1.

Product 5

N-Tallow-1,3-diaminopropane (41.0 g, 0.12 mol, 1 eq.) was melted at 75°C. Vacuum was applied to the reaction after N-Tallow-1,3-diaminopropane was melted, and then Cinnamaldehyde (16.2 g, 0.12 mol, 1 eq.) was added dropwise – 1 drop/sec. The reaction was on for 10h. Water* was collected in a receiver flask. The final product (44.3 g) was an orange-brown, semi-solid. NMR and IR as for Product 1.

Product 6

N-Tallow-1,3-diaminopropane (40.5 g, 0.12 mol, 1 eq.) and p-toluenesulfonic acid (2.0 g, 2 wt%) was melted at 75°C along with 2-butoxyethanol (56.4 g). Then vacuum was applied and Cinnamaldehyde (15.9 g, 0.12 mol, 1 eq.) was added dropwise. After 5h a sample was collected, and additional p-toluenesulfonic acid (2.0 g, 2 wt%). After five more hours, the reaction was stopped. Water* was collected in a receiver flask. The final product (109.3 g) was a brown-black, viscous liquid. NMR and IR as for Product 1.

Product 7

N-Tallow-1,3-diaminopropane (21.9 g, 0.065 mol, 1 eq.) and DDQ (0.9 g, 2 wt%) was melted at 75°C. Then Cinnamaldehyde (8.3 g, 0.065 mol, 1 eq.) was added drop wise before vacuum was applied. The reaction was stopped after 5h. Water* was collected in a receiver flask. The final product (22.6 g) was a brown-black, viscous liquid. NMR and IR as for Product 1.

Product 8

N-Tallow-1,3-diaminopropane (20.7 g, 0.062 mol, 1 eq.) was dissolved in Xylene (21.4 g), first at room temperature, and then at 40°C in order to dissolve all of it. The reaction was then

* Water was observed both in the condenser and receiver flask, but due to vacuum it condensed. Since water is more a measurement of the reaction taking place, not a wanted product in these reactions, it is not critical to measure the exact amount of water loss. It is also not expedient to stop/pause the reaction in order to collect every water drop.

cooled down to room temperature before Cinnamaldehyde (8.3 g, 0.062 mol, 1 eq.) was added dropwise. Then DDQ (0.23 g, 1 wt%) was added, and the reaction was then left for 2h with stirring. After 2 hours, the temperature was raised to 150°C in order to start the Dean-Stark reaction. Maximum temperature during the reaction was 180°C. Water (0.9 mL) was collected in the Dean-Stark trap. The final product (21.3 g) was a brown-black, viscous liquid. NMR and IR as for Product 1.

Product 9

N-Tallow-1,3-diaminopropane (10.1 g, 0.030 mol, 1 eq.) and B(OCH₂CF₃)₃ (0.1 g, 1 wt%) was melted at 75°C. When everything was melted, vacuum was applied to the reaction, then Cinnamaldehyde (3.9 g, 0.030 mol, 1 eq.) was added dropwise. Water was collected on ice bath. The reaction was left with stirring for 5h. Water* was collected in a receiver flask. The final product (14.9 g) was a brown-black, viscous liquid. NMR and IR as for Product 1.

Product 10

N-Tallow-1,3-diaminopropane (11.5 g, 0.034 mol, 1 eq.) was dissolved in Xylene (10.8 g), first at room temperature, and then at 40°C to dissolve all. The reaction was then cooled down to room temperature before Cinnamaldehyde (4.4 g, 0.034 mol, 1 eq.) was added dropwise. Then B(OCH₂CF₃)₃ (0.12 g, 1 wt%) was added, and the reaction was then left for 2h with stirring. After 2 hours, the temperature was raised to 150°C in order to start the Dean-Stark reaction. Maximum temperature during the reaction was 180°C. Water (0.49 mL) was collected in the Dean-Stark trap. The final product (19.1 g) was a brown-black, viscous liquid. NMR and IR as for Product 1.

Product 11

N-Oleyl-1,3-diaminopropane (50.6 g, 0.16 mol, 1 eq.) and Toluene (52.3 g) was melted at 40°C. Then Cinnamaldehyde (20.7 g, 0.16 mol, 1 eq.) was added dropwise before B(OCH₂CF₃)₃ (0.5 g, 1 wt%) was added. The temperature was then raised to 100°C for 20 min, then to 130°C for 1h, then to 140°C for 1.5h, then to 150°C for 1.5h, and then to 160°C until the Dean-Stark reaction was finished. Water (2.1 mL) was collected in the Dean-Stark trap. The final product (71.8 g) was a brown-black, viscous liquid. NMR and IR as for Product 1.

Product 12

N-Oleyl-1,3-diaminopropane (50.1 g, 0.15 mol, 1 eq.) was melted at 40°C before Cinnamaldehyde (20.4 g, 0.15 mol, 1 eq.) was added dropwise. When Cinnamaldehyde was added, p-toluenesulfonic acid (0.70 g, 1 wt%) was added to the reaction and vacuum applied. Then the temperature was raised to 75°C. The reaction was left with stirring for 5h. Water* was collected in a receiver flask. The final product (65.8 g) was a brown-black, viscous liquid. NMR and IR as for Product 1.

Product 13

N-Oleyl-1,3-diaminopropane (50.1 g, 0.16 mol, 1 eq.) and Toluene (50.0 g) was melted at 40°C. Then Cinnamaldehyde (20.4 g, 0.16 mol, 1 eq.) was added dropwise before p-toluenesulfonic

* Water was observed both in the condenser and receiver flask, but due to vacuum it condensed. Since water is more a measurement of the reaction taking place, not a wanted product in these reactions, it is not critical to measure the exact amount of water loss. It is also not expedient to stop/pause the reaction in order to collect every water drop.

acid (0.70 g, 1 wt%) was added. The temperature was then raised to 140°C for 3h, and then to 160°C until the Dean-Stark reaction was finished. Water (2.1 mL) was collected in the Dean-Stark trap. The final product (71.7 g) was a brown-black, viscous liquid. NMR and IR as for Product 1.

Product 14

N-Oleyl-1,3-diaminopropane (50.3 g, 0.16 mol, 1 eq.) was melted at 40°C before Cinnamaldehyde (20.4 g, 0.16 mol, 1 eq.) was added dropwise. When Cinnamaldehyde was added, DDQ (0.70 g, 1 wt%) was added to the reaction and vacuum applied. Then the temperature was raised to 75°C. The reaction was left with stirring for 5h. Water* was collected in a receiver flask. The final product (71.7 g) was a brown-black, viscous liquid. NMR and IR as for Product 1.

Product 15

N-Oleyl-1,3-diaminopropane (50.3 g, 0.16 mol, 1 eq.) and Toluene (50.2 g) was melted at 40°C. Then Cinnamaldehyde (20.4 g, 0.16 mol, 1 eq.) was added dropwise before DDQ (0.70 g, 1 wt%) was added. The temperature was then raised to 140°C for 2h, and then to 160°C until the Dean-Stark reaction was finished. Water (1.8 mL) was collected in the Dean-Stark trap. The final product (71.3 g) was a brown-black, viscous liquid. NMR and IR as for Product 1.

Product 16

N-Oleyl-1,3-diaminopropane (30.0 g, 0.092 mol, 1 eq.) and Toluene (100 mL) was melted at 40°C. Then Cinnamaldehyde (12.2 g, 0.092 mol, 1 eq.) was added dropwise before B(OCH₂CF₃)₃ (0.41 g, 1 wt%) was added. The temperature was then raised to 140°C for 2h, then for 1h at 150°C, and then the temperature was raised to 160 °C until the Dean-Stark reaction was finished. Water (0.1 g) was collected in the Dean-Stark trap. The final product (41.3 g) was a brown-black, viscous liquid. NMR and IR as for Product 1.

Product 17

N-Oleyl-1,3-diaminopropane (50.0 g, 0.154 mol, 1 eq.) was melted at 40°C before Cinnamaldehyde (20.4 g, 0.154 mol, 1 eq.) was added dropwise. When Cinnamaldehyde was added, B(OCH₂CF₃)₃ (0.70 g, 1 wt%) was added to the reaction and vacuum applied. Then the temperature was raised to 75°C. The reaction was left with stirring for 5h. Water* was collected in a receiver flask. The final product (69.5 g) was a red, oily liquid. NMR and IR as for Product 1.

Product 18

N-Oleyl-1,3-diaminopropane (50.4 g, 0.16 mol, 1 eq.) was melted at 40°C before Citral (23.5 g, 0.16 mol, 1 eq.) was added dropwise. When Citral was added, p-toluenesulfonic acid (0.74 g, 1 wt%) was added to the reaction and vacuum applied. Then the temperature was raised to 75°C. The reaction was left with stirring for 5h. Water (1.9 g) was collected in a receiver flask. The final product (73.2 g) was a brown-black, viscous liquid.

* Water was observed both in the condenser and receiver flask, but due to vacuum it condensed. Since water is more a measurement of the reaction taking place, not a wanted product in these reactions, it is not critical to measure the exact amount of water loss. It is also not expedient to stop/pause the reaction in order to collect every water drop

$^1\text{H-NMR}$ (400 MHz, CDCl_3): δ 0.88 (t, $J = 4.0$ Hz), 1.10-1.40 (m), 1.40-1.55 (m), 1.55-1.75 (m), 1.75-1.90 (m), 1.90-2.05 (m), 2.10-2.20 (m), 2.20-2.30 (m), 2.55-2.75 (m), 3.00-3.10 (m), 3.15-3.25 (m), 5.00-5.20 (m), 5.25-5.45 (m) (*Annotation of number of protons was difficult due to impure product*); $^{13}\text{C-NMR}$ (100 MHz, CDCl_3): δ 14.05, 22.64, 25.63, 26.24, 27.16, 27.20, 27.72, 29.20-29.72 (12C), 31.87, 32.56, 45.03, 51.65, 52.88, 72.18, 129.74, 129.75, 129.82, 129.84, 130.26, 131.71; IR (neat): ν 2921, 2852, 1660, 1621, 1456, 1375, 1125, 966, 721, 682 cm^{-1} .

Product 19

N-Oleyl-1,3-diaminopropane (50.0 g, 0.15 mol, 1 eq.) and Toluene (50.0 g) was melted at 40°C. Then Citral (23.5 g, 0.15 mol, 1 eq.) was added dropwise before p-toluenesulfonic acid (0.73 g, 1 wt%) was added. The temperature was then raised to 140°C for 2h, and then to 160°C until the Dean-Stark reaction was finished. Water (2.5 mL) was collected in the Dean-Stark trap. The final product (74.8 g) was a brown-black, viscous liquid. NMR and IR as for product 18.

Product 20

N-Oleyl-1,3-diaminopropane (50.0 g, 0.15 mol, 1 eq.) was melted at 40°C before Citral (23.5 g, 0.15 mol, 1 eq.) was added dropwise. When Citral was added, DDQ (0.73 g, 1 wt%) was added to the reaction and vacuum applied. Then the temperature was raised to 75°C. The reaction was left with stirring for 5h. Water (1.0 g) was collected in a receiver flask. The final product (74.3 g) was a brown-black, viscous liquid. NMR and IR as for product 18

Product 21

N-Oleyl-1,3-diaminopropane (50.1 g, 0.15 mol, 1 eq.) and Toluene (50.1 g) was melted at 40°C. Then Citral (23.5 g, 0.15 mol, 1 eq.) was added dropwise before DDQ (0.73 g, 1 wt%) was added. The temperature was then raised to 140°C for 2.5h, and then to 160°C until the Dean-Stark reaction was finished. Water (2.2 mL) was collected in the Dean-Stark trap. The final product (75.2 g) was a brown-black, viscous liquid. NMR and IR as for product 18.

Product 22

N-Oleyl-1,3-diaminopropane (30.1 g, 0.093 mol, 1 eq.) and Toluene (100 mL) was melted at 40°C. Then Citral (14.1 g, 0.093 mol, 1 eq.) was added dropwise before $\text{B}(\text{OCH}_2\text{CF}_3)_3$ (0.47 g, 1 wt%) was added. The temperature was then raised to 140°C for 2h, then for 1h at 150°C, and then the temperature was raised to 160°C until the Dean-Stark reaction was finished. Water (0.2 g) was collected in the Dean-Stark trap. The final product (45.6 g) was an orange-red, oily liquid. NMR and IR as for product 18.

Product 23

N-Oleyl-1,3-diaminopropane (50.0 g, 0.15 mol, 1 eq.) was melted at 40°C before Citral (23.4 g, 0.15 mol, 1 eq.) was added dropwise. When Citral was added, $\text{B}(\text{OCH}_2\text{CF}_3)_3$ (0.73 g, 1 wt%) was added to the reaction and vacuum applied. Then the temperature was raised to 75°C. The reaction was left with stirring for 5h. Water (2.3 g) was collected in a receiver flask. The final product (71.0 g) was an orange, oily liquid. NMR and IR as for product 18.

Product 24

N-Oleyl-1,3-diaminopropane (50.1 g, 0.15 mol, 1 eq.) was melted at 40°C before Hexylcinnamaldehyde (33.4 g, 0.15 mol, 1 eq.) was added dropwise. When Hexylcinnamaldehyde was added, p-toluenesulfonic acid (0.83 g, 1 wt%) was added to the reaction and vacuum applied. Then the temperature was raised to 75°C. The reaction was left with stirring for 5h. Water* was collected in a receiver flask. The final product (84.8 g) was a yellow, oily liquid.

¹H-NMR (400 MHz, CDCl₃): δ 0.89 (6H, m), 1.05-1.40 (24H, m), 1.40-1.75 (10H, m), 1.75-1.90 (2H, m), 1.90-2.10 (2H, m), 2.47 (2H, t, *J* = 8Hz), 2.50-2.65 (2H, m), 2.65-2.80 (2H, m), 3.45-3.65 (2H, m), 5.27-5.45 (2H, m), 6.70 (1H, s), 7.11-7.52 (5H, m), 7.88 (1H, s); ¹³C-NMR (100 MHz, CDCl₃): δ 14.13 (2C), 22.66, 22.70, 26.70, 27.22, 27.46, 28.74, 29.29-29.79 (13C), 30.17, 31.66, 31.93, 48.26, 50.15, 59.71, 127.56, 128.38, 128.96, 129.83, 129.91, 136.67, 138.30, 141.95, 165.21; IR (neat): ν 2921, 2852, 1629, 1457, 1376, 1338, 1127, 965, 750, 722, 696, 509 cm⁻¹.

Product 25

N-Oleyl-1,3-diaminopropane (50.0 g, 0.15 mol, 1 eq.) was melted at 40°C before Hexylcinnamaldehyde (33.3 g, 0.15 mol, 1 eq.) was added dropwise. When Hexylcinnamaldehyde was added, DDQ (0.83 g, 1 wt%) was added to the reaction and vacuum applied. Then the temperature was raised to 75°C. The reaction was left with stirring for 5h. Water (1.4 g) was collected in a receiver flask. The final product (84.0 g) was a brown-black, viscous liquid.

Product 26

N-Oleyl-1,3-diaminopropane (30.1 g, 0.093 mol, 1 eq.) and Toluene (100 mL) was melted at 40°C. Then Hexylcinnamaldehyde (20.1 g, 0.093 mol, 1 eq.) was added dropwise before p-toluenesulfonic acid (0.55 g, 1 wt%) was added. The temperature was then raised to 140°C for 2h, then for 1h at 150°C, and then the temperature was raised to 160°C until the Dean-Stark reaction was finished. Water (0.3 g) was collected in the Dean-Stark trap. The final product (50.6 g) was a dark orange, oily liquid.

Product 27

N-Oleyl-1,3-diaminopropane (30.0 g, 0.092 mol, 1 eq.) and Toluene (100 mL) was melted at 40°C. Then Hexylcinnamaldehyde (20.0 g, 0.092 mol, 1 eq.) was added dropwise before DDQ (0.50 g, 1 wt%) was added. The temperature was then raised to 140°C for 2h, then for 1h at 150°C, and then the temperature was raised to 160°C until the Dean-Stark reaction was finished. Water (0.9 g) was collected in the Dean-Stark trap. The final product (49.8 g) was a brown-black, viscous liquid.

Product 28

N-Oleyl-1,3-diaminopropane (50.0 g, 0.15 mol, 1 eq.) was melted at 40°C before Hexylcinnamaldehyde (33.4 g, 0.15 mol, 1 eq.) was added dropwise. When

* Water was observed both in the condenser and receiver flask, but due to vacuum it condensed. Since water is more a measurement of the reaction taking place, not a wanted product in these reactions, it is not critical to measure the exact amount of water loss. It is also not expedient to stop/pause the reaction in order to collect every water drop.

Hexylcinnamaldehyde was added, $B(OCH_2CF_3)_3$ (0.84 g, 1 wt%) was added to the reaction and vacuum applied. Then the temperature was raised to 75°C. The reaction was left with stirring for 5h. Water (2.2 g) was collected in a receiver flask. The final product (82.0 g) was a yellow, oily liquid.

Product 29

N-Oleyl-1,3-diaminopropane (30.0 g, 0.092 mol, 1 eq.) and Toluene (100 mL) was melted at 40°C. Then Hexylcinnamaldehyde (20.0 g, 0.092 mol, 1 eq.) was added dropwise before $B(OCH_2CF_3)_3$ (0.53 g, 1 wt%) was added. The temperature was then raised to 140°C for 2h, then for 1h at 150°C, and then the temperature was raised to 160°C until the Dean-Stark reaction was finished. Water (0.6 g) was collected in the Dean-Stark trap. The final product (49.9 g) was a yellow, oily liquid.

Test methods:

High Pressure, High Temperature, static Autoclave test

Tests were conducted using standard static autoclave equipment (Figure 35 and figure 36). The test was performed on a fluid consisting of 80 % brine (3% NaCl) and 20% kerosene. The test cell was primed with fluid and sparged with CO₂ for 1h prior to corrosion inhibitor being added and the test fluids sparged with CO₂ for a further 30 minutes to remove oxygen in the head space of the autoclave. The test coupons were then mounted in the autoclave which was subsequently sealed. The autoclave was pressurized to 1 bar with CO₂ and heated to test temperature for 3 days. At the end of the test the coupons were removed, cleaned, reweight and the corrosion rate calculated. The coupons were analyzed for any evidence of pitting or localized corrosion using an optical microscope. The corrosion inhibitor performance was established by weightless measurements and investigation of the surface condition post-test and by comparison of the inhibited corrosion rate to the baseline uninhibited corrosion rate.

- Brine phase 3% w/v NaCl
- Water cut 80%
- Inhibitor dosage 500 ppm, where 100 ppm are active product
- Temperature 150 °C
- Coupon Material Carbon steel (C1018)
- Pressure 1 bar CO₂
- Test duration 72 hours



Figure 35: HPHT static Autoclave test equipment



Figure 36: Assembled HPHT static Autoclave test equipment

Kettle-test

Equipment and Maintenance

The following test equipment is required:

- Hot plate/magnetic stirrer with thermocouple
- Magnetic stirring bar
- Glass corrosion cells, lids and stopper
- Metal clamps for lids
- Gas sparge tubes linked to CO₂ supply
- Condensers connected to water supply
- LPR Probe & electrodes attached to ACM potentiostat
- PC for data logging
- ACM Potentiostat
- Micro Pipette (5-100 µL)
- Silicon carbide paper

The following reagents are required:

- Brine Phase – Synthetic brines are made according to customer specification using analytical grade salts. Sulphate/bicarbonate ions may need to be omitted, and calcium ions replace with two molar equivalents of sodium ions to prevent scale formation during the tests, this typically occurs at temperatures above 50°C and can be seen either by clouding of the brine or a gradual decline in baseline corrosion rates (trending towards zero). Salty brines may also show a tendency to block/salt out the sparge tube at elevated temperatures. If salt deposition is problem, place a split 1" length of plastic tubing on the sparge tube outlet, this will ensure that the sparge does not become blocked during testing.
- Oil Phase – Field Crude (this must be inhibitor free) or odourless kerosene (if a generic oil phase is required). Where Field Crude is used it must not be sour, and the tests must be performed only if ventilation allows, i.e. in a fume hood.
- Formulation containing the Corrosion inhibitor
- Acetone (for cleaning)
- ~5 % Hydrochloric acid solution (for cleaning)

Procedure

Place a clean test vessel on a hotplate, and add a magnetic stir bar and the brine phase. Place the lid on the vessel and secure with clips. Insert a condenser, sparge tube and thermocouple respectively in the three

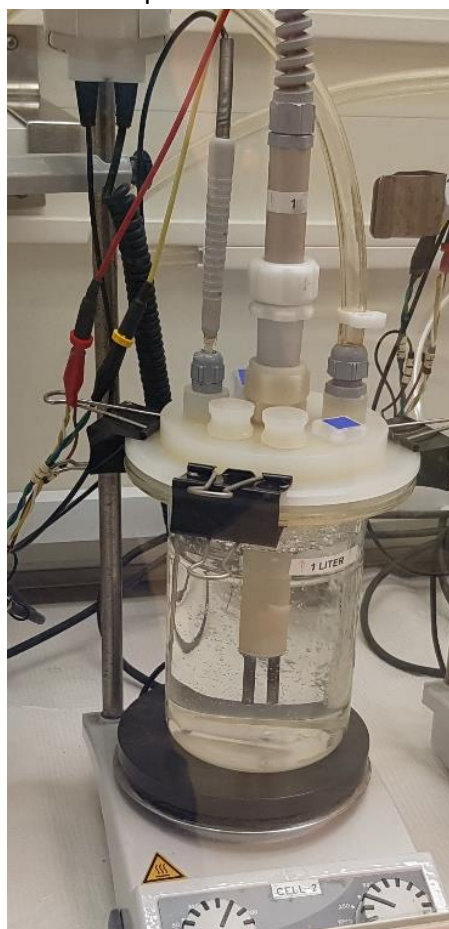


Figure 37: Kettle-test set-up for one test cell

small ports on the lid. Add a stopper to the central port. Start the CO₂ flow and ensure a steady stream of bubbles through the brine phase (300-500 ml/min). Turn on the condensers, begin stirring (250 rpm) and heat to test temperature (70°C). Make sure that no leads are in contact with the hotplate. Sparge for at least 1 hour to deaerate the system. Prepare electrodes and attach to LPR probe. After deaeration is complete, remove the stopper from the central port and carefully insert the LPR probe. Check again that no leads are in contact with the hotplate. Add the oil phase through either the thermocouple or condenser port taking care not to get oil on the LPR electrodes. Begin logging data on the computer. Establish baseline for minimum of two hours or until it is stable. Treat with corrosion inhibitor. Monitor corrosion rate for a day, and then end data logging. Turn off the hotplate and condenser, remove the gas-spargers and stop CO₂ flow. Dismantle and clean the test equipment when cool enough to handle.

Some of the test cells were tested in 100% brine, others in 80% brine and 20% kerosene.

The final set-up for one cell is pictured in figure 37.

Making of formulations and brines for both test methods

The brines used in both test methods are a 3% w/v NaCl solution, which were made by mixing NaCl and distilled water at the right ratio.

For both tests there was used a formulation consisting of 79% 2-butoxyethanol, 20% active product and 1% 2-ME. The formulations were made adding active product into the 2-butoxyethanol and then 2-ME to the end. In the Kettle-test formulations without 2-ME was also used. In this case the formulation contained 80% 2-butoxyethanol and 20% active product. These were made by adding active product to 2-butoxyethanol.

References

- Barnes, P. (2018). [High pressure, high temperature, static Autoclave tests].
- Becker, J. R. (1998). *Corrosion and scale handbook*. Tulsa, Okla: PennWell.
- Chen, H. J., Jepson, W. P., & Hong, T. J. (2000). High temperature corrosion inhibition performance of imidazoline and amide. *CORROSION 2000*.
- Chilingar, G. V., Mourhatch, R., & Al-Qahtani, A. (2013). *The Fundamentals of Corrosion and Scaling for Petroleum & Environmental Engineers*. Burlington: Elsevier Science.
- Darling, D., & Rakshpal, R. (1998). *Green chemistry applied to corrosion and scale inhibitors*. Retrieved from
- Davis, J. R. (2000). *Corrosion : Understanding the Basics*. Materials Park: A S M International.
- Eynde, J. J. V., Delfosse, F., Lor, P., & Haverbeke, Y. V. (1995). *Tetrahedron*, 51, 5813-5818.
- Fink, J. (2003). *Oil Field Chemicals*: Elsevier Science.
- Fisher, L. (1993). Corrosion Inhibitors and Neutralizers Past, Present and Future. *L. E. Fisher, Paper(537)*.
- Guimaraes, P. I. C., Monterio, A. P., & Mainier, F. B. (1994). New Corrosion Inhibitors in solid form to protect carbon steel pipes in acidizing operations. *Proceeding Volume, 2*.
- Hart, D. J. (2012). *Organic chemistry : a brief course* (13th ed. ed.). Belmont, Calif.: Brooks/Cole Cengage Learning.
- Hart, H., Hadad, C. M., Craine, L. E., & Hart, D. J. (2011). *Organic chemistry: a short course*: Cengage Learning.
- Hoffmann, H., & Kremer, G. (1996). 5530131.
- INSA. (2013a). Erosion and cavitation corrosion. Retrieved from http://www.cdcorrosion.com/mode_corrosion/corrosion_erosion_gb.htm
- INSA. (2013b). Stress corrosion cracking (SCC). Retrieved from http://www.cdcorrosion.com/mode_corrosion/stress_corrosion_cracking.htm
- Kelland, M. A. (2014). *Production Chemicals for the Oil and Gas Industry, Second Edition* (2nd ed. ed.). Hoboken: Taylor and Francis.
- Kennard, M. A., & McNulty, J. G. (1992). Conventional pipeline-pigging technology: Pt. 2: Crrosion-Inhibitor deposition using pigs. *Pipes Pipelines Int*.
- Lanigan, R. M., Starkov, P., & Sheppard, T. D. (2013). Direct synthesis of amides from carboxylic acids and amines using B(OCH₂CF₃)₃. *The Journal of organic chemistry*, 78(9), 4512. doi:10.1021/jo400509n
- Martin, R. (2009). *Control of top-of-line corrosion in a sour gas gathering pipeline with corrosion inhibitors*. Paper presented at the CORROSION 2009.
- Moke, H. C., & Leathers, J. M. (1967). Process for the purification of amines. In: Google Patents.
- Molander, G. A., Katritzky, A. R., & Taylor, R. J. K. (2005). *Comprehensive organic functional group transformations II : Vol. 4 : Carbon with two heteroatoms, each attached by a single bond* (Vol. Vol. 4). Oxford: Elsevier Pergamon.
- Muhlbauer, H. G., & Cour, T. H. (1964). Purification of amines. In: Google Patents.
- Obeyesekere, N. U., Naraghi, A. R., Chen, L., Zhou, S., & Wang, S. (2005). *Novel Corrosion Inhibitors for High Temperature Applications*. Paper presented at the CORROSION 2005.
- Okafor, P., Liu, C., Zhu, Y., & Zheng, Y. (2011). Corrosion and corrosion inhibition behavior of N80 and P110 carbon steels in CO₂-saturated simulated formation water by rosin amide imidazoline. *Industrial & Engineering Chemistry Research*, 50(12), 7273-7281.
- Park, N. G., Morello, L., & Abriam, G. (2009). *Understanding Inhibition of Sour Systems with Water Soluble Corrosion Inhibitors*. Paper presented at the CORROSION 2009.
- Peabody, A. W., Bianchetti, R. L., National Association of Corrosion, E., & International, N. (2001). *Peabody's control of pipeline corrosion* (2nd ed. ed.). Houston, Tex: NACE International.
- Perez, N. (2004). *Electrochemistry and corrosion science*. Boston: Kluwer Academic.

- Pähler, M., Santana, J. J., Schuhmann, W., & Souto, R. M. (2011). Application of AC-SECM in Corrosion Science: Local Visualisation of Inhibitor Films on Active Metals for Corrosion Protection. *Chemistry-A European Journal*, 17(3), 905-911.
- Ramachandran, S., Ahn, Y. S., Greaves, M., Jovancicevic, V., & Bassett, J. (2006). *Development of high temperature, high pressure corrosion Inhibitor*. Paper presented at the CORROSION 2006.
- Ramachandran, S., Ahn, Y. S., Jovancicevic, V., & Bassett, J. (2005). *Further advances in the development of erosion corrosion inhibitors*. Paper presented at the CORROSION 2005.
- Standards, U. S. N. B. o., Bennett, L. H., & Laboratories, B. M. I. C. (1978). *Economic effects of metallic corrosion in the United States: a report to the Congress: The Bureau : for sale by the Supt. of Docs., U.S. Govt. Print. Off.*
- Stansbury, E. E., & Buchanan, R. A. (2000). Fundamentals of electrochemical corrosion. In *Fundamentals of electrochemical corrosion*. Materials Park, OH: Materials Park, OH: ASM International.
- Steelfab. (2017a, 26.06.2017). A Guide To Crevice Corrosion & How To Treat It. Retrieved from <https://steelfabservices.com.au/a-guide-to-crevice-corrosion-how-to-treat-it/>
- Steelfab. (2017b, 26.06.2017). A Guide To Galvanic Corrosion & How To Treat It. Retrieved from <https://steelfabservices.com.au/a-guide-to-galvanic-corrosion-how-to-treat-it/>
- Steelfab. (2017c, 17.07.2017). A Guide To Intergranular Corrosion & How To Treat It. Retrieved from <https://steelfabservices.com.au/a-guide-to-intergranular-corrosion-how-to-treat-it/>
- Steelfab. (2017d, 26.06.2017). Pitting Corrosion & How To Treat It. Retrieved from <http://steelfabservices.com.au/pitting-corrosion-how-to-treat-it/>
- Stewart, S., Menendez, C., Jovancicevic, V., & Moloney, J. (2009). New Corrosion Inhibitor Evaluation Approach for Highly Sour Service Conditions. *CORROSION 2009*.
- Strenitz, M. (2018). [Characterization of products by the use of LCMS, GPC and GC].
- Tandon, M., Shadley, J. R., Rybicki, E. F., Roberts, K. P., Ramachandran, S., & Jovancicevic, V. (2006). *Flow loop studies of inhibition of erosion-corrosion in CO2 environments with sand*. Paper presented at the CORROSION 2006.
- Tanks, A. (2017). MIC Corrosion, Microbiologically Influenced Corrosion. Retrieved from <http://atmtanks.com.au/maintenance/mic-specialists/>
- Wang, H., Jepson, W. P., Wang, H., & Shi, H. (2002). *Why corrosion inhibitors do not perform well in some multiphase conditions: a mechanistic study*. Paper presented at the CORROSION 2002.
- Wong, J. E., & Park, N. (2009). *Further investigation on the effect of corrosion inhibitor actives on the formation of iron carbonate on carbon steel*. Paper presented at the CORROSION 2009.
- Wylde, J. J., Reid, M., Kirkpatrick, A., Obeyesekere, N., & Glasgow, D. (2013). *When To Batch and When Not To Batch: An Overview of Integrity Management and Batch Corrosion Inhibitor Testing Methods and Application Strategies*. Paper presented at the SPE International Symposium on Oilfield Chemistry.

Attachment

High pressure, high temperature, static Autoclave Test

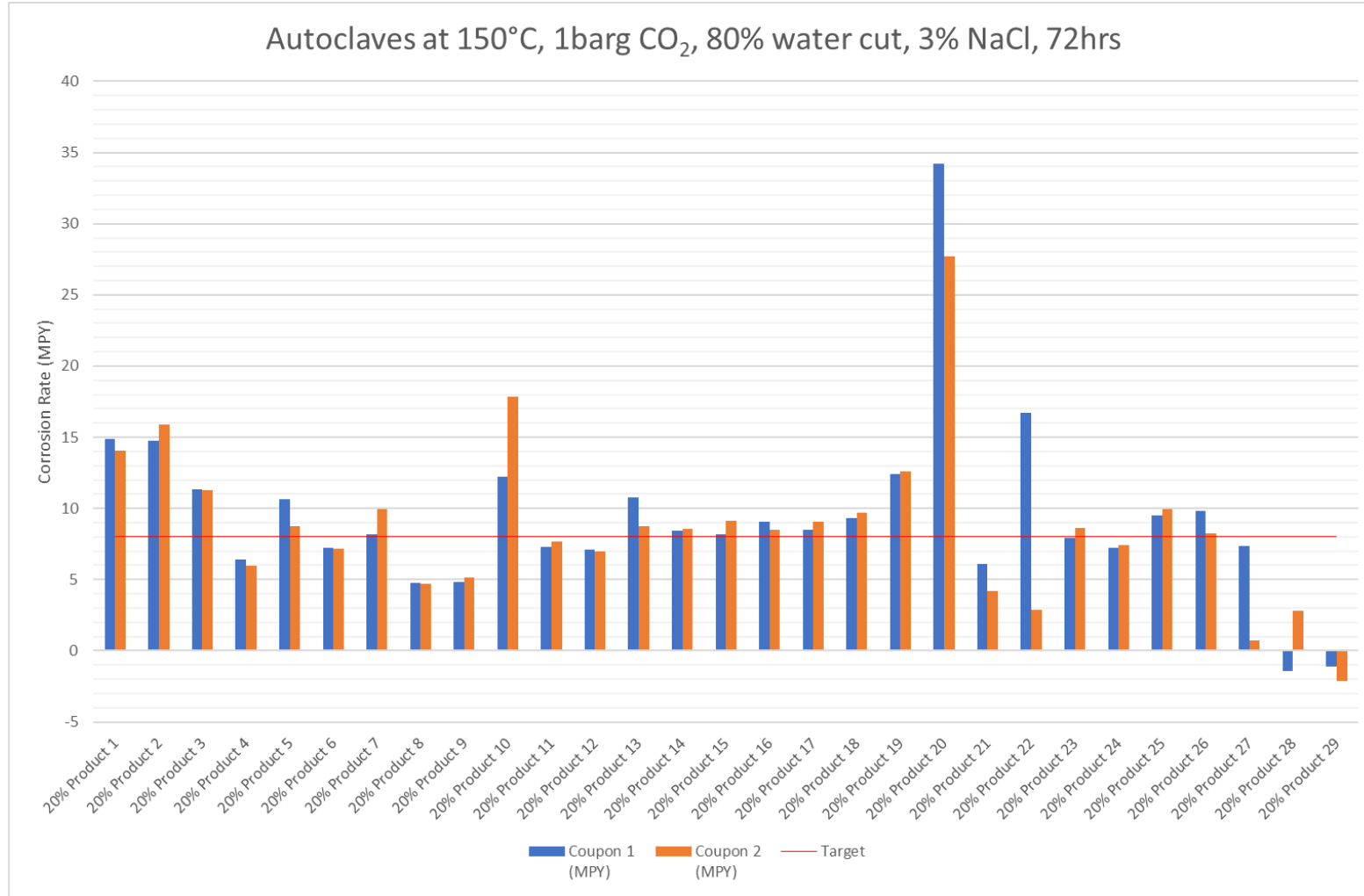


Figure 38: Corrosion rates for each coupon from the HPHT static autoclave test



Figure 39: Product 1



Figure 42: Product 4



Figure 40: Product 2



Figure 43: Product 5



Figure 41: Product 3



Figure 44: Product 6



Figure 45: Product 7



Figure 48: Product 10



Figure 46: Product 8



Figure 49: Product 11



Figure 47: Product 9



Figure 50: Product 13



Figure 51: Product 14



Figure 54: Product 19



Figure 52: Product 15



Figure 55: Product 21



Figure 53: Product 18



Figure 56: Product 16



Figure 57: Product 25



Figure 60: Product 26



Figure 58: Product 22



Figure 61: Product 23



Figure 59: Product 17



Figure 62: Product 27



Figure 63: Product 28



Figure 64: Product 29

Table 4: Overview of corrosion rates and comments regarding surface conditions for HPHT, static autoclave tests

Product	Corrosion Rate 1	Corrosion Rate 2	Average	Surface condition
1	14.851	14.062	14.457	Product 1 averaged 14.46MPY across both test specimens. Compared to Product 2 and 3, Product 1 had the most tenacious siderite scale on the surface ie the most difficult to remove.
2	14.781	15.895	15.338	Product 2 (Deans-Stark method) averaged 15.34MPY across both test specimens and of the 3 tests these coupons had the better surface condition
3	11.324	11.254	11.289	Product 3 (Tosic acid catalyst) averaged 11.29MPY across both test specimens with good surface conditions however there was some patterns on the surface, particularly on the back which is likely due to emulsion effects
4	6.381	5.964	6.173	Product 4 averaged 6.17MPY across both test specimens with some residual siderite present on the surface.
5	10.651	8.725	9.688	Product 5 averaged 9.69MPY across both test specimens with some evidence of pitting occurring.
6	7.217	7.193	7.205	Product 6 averaged 7.21MPY across both test specimens with good surface condition albeit with a low residual amount of siderite on the surface
7	8.168	9.491	8.830	Product 7 averaged 8.83MPY across the two test specimens with corrosion occurring more on the top halves of the coupons
8	4.780	4.687	4.734	Product 8 averaged 4.73MPY across both test specimens although siderite is still present on the surface the surface looks quite good
9	4.850	5.128	4.989	Product 9 averaged 4.99MPY across both test specimens with siderite present on the surface with evidence of localized pitting on the coupons surfaces.
10	12.229	17.867	15.048	Product 10 averaged 15.05MPY across the two test specimens with corrosion occurring more on the top halves of the coupons with more etching around the attachment point
11	7.309	7.657	7.483	Product 11 averaged 7.48MPY across the two test specimens with good surface conditions albeit with some minor etching at the bottom which is likely due to emulsion at this point
12	7.124	7.008	7.066	Product 12 averaged 7.07MPY across the two test specimens although there appears to be some etching on the top half of the coupon perhaps due to water in oil emulsion??
13	10.744	8.725	9.735	Product 13 averaged 9.73MPY across the two test specimens with excellent surface condition.
14	8.423	8.562	8.493	Product 14 averaged 8.45MPY across the two test specimens with excellent surface conditions perhaps with a slight dusting of siderite present on the surface??
15	8.168	9.119	8.644	Product 15 averaged 8.64MPY across the two test specimens with good surface condition but with the beginnings of a single pit on the back of one coupon (2875)

Table 5: Overview of corrosion rates and comments regarding surface conditions for HPHT, static autoclave tests

Product	Corrosion Rate 1	Corrosion Rate 2	Average	Surface condition
18	9.073	8.470	8.772	Product 18 averaged 8.77MPY across the two test specimens with good surface condition with odd markings on the backs of the coupons. No pitting observed though
19	8.516	9.073	8.795	Product 19 averaged 8.79MPY across the two test specimens surface condition is reasonable but is the worst of this series of three tests with both coupons exhibiting a dark boarder on the sides and bottom on both the front and back of the coupons.
20	9.328	9.699	9.514	Product 20 averaged 9.51MPY across the two test specimens with good surface condition
21	12.433	12.623	12.528	Product 21 averaged 12.53MPY across the two test specimens with good surface condition
24	34.227	27.683	30.955	Product 24 averaged 30.96MPY across the two test specimens with substantial siderite present on the coupon surfaces
16	6.080	4.177	5.129	Product 16 averaged 5.13MPY across the two test specimens with reasonable surface condition with some etching on the sides and bottom of the test coupons
25	16.684	2.901	9.793	Product 25 averaged 9.79MPY across the two test specimens with poor surface condition and siderite present on the surfaces hence the difference in corrosion rates between the two coupons.
22	7.936	8.609	8.273	Product 22 averaged 8.27MPY across the two test specimens with Excellent surface condition
17	7.240	7.449	7.345	Product 17 averaged 7.34MPY across the two test specimens with poor surface condition and siderite still present on the surfaces
26	9.491	9.932	9.712	Product 26 averaged 9.71MPY across the two test specimens with good surface conditions with some emulsion markings on the surface. However, a large pit was present on the back of one of the coupons.
23	9.839	8.261	9.050	Product 23 averaged 9.05MPY across the two test specimens with excellent surface condition
27	7.333	0.696	4.015	Product 27 averaged 4.01MPY across the two test specimens with heavy siderite deposition on the surfaces
28	-1.439	2.785	0.673	Product 28 averaged 0.67MPY across the two test specimens with heavy siderite deposition on the surfaces and some pitting on the bottom of 2818
29	-1.114	-2.112	-1.613	Product 29 averaged -1.61MPY across the two test specimens with heavy siderite deposition on the surfaces with a large pit on 2820

Kettle-test results

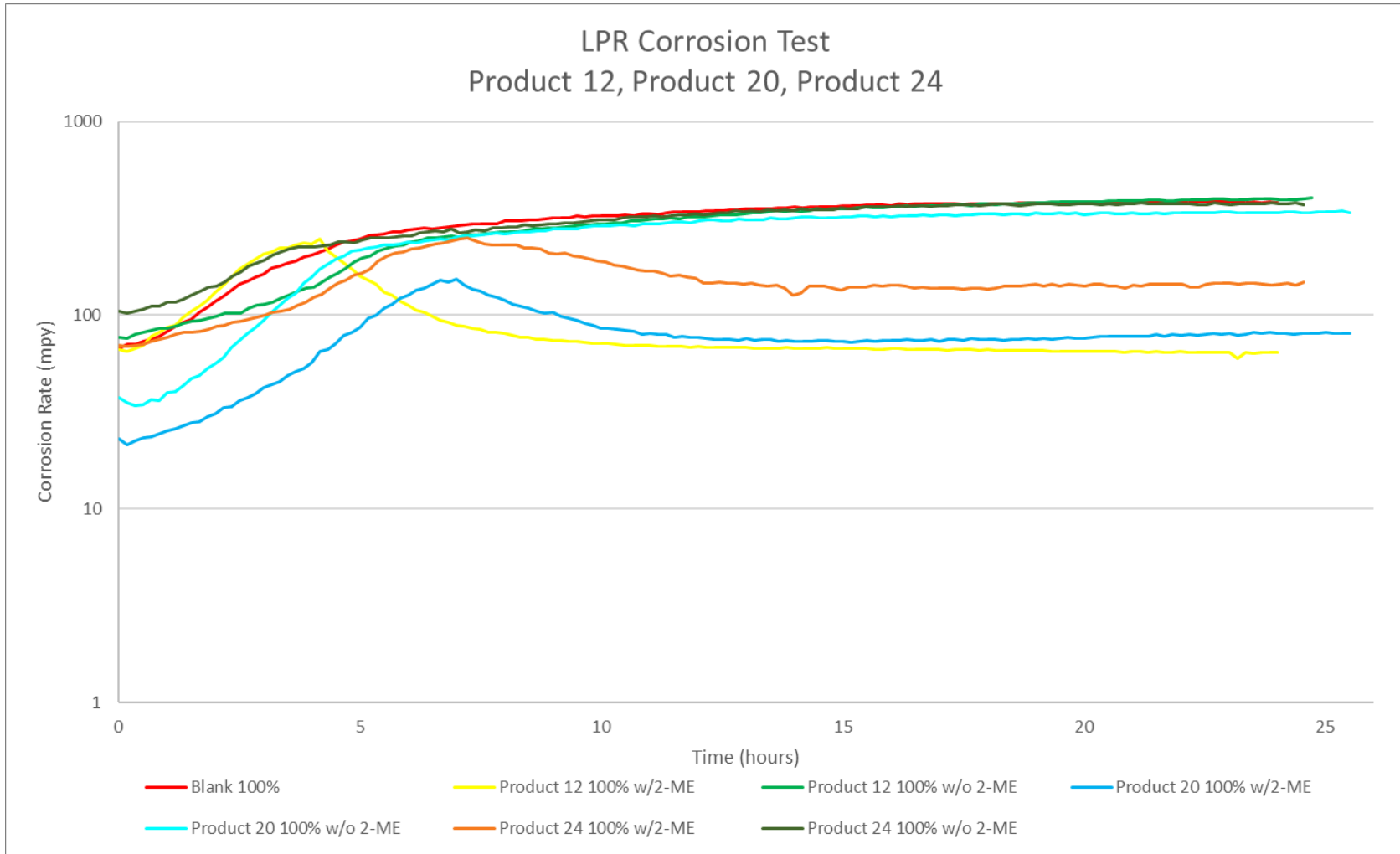


Figure 65: LPR graph including results from cells with 100% brine

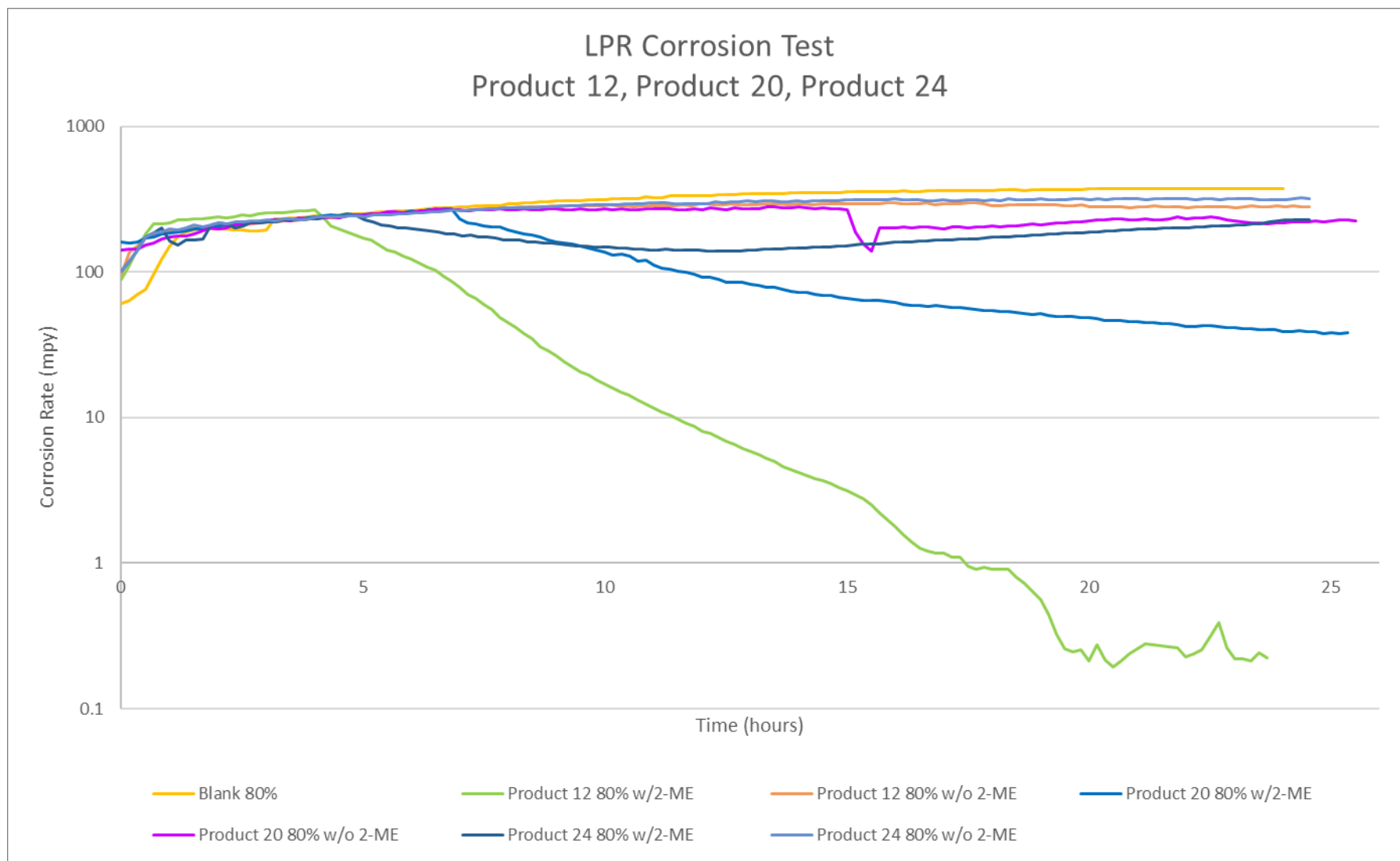


Figure 66: LPR graph including results from cells with 80% brine, 20% kerosene

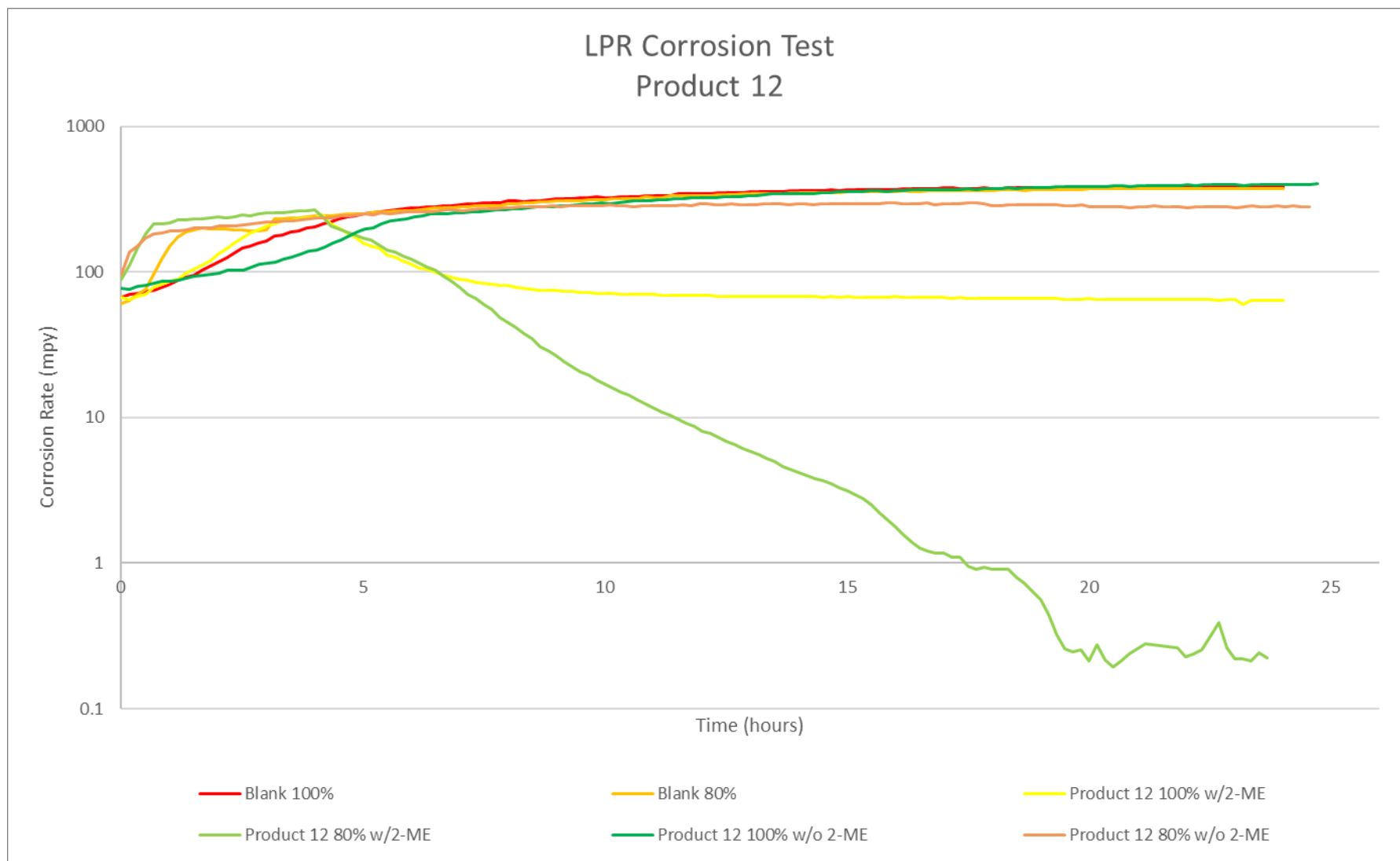


Figure 67: LPR graph including results of Product 12

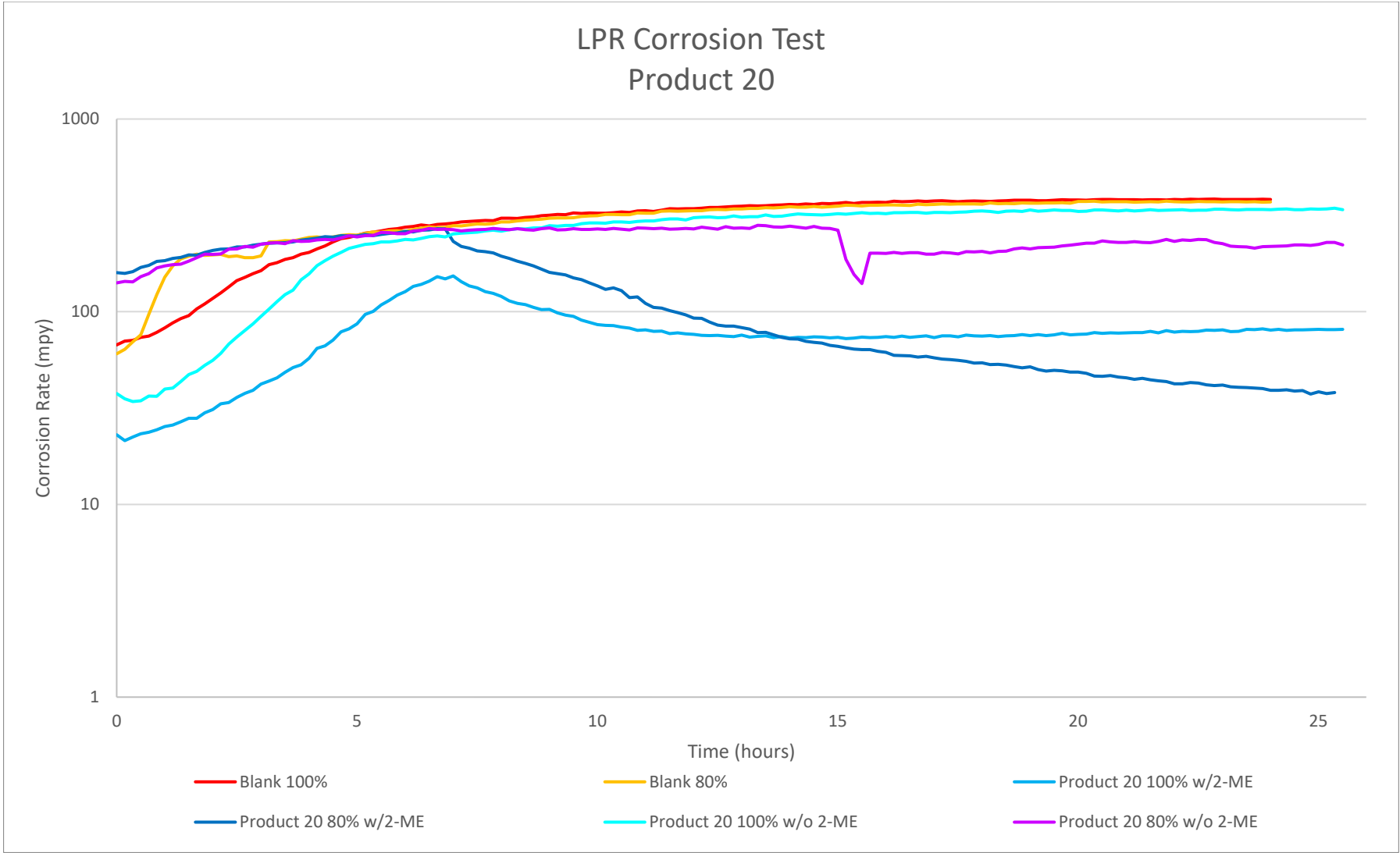


Figure 68: LPR graph including results of Product 20

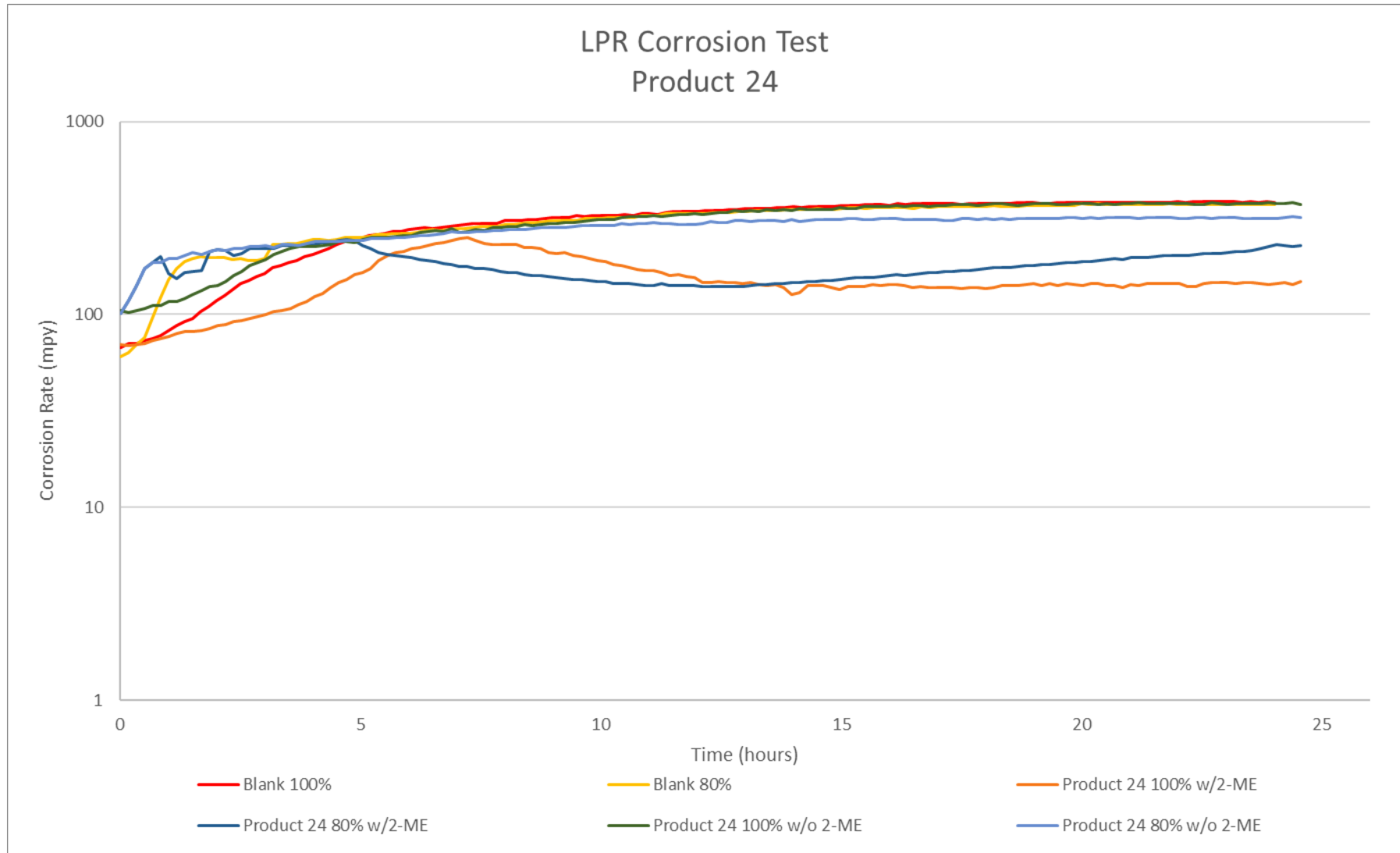


Figure 69: LPR graph including results of Product 24

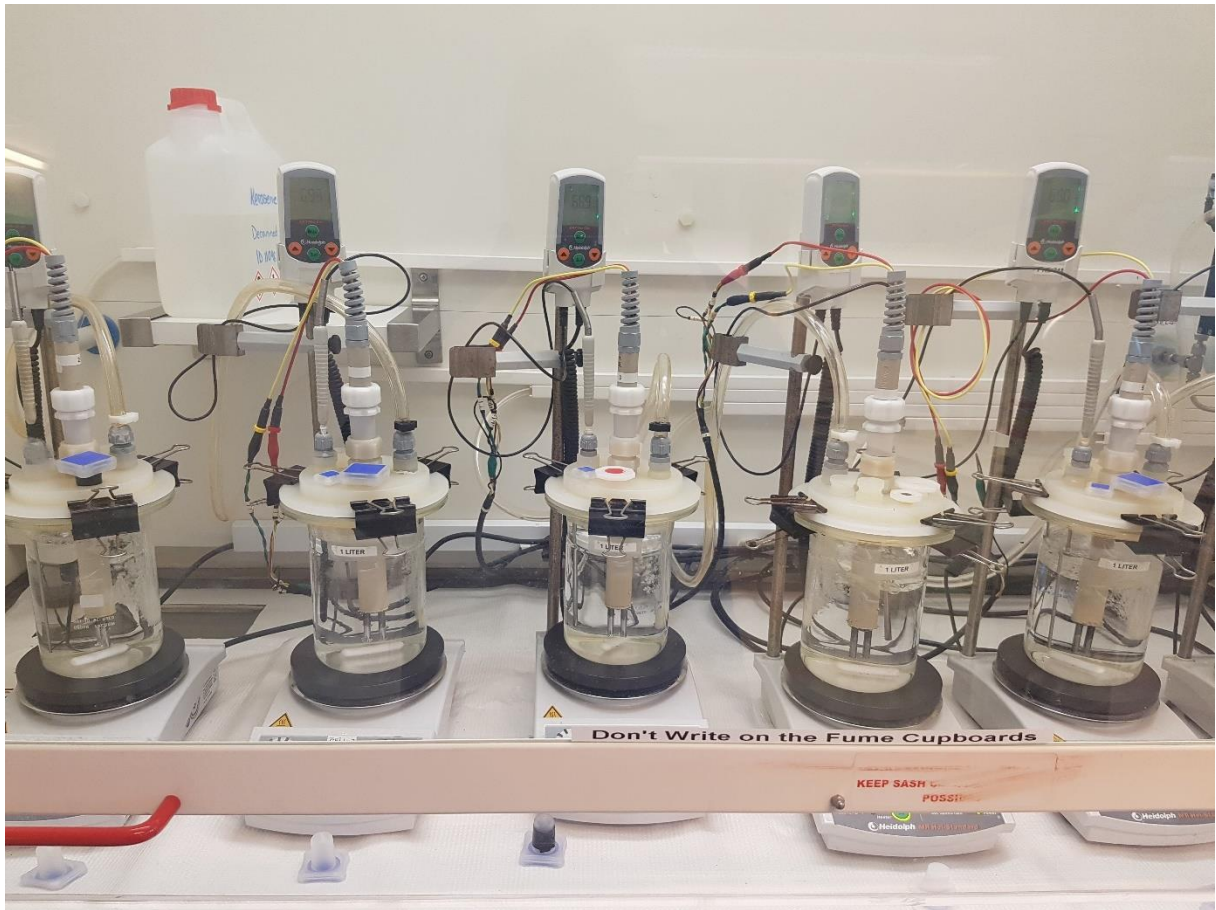


Figure 70: Full Kettle-test set-up with 5 test-cells



Figure 71: Product 24 in 80% brine w/2-ME

Infrared (IR) Spectroscopy

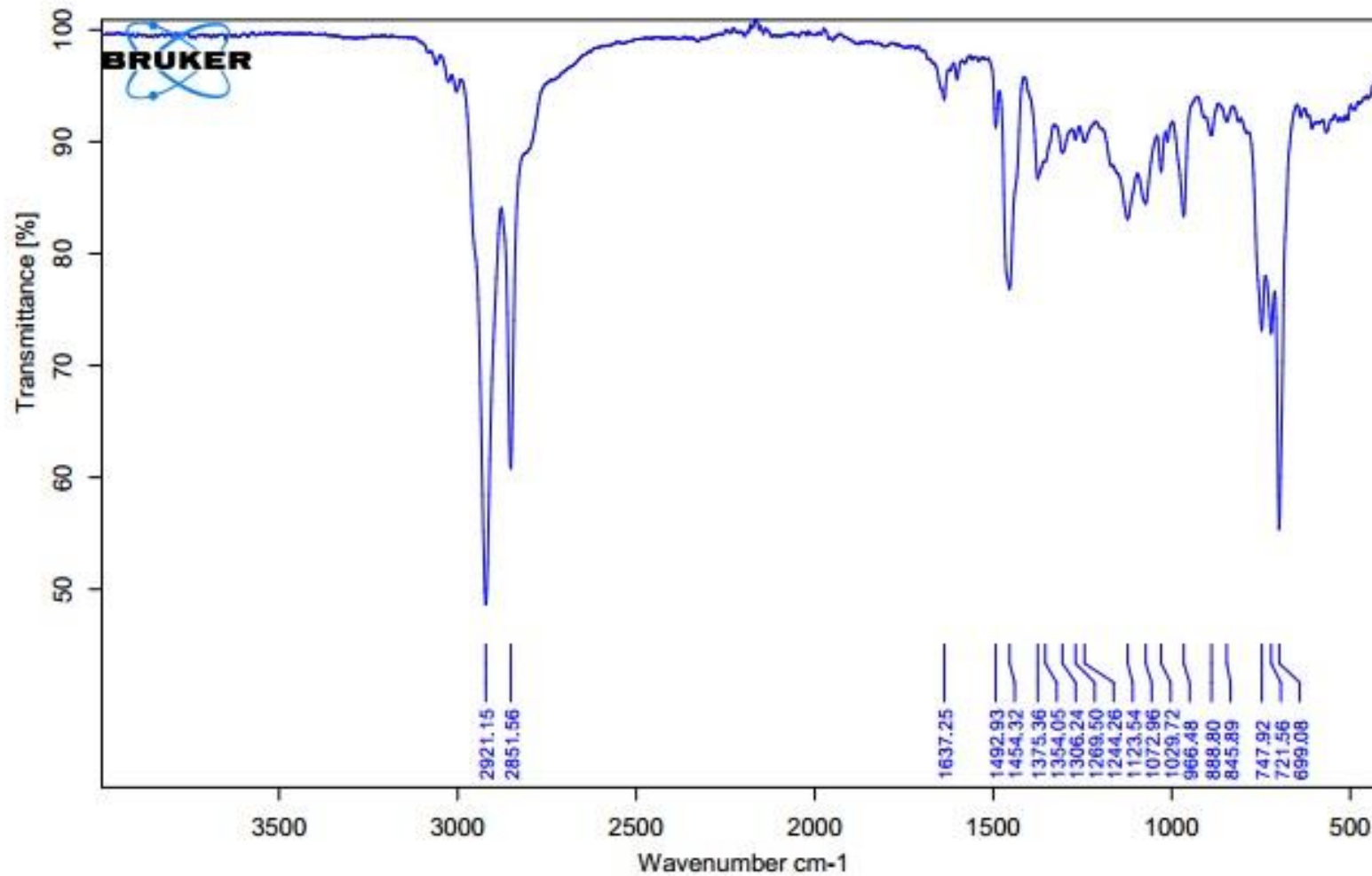


Figure 72: IR of product 12

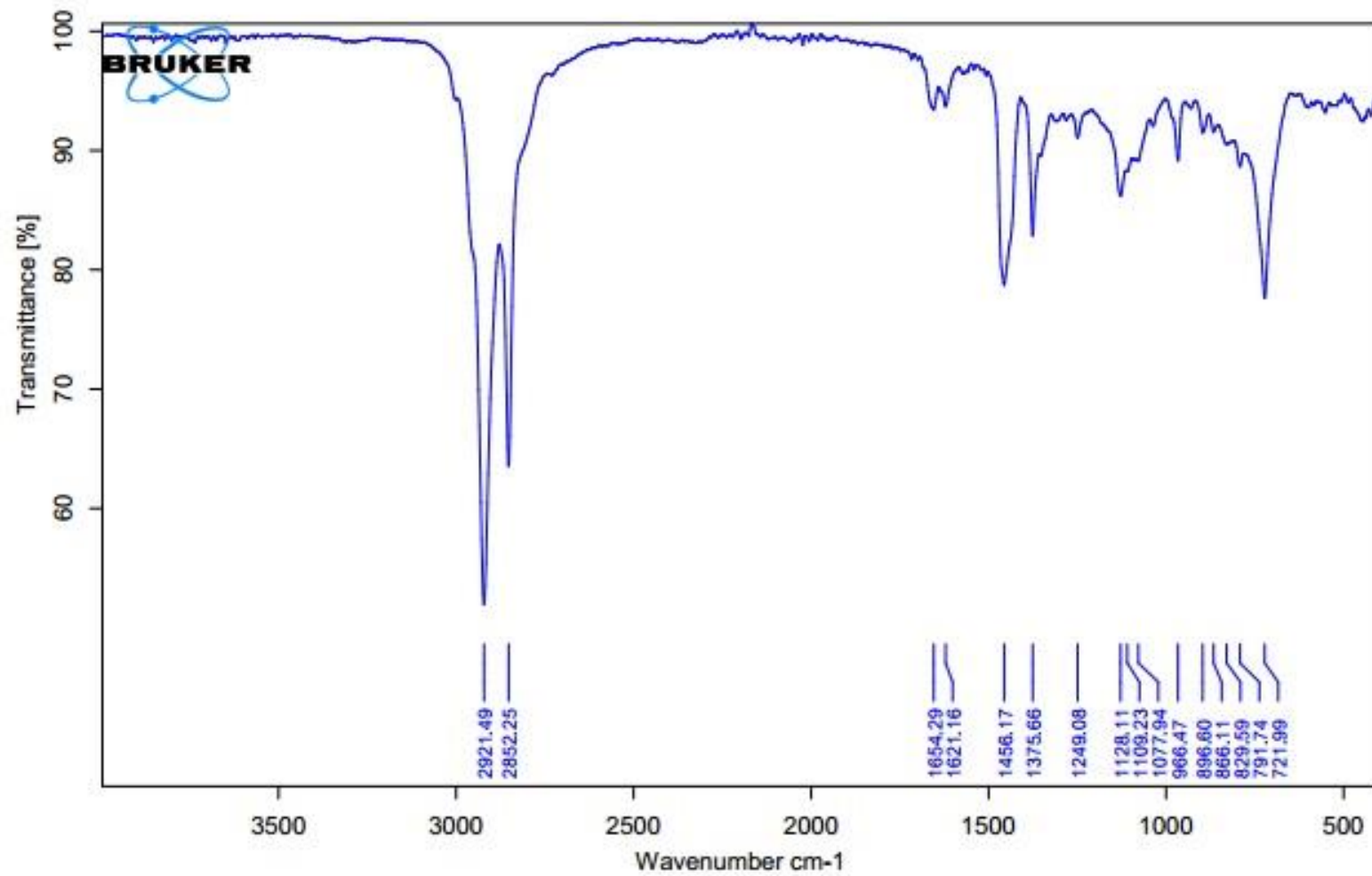


Figure 73: IR of Product 20

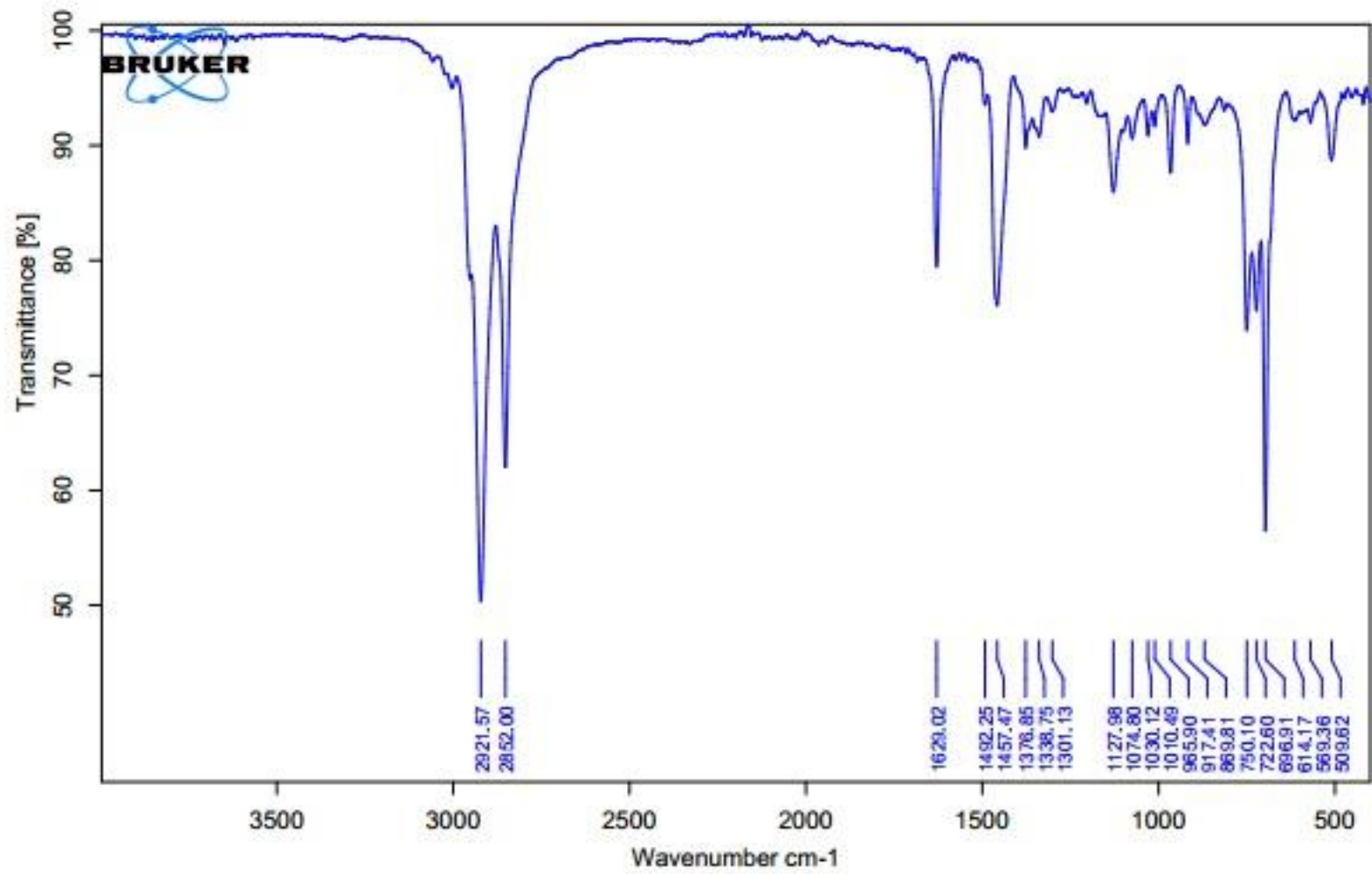


Figure 74: IR of Product 24

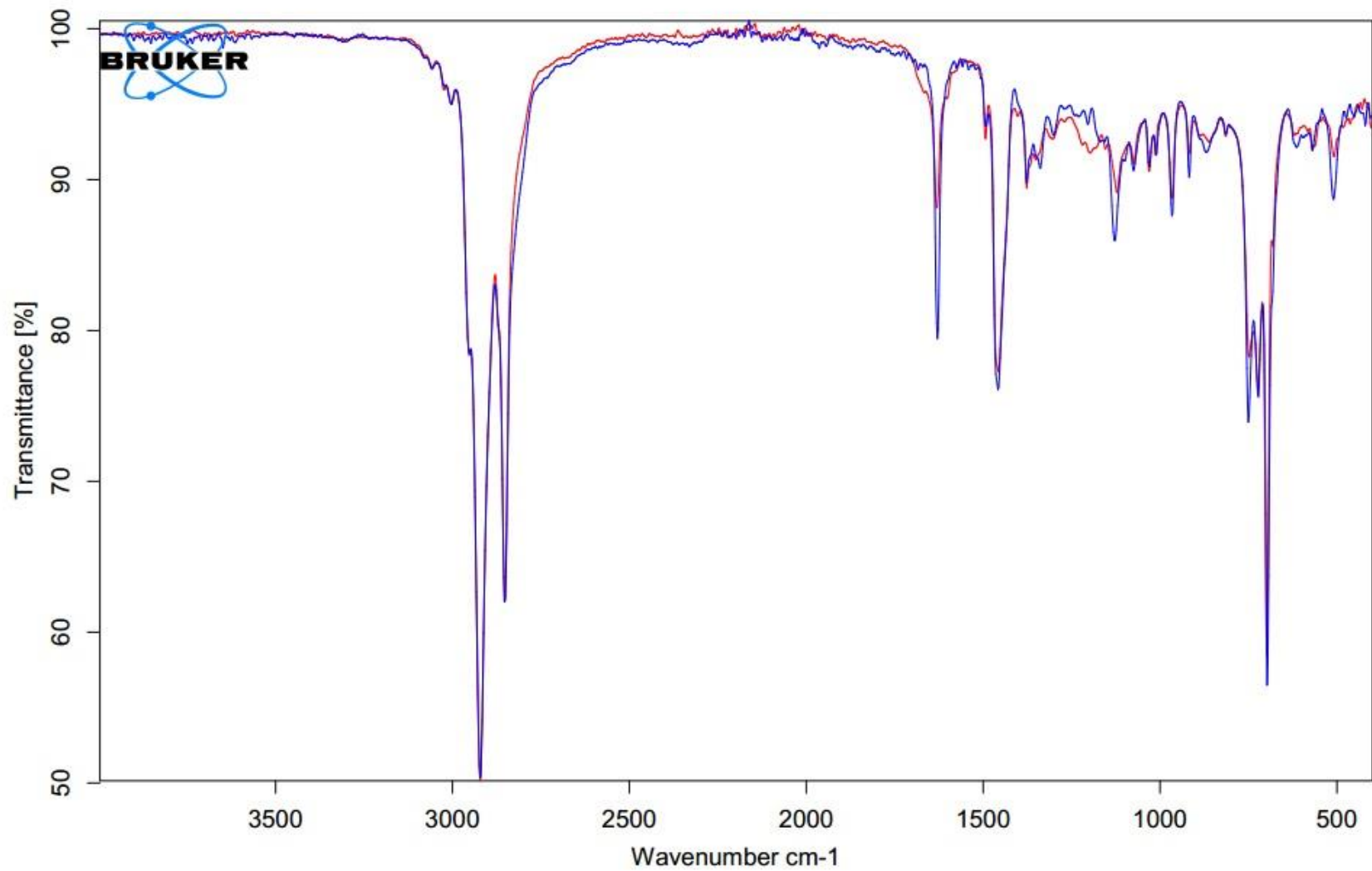


Figure 75: IR of Product 24 and Product 24 reheated where the blue spectra is Product 24 and the red spectra is product 24 reheated.

NMR

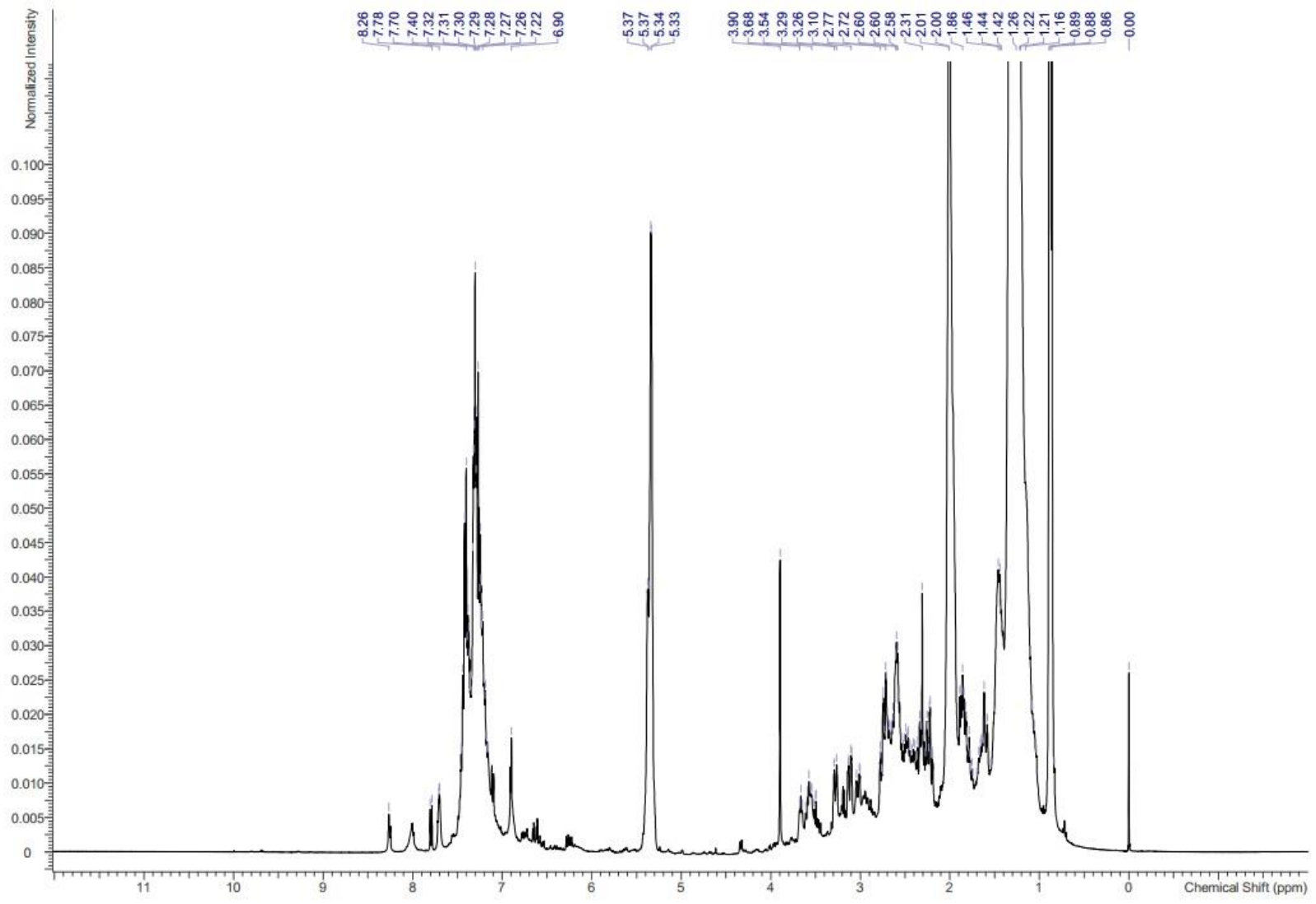


Figure 76: ¹H-NMR of Product 12

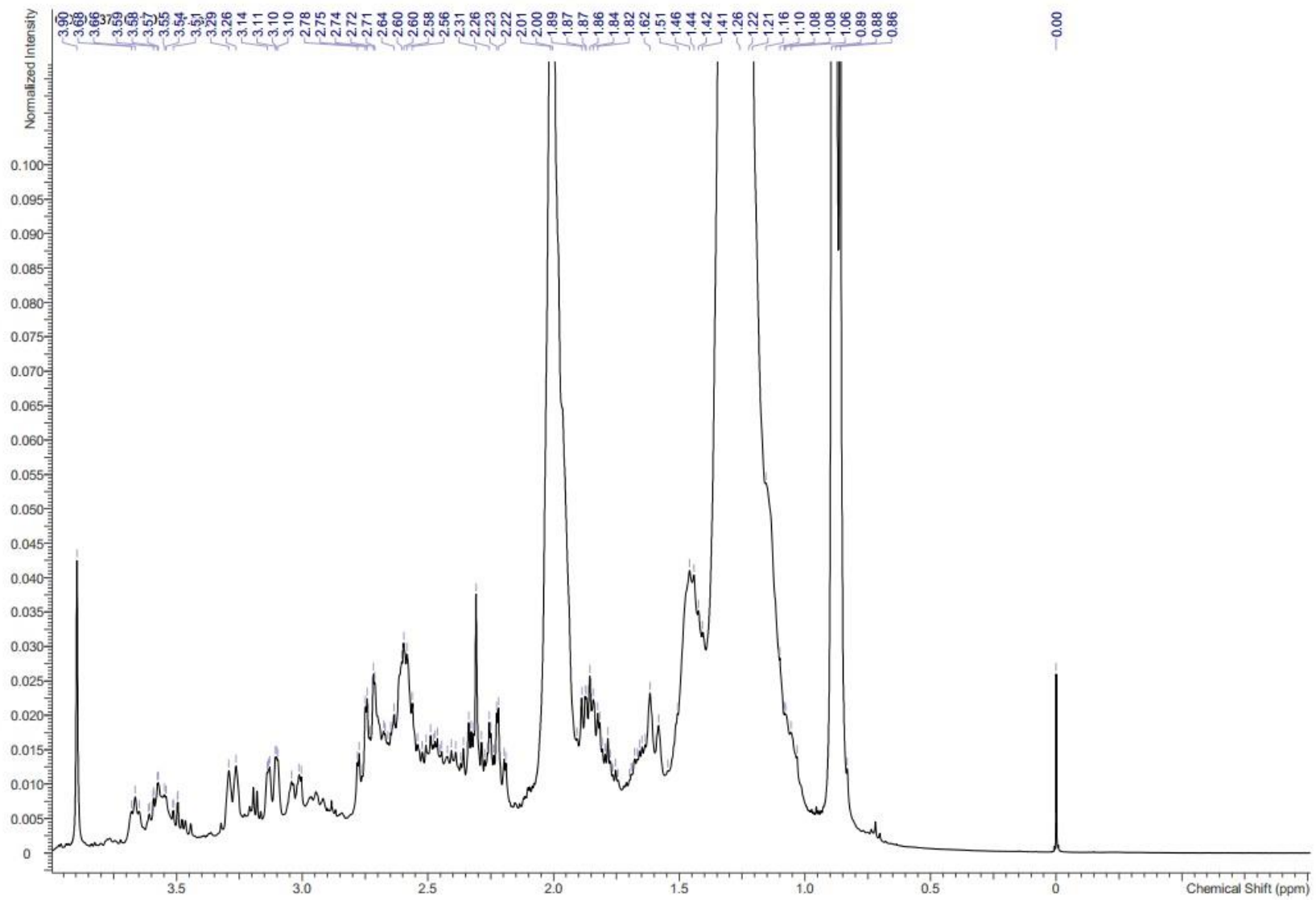


Figure 77: ¹H-NMR of Product 12

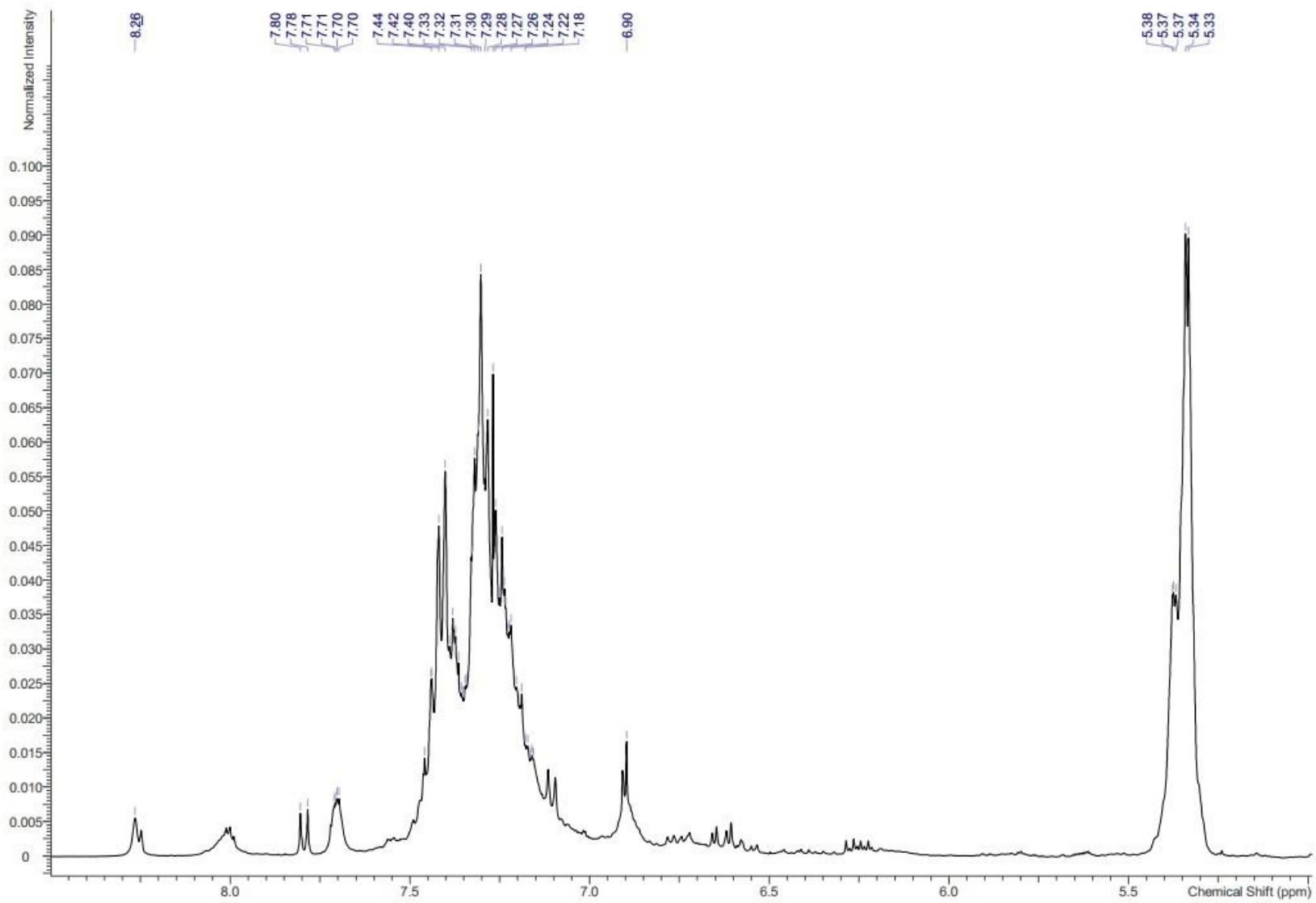


Figure 78: ¹H-NMR of Product 12

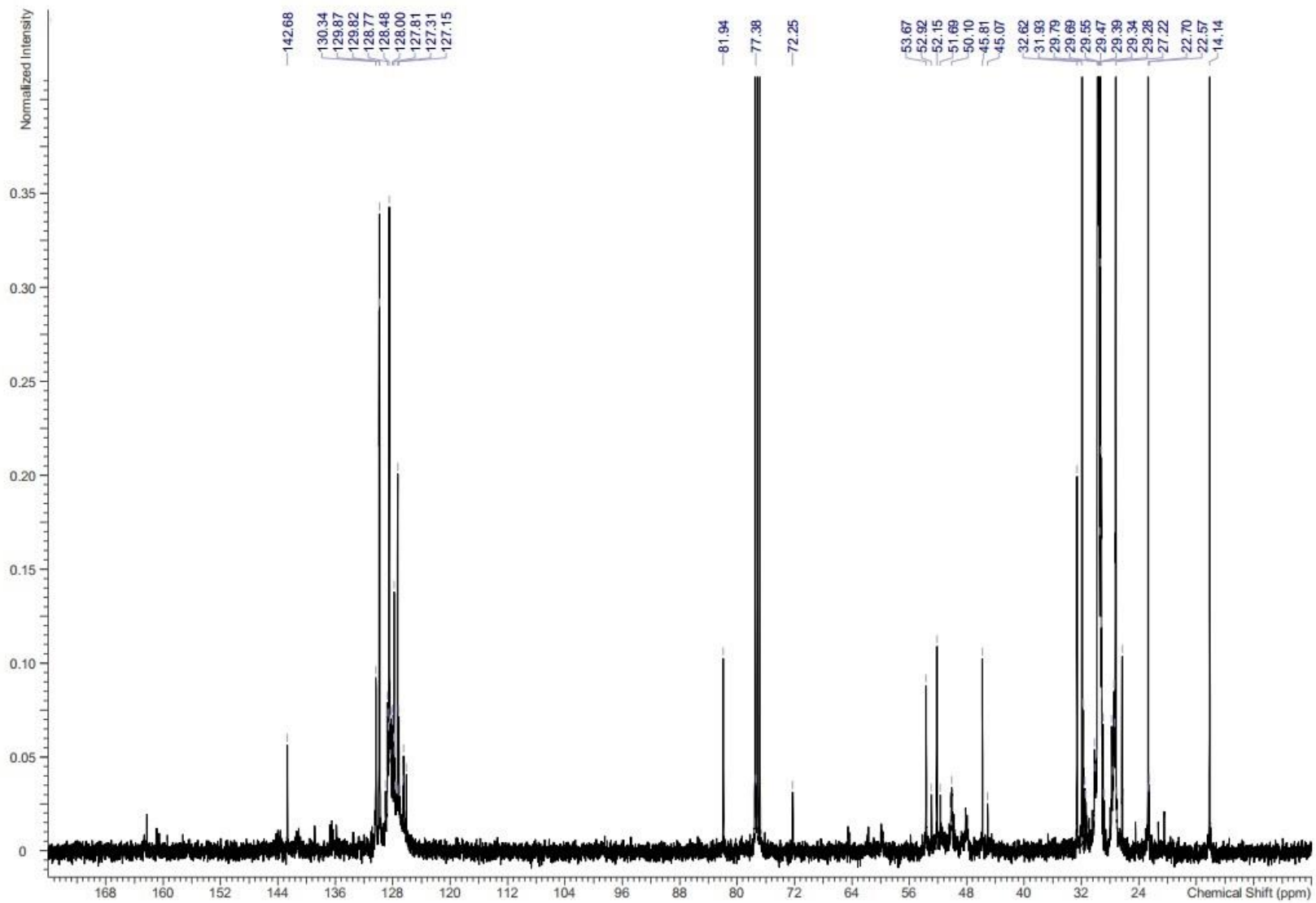


Figure 79: ^{13}C -NMR of Product 12

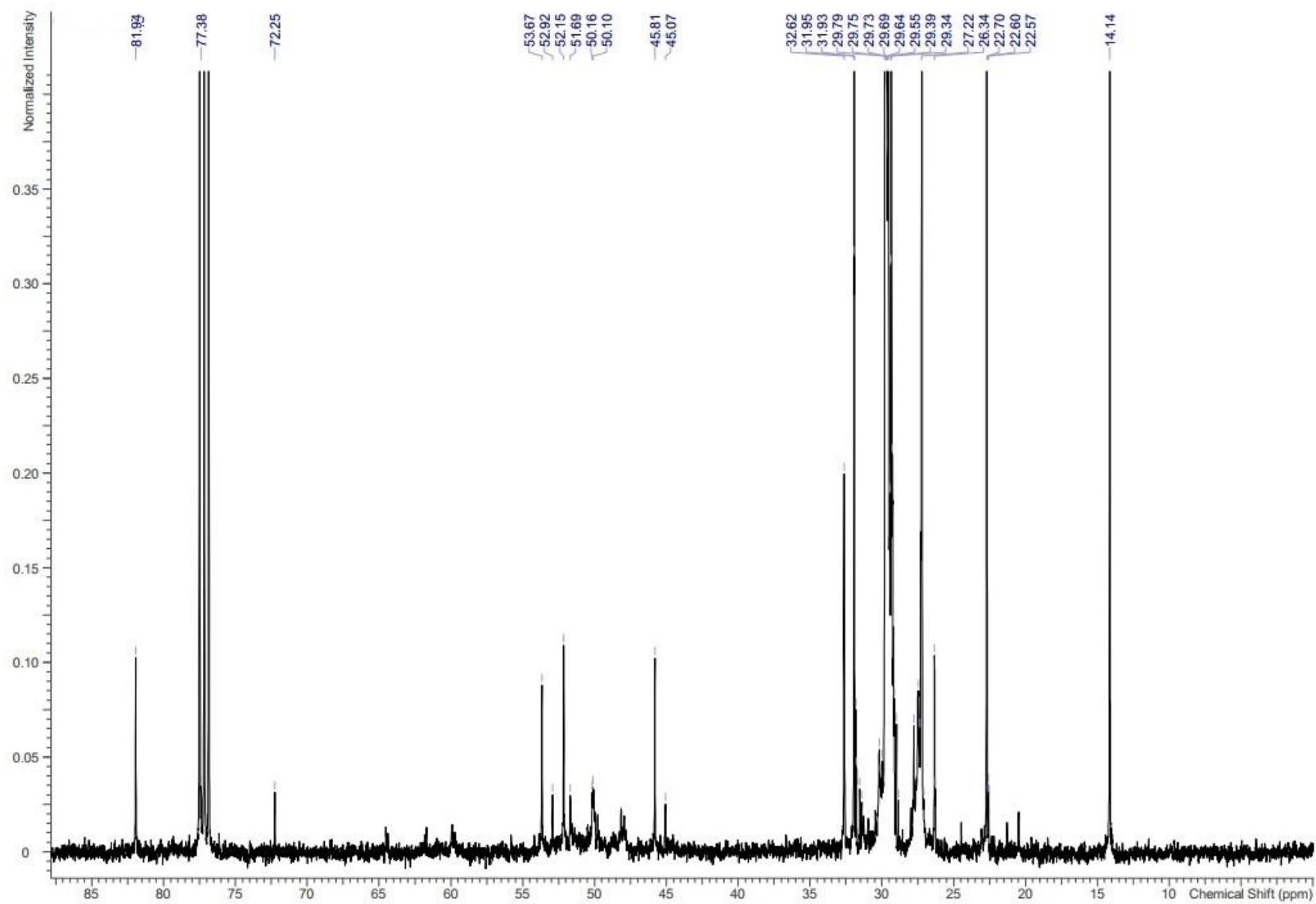


Figure 80: ^{13}C -NMR of Product 12

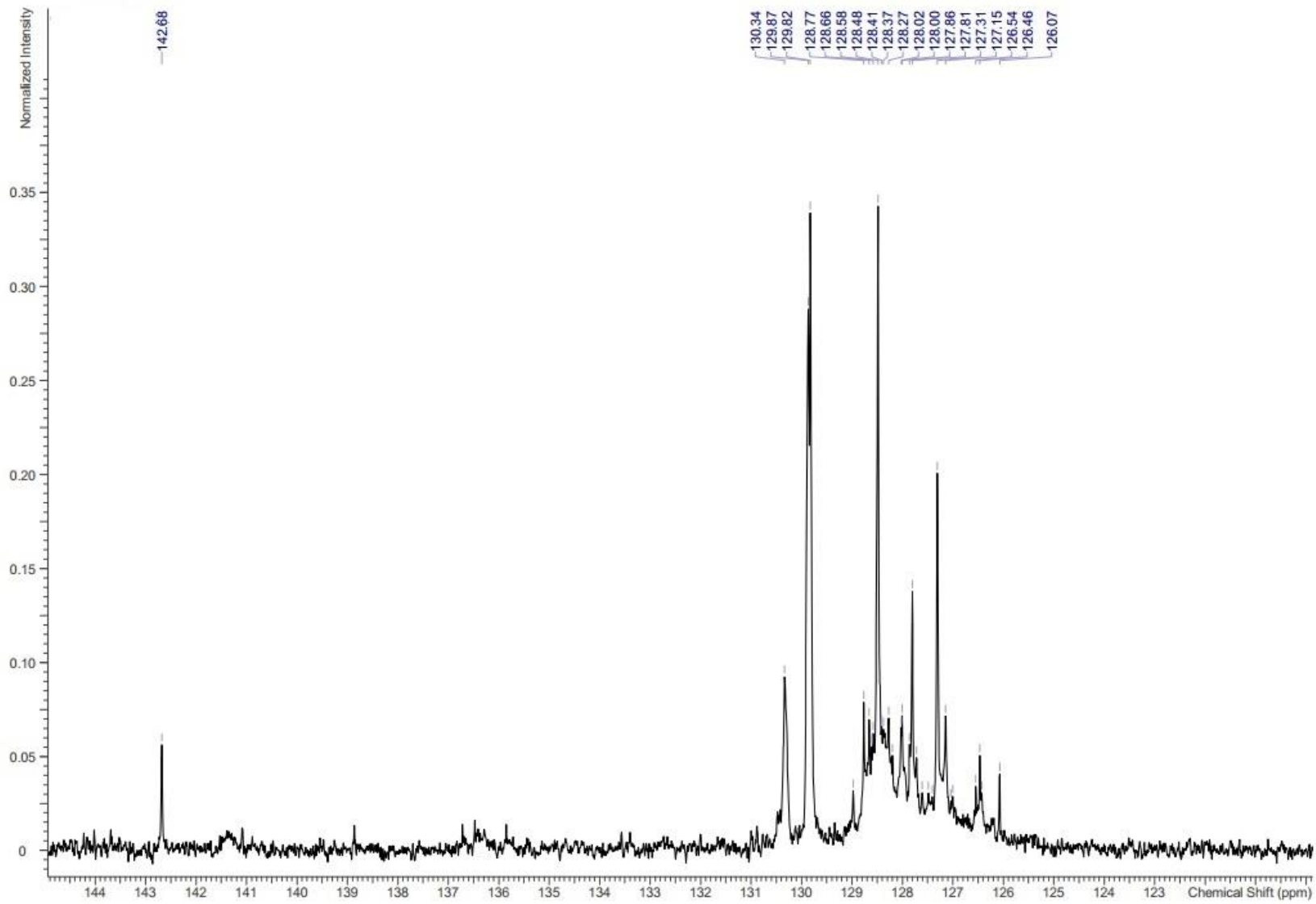


Figure 81: ^{13}C -NMR of Product 12

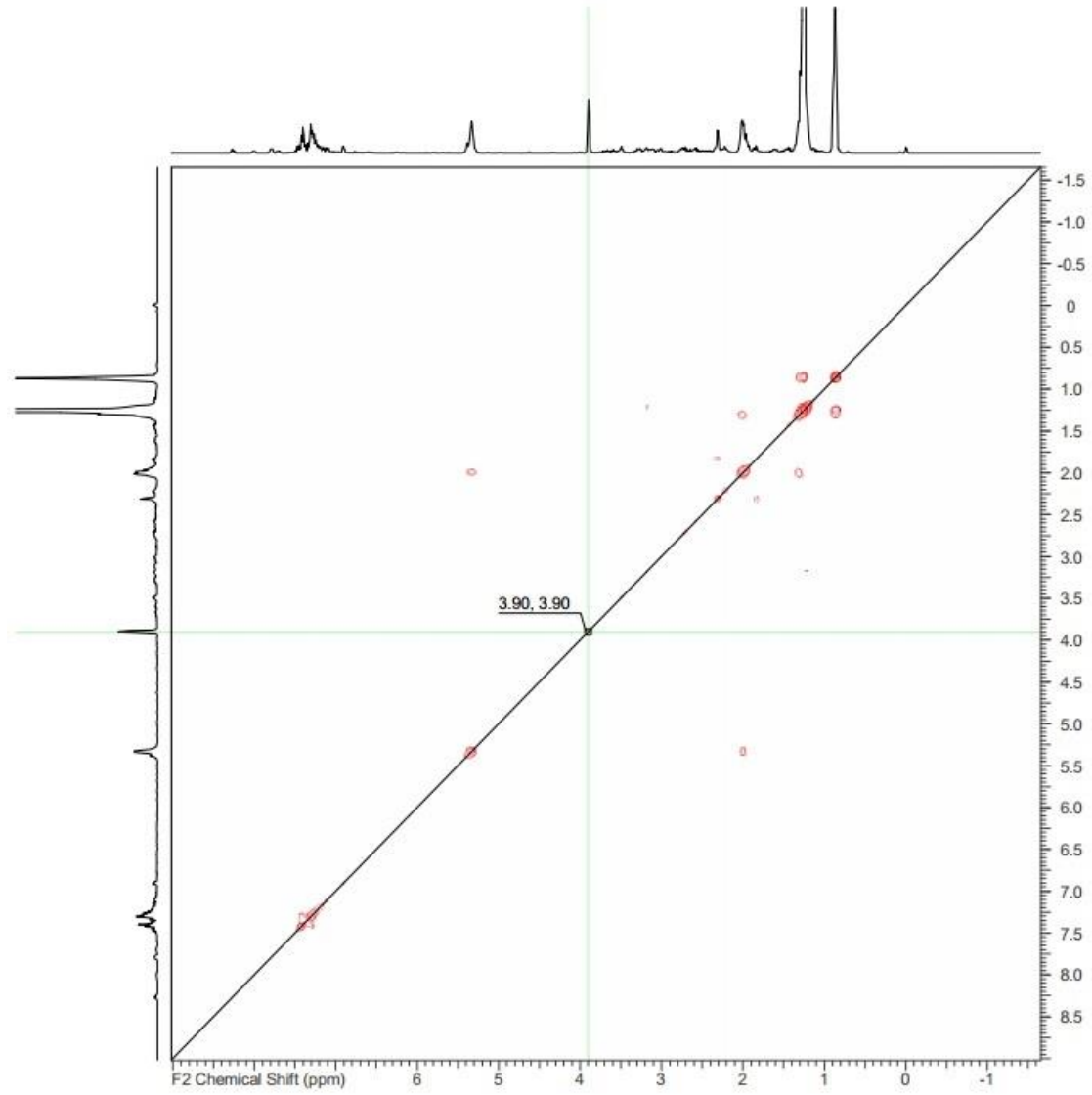


Figure 82: 2D-NMR COSY of Product 12

Y

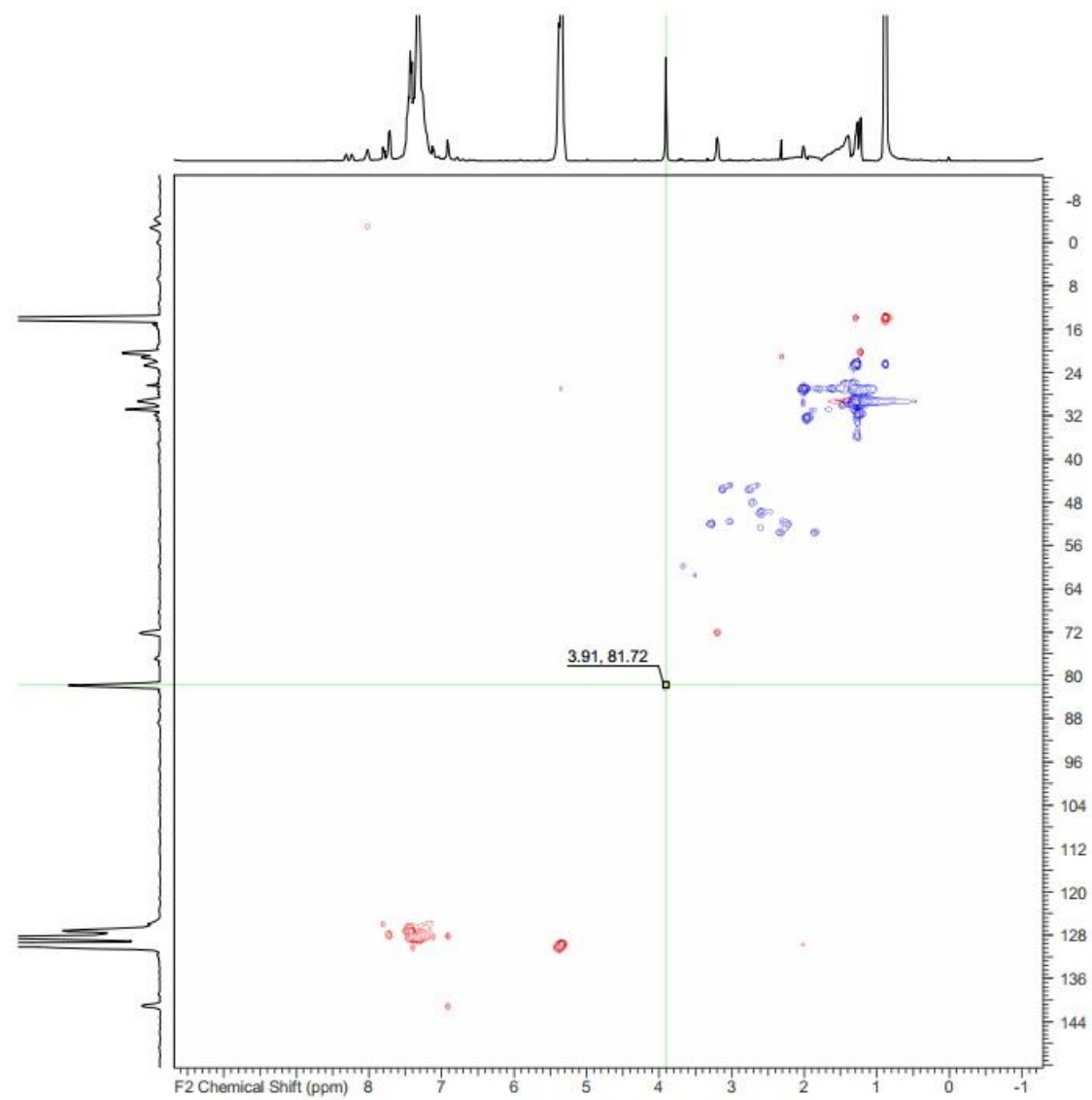


Figure 83: 2D-NMR HSQC of Product 12

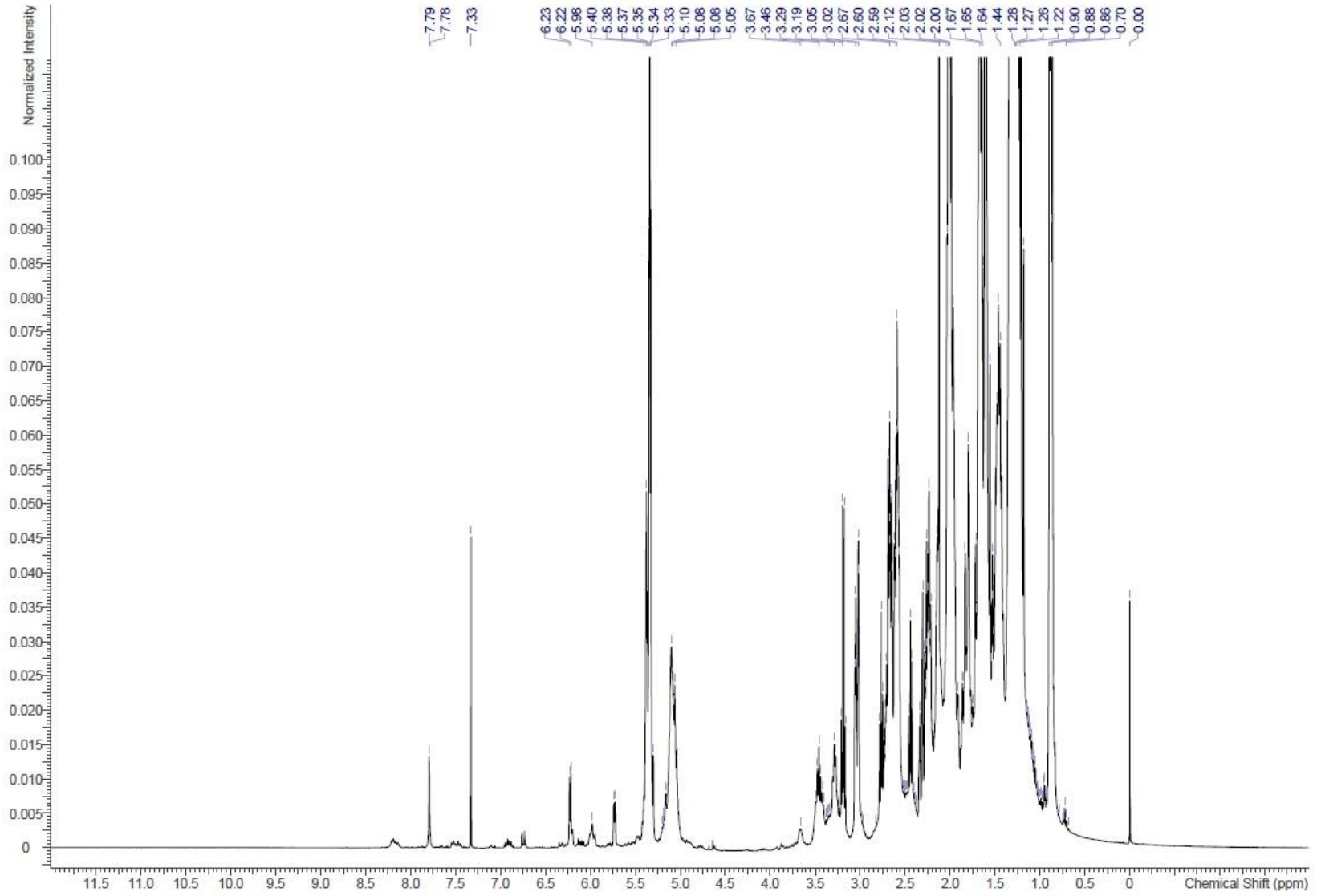


Figure 84: ¹H-NMR of Product 20

Æ

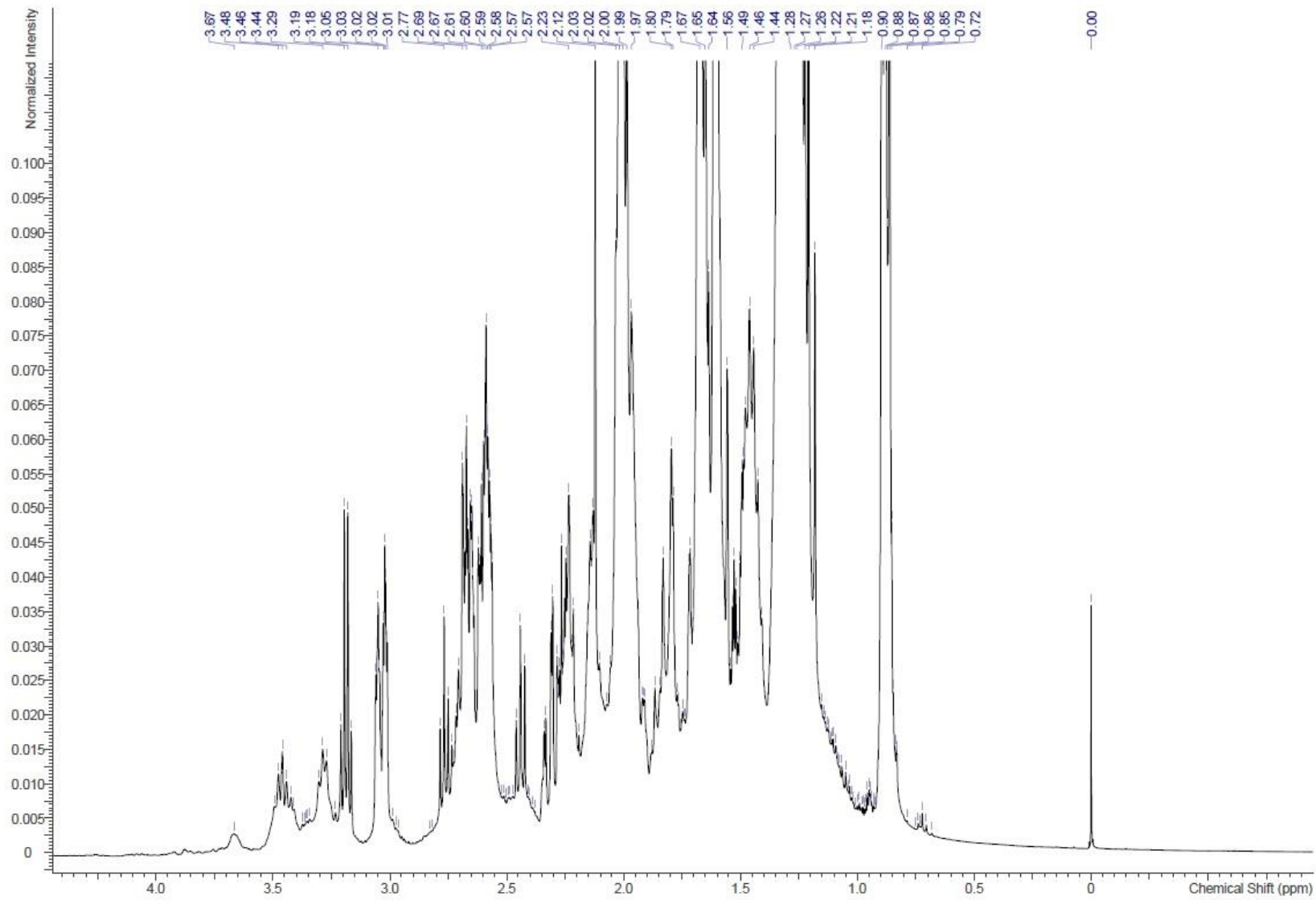


Figure 85: ¹H-NMR of Product 20

∅

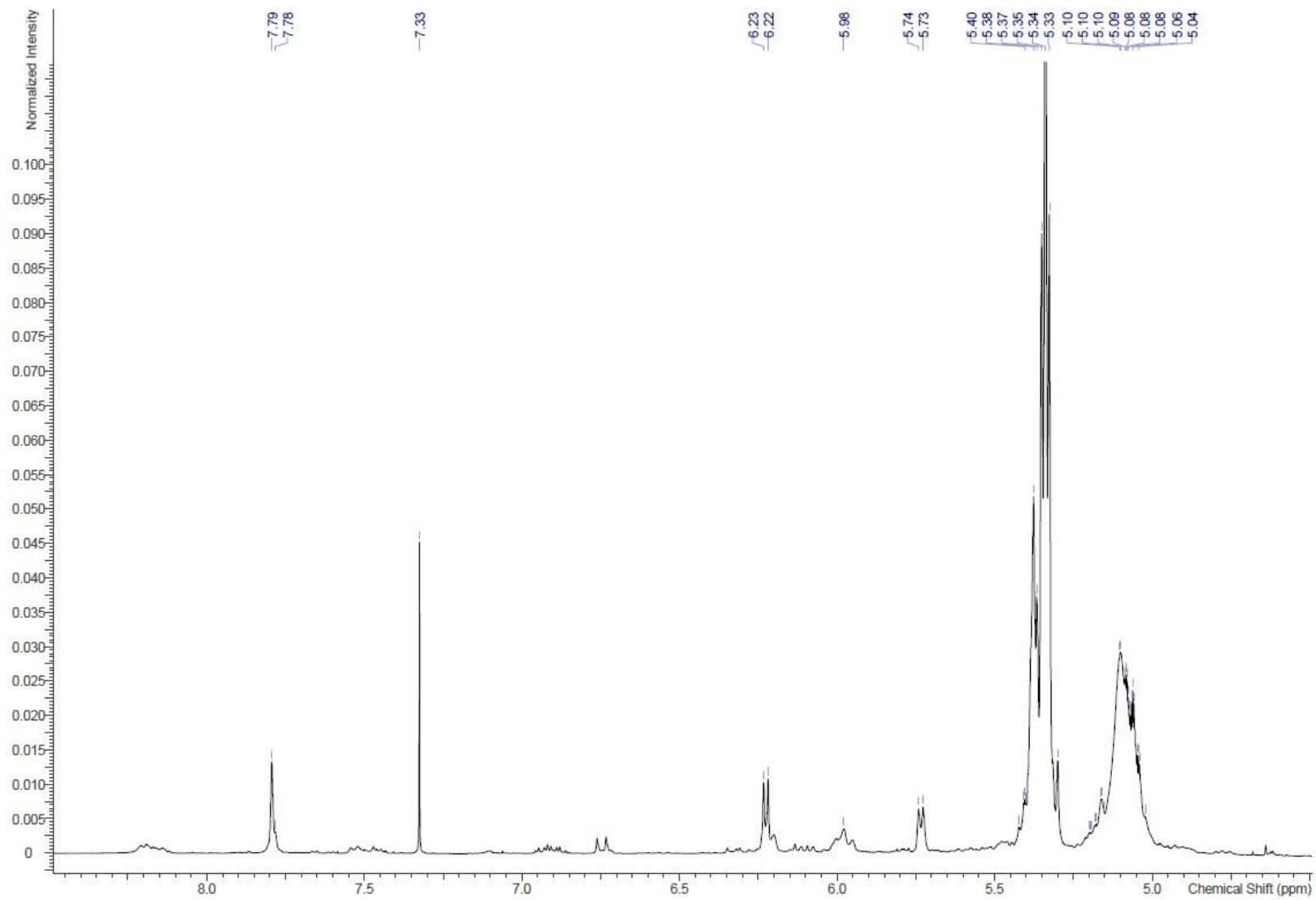


Figure 86: $^1\text{H-NMR}$ of Product 20

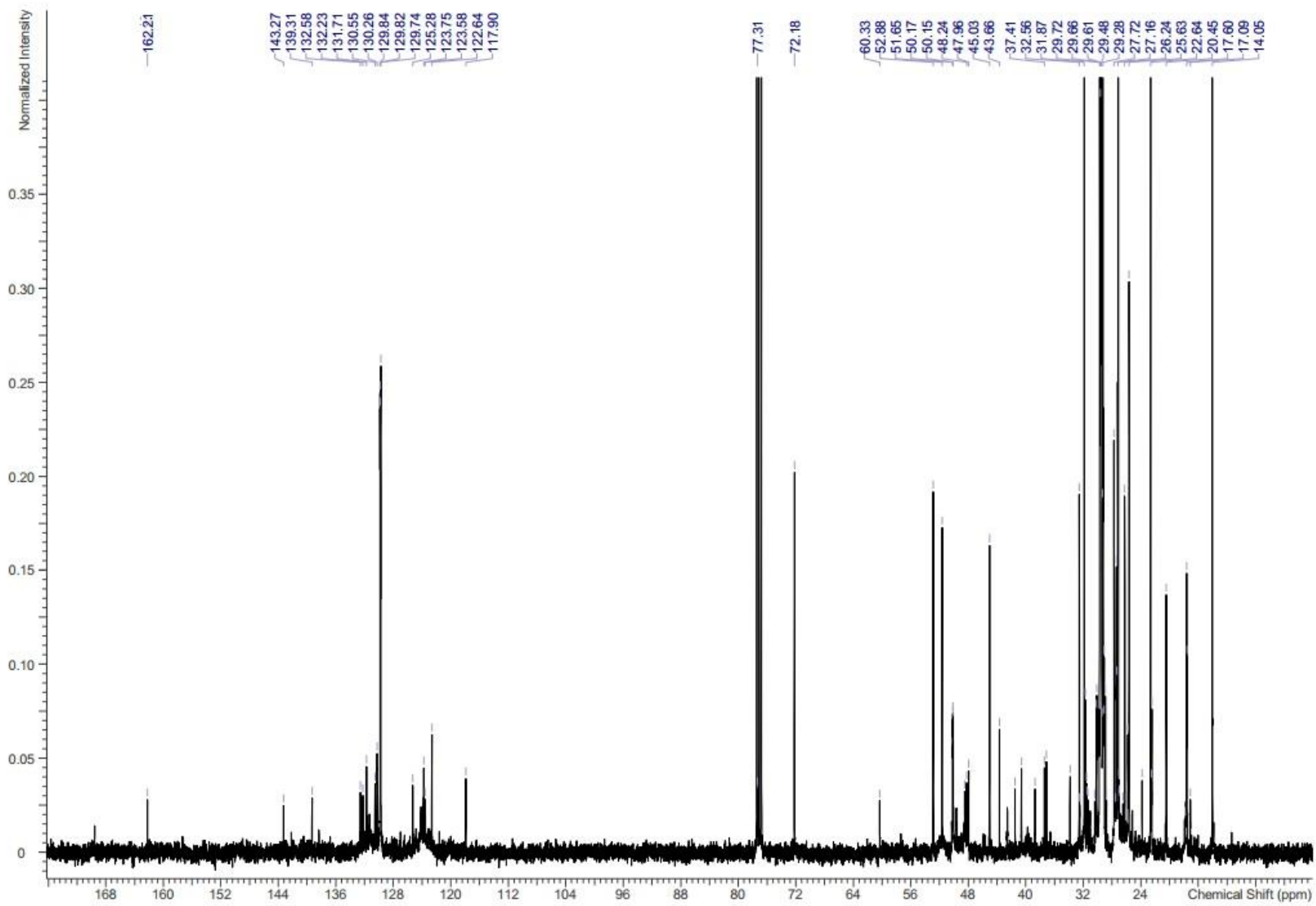


Figure 87: ^{13}C -NMR of Product 20

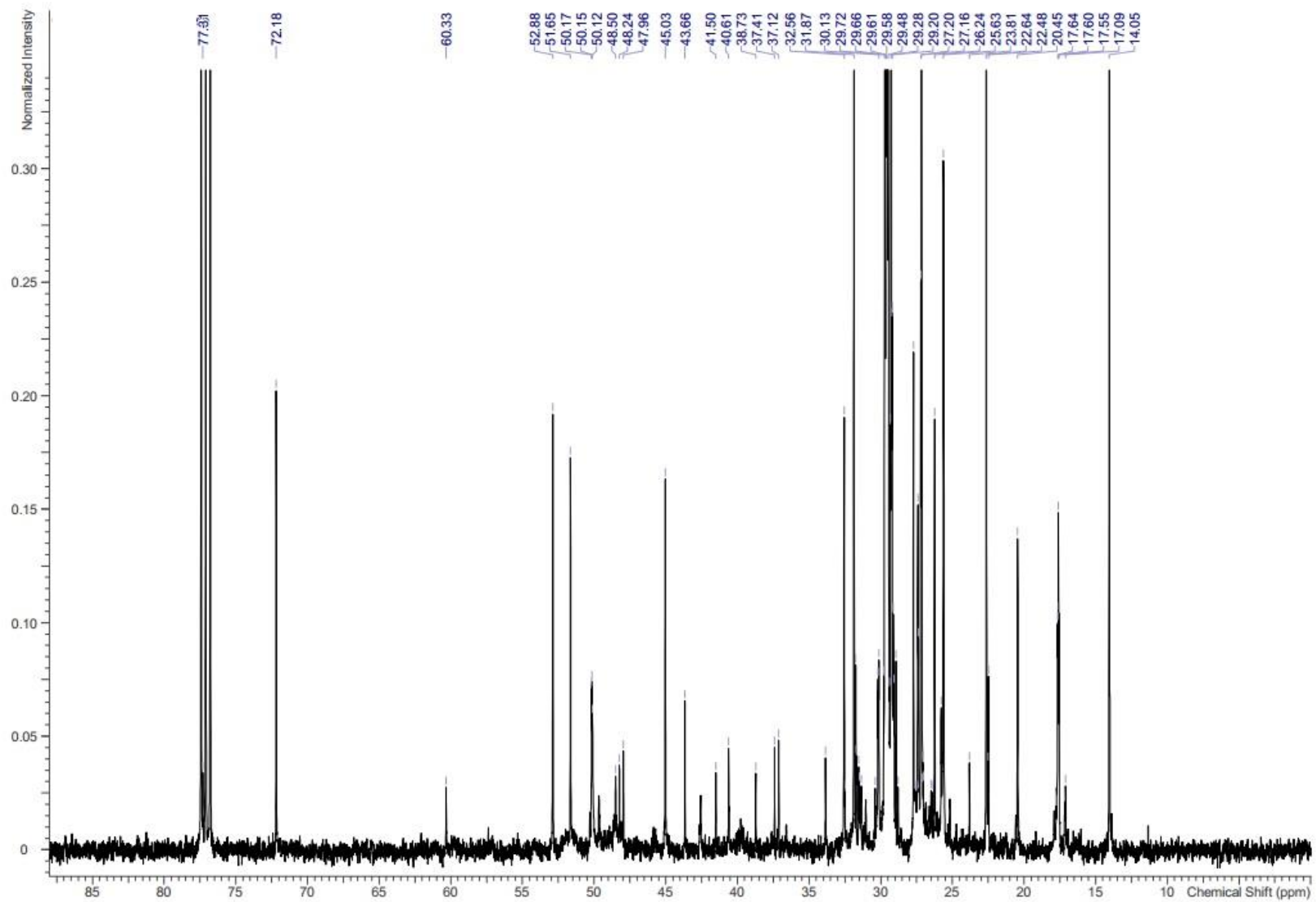


Figure 88: ^{13}C -NMR of Product 20

BB

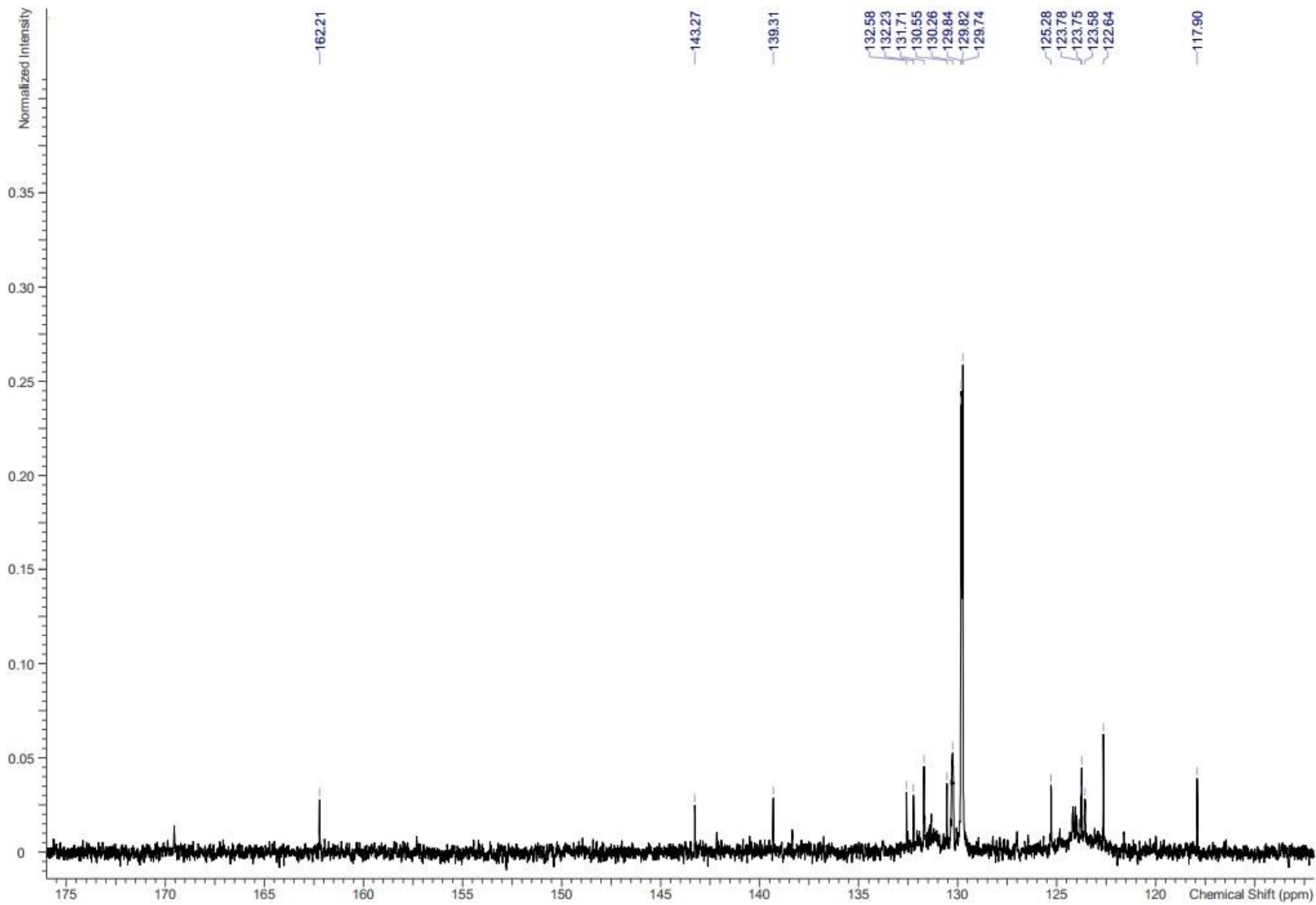


Figure 89: ¹³C-NMR of Product 20

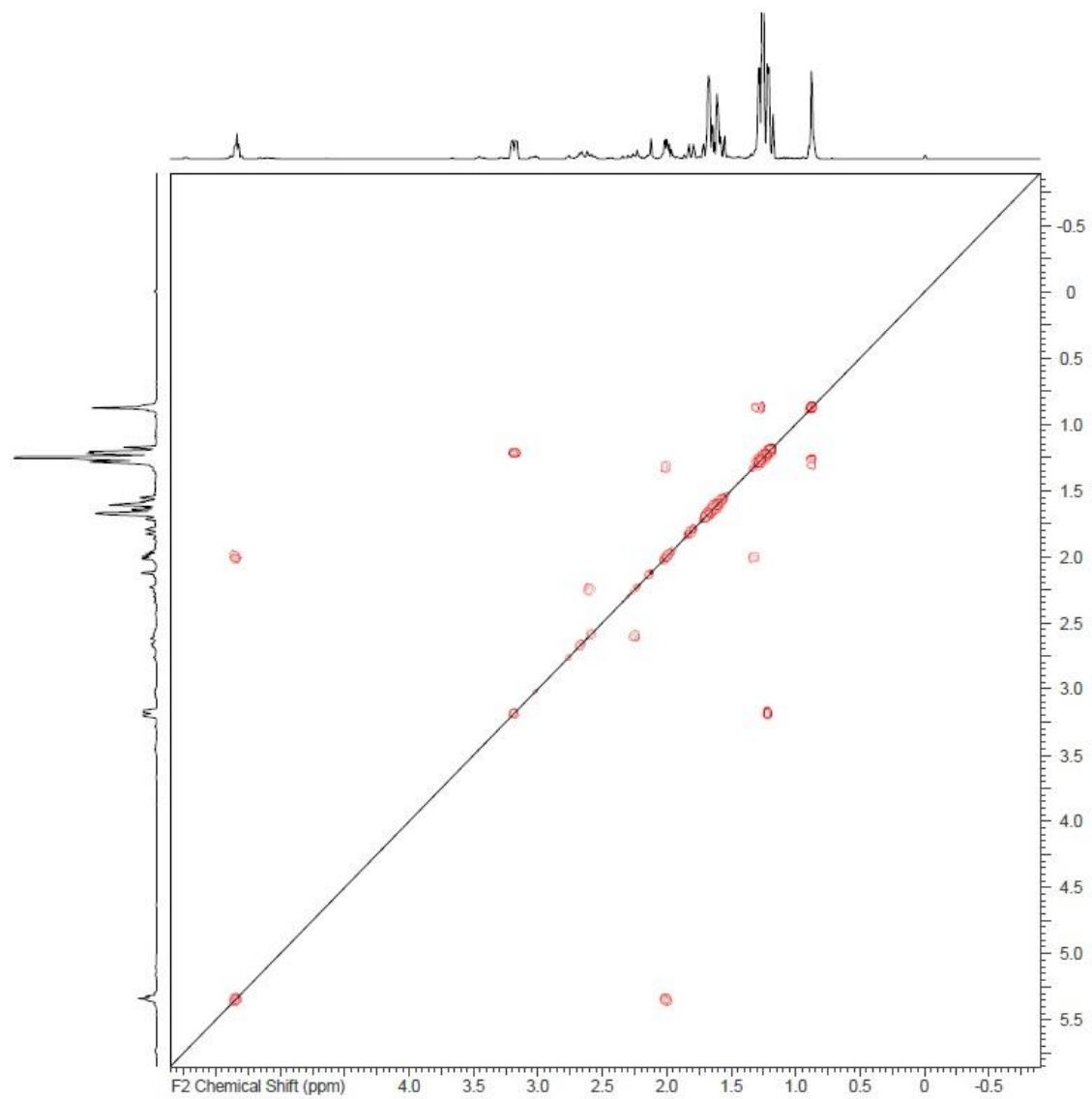


Figure 90: 2D-NMR COSY of Product 20

DD

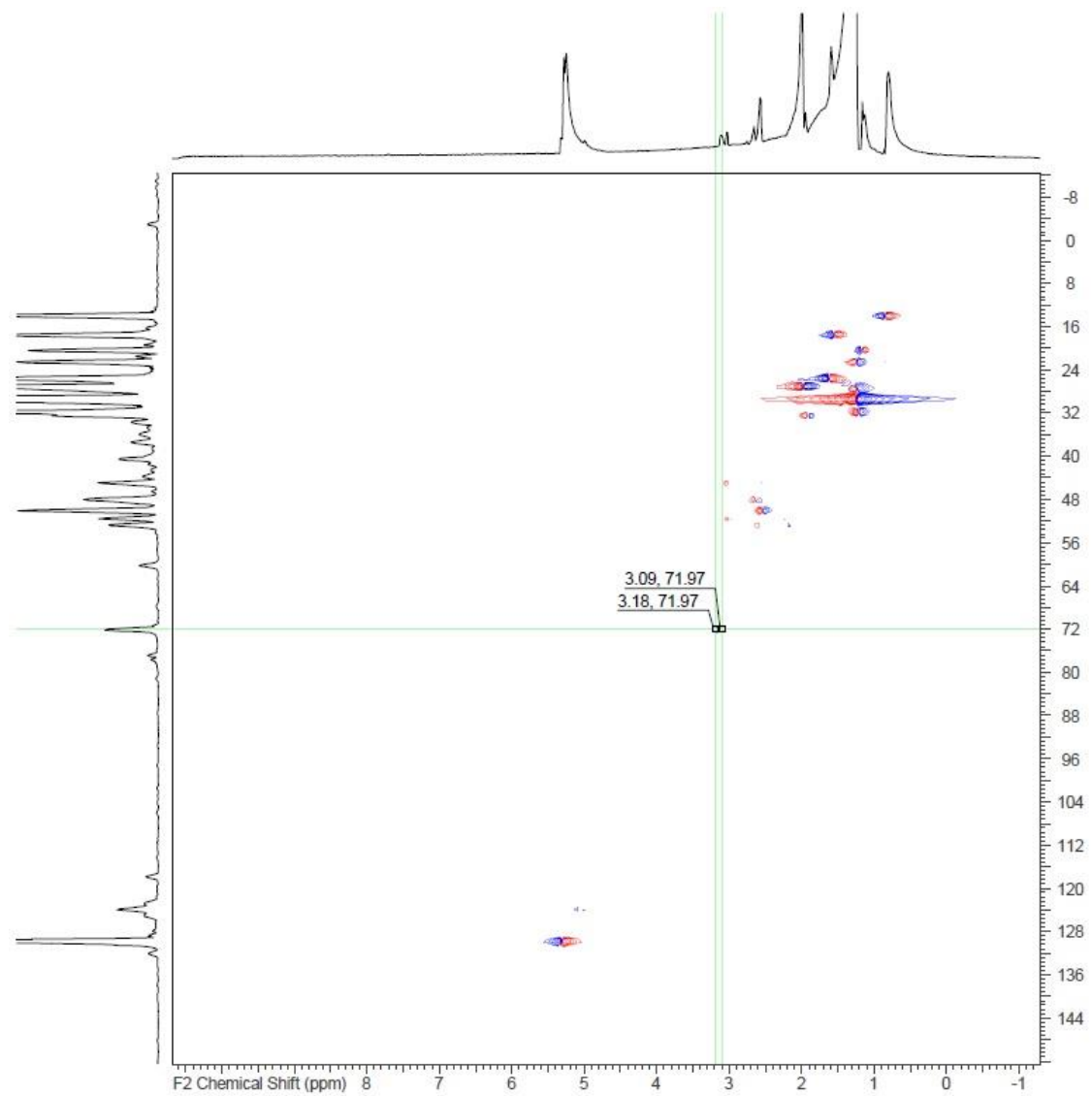


Figure 91: 2D-NMR HSQC of Product 20

EE

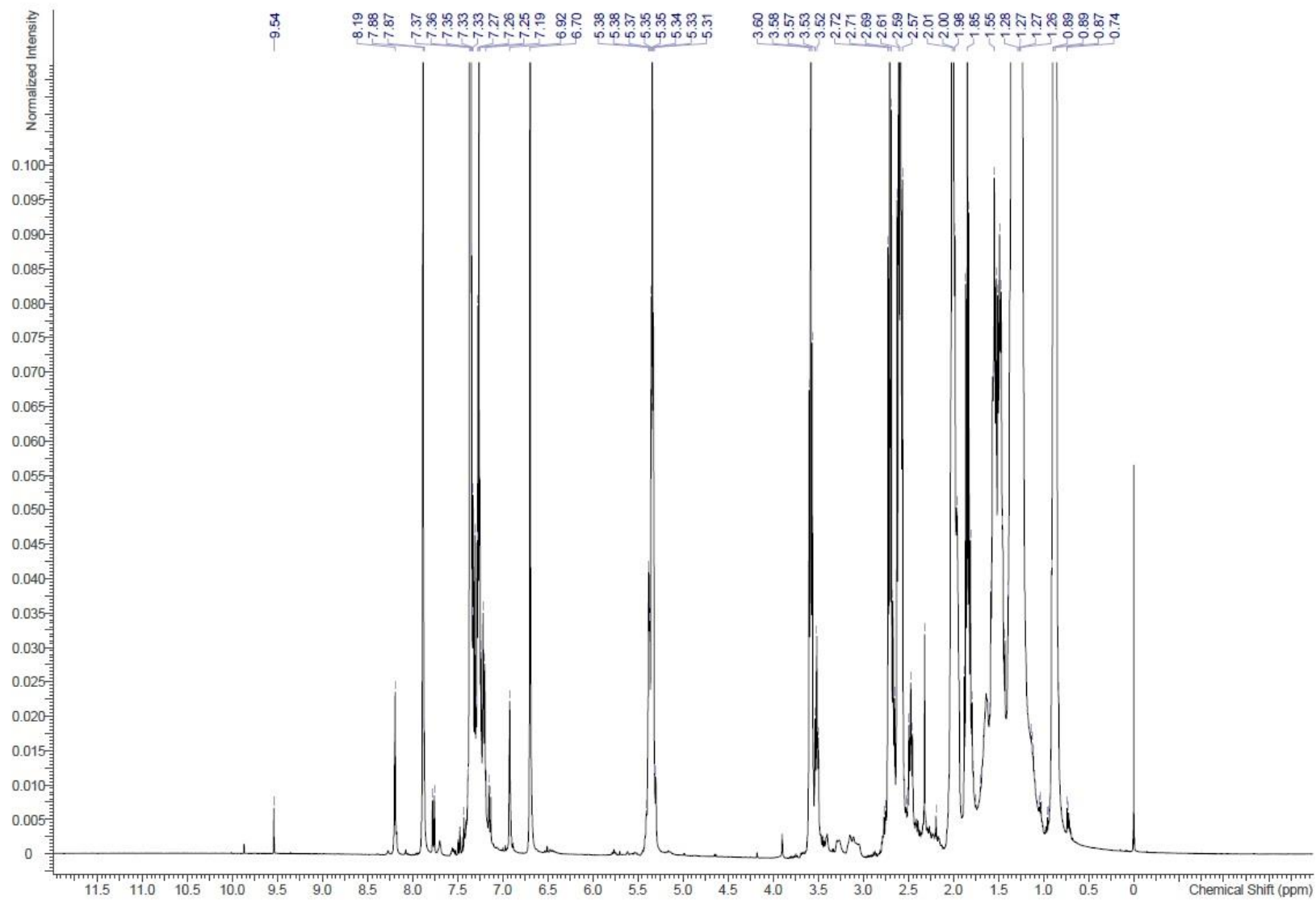


Figure 92: ¹H-NMR of Product 24

FF

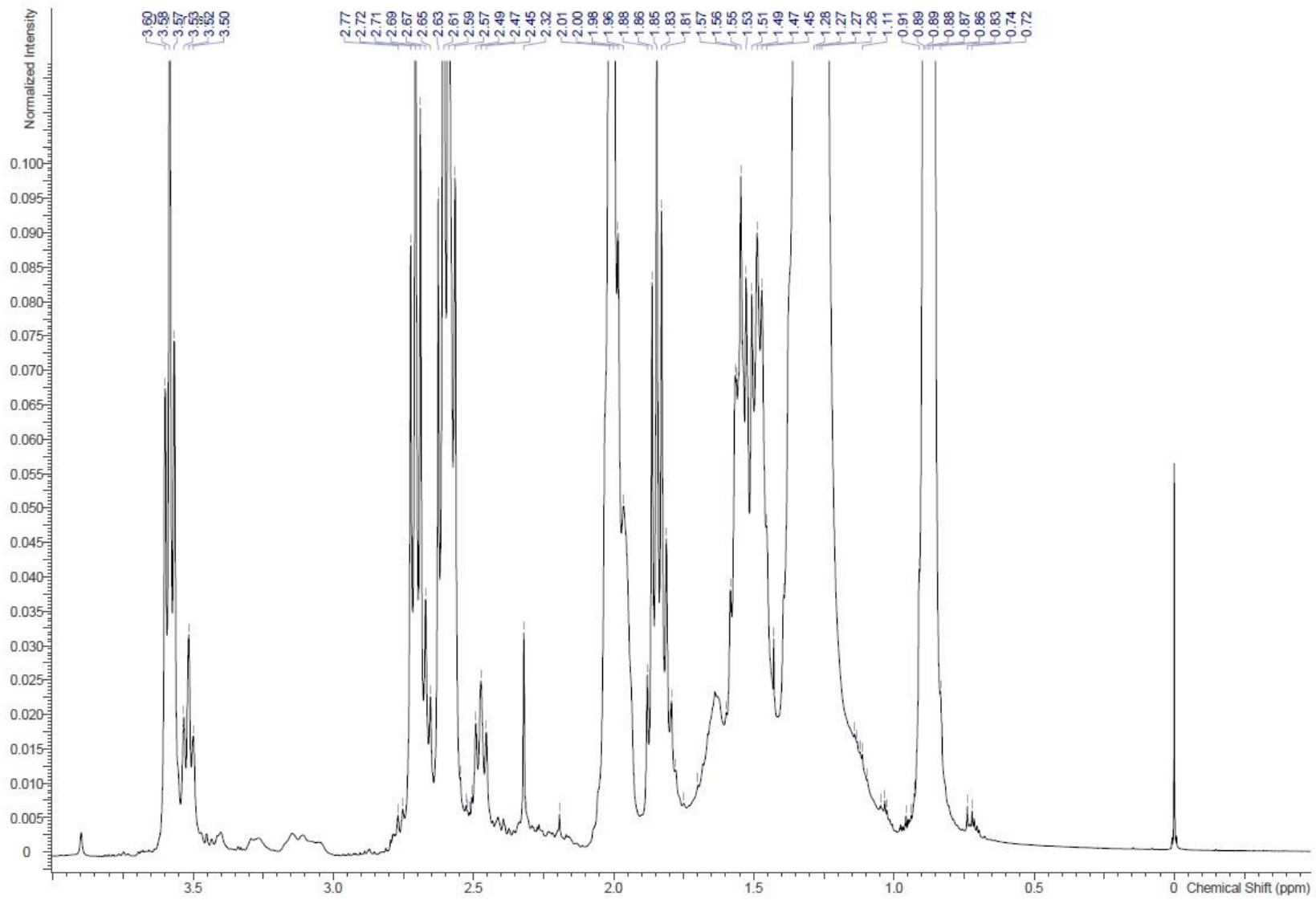


Figure 93: ¹H-NMR of Product 24

GG

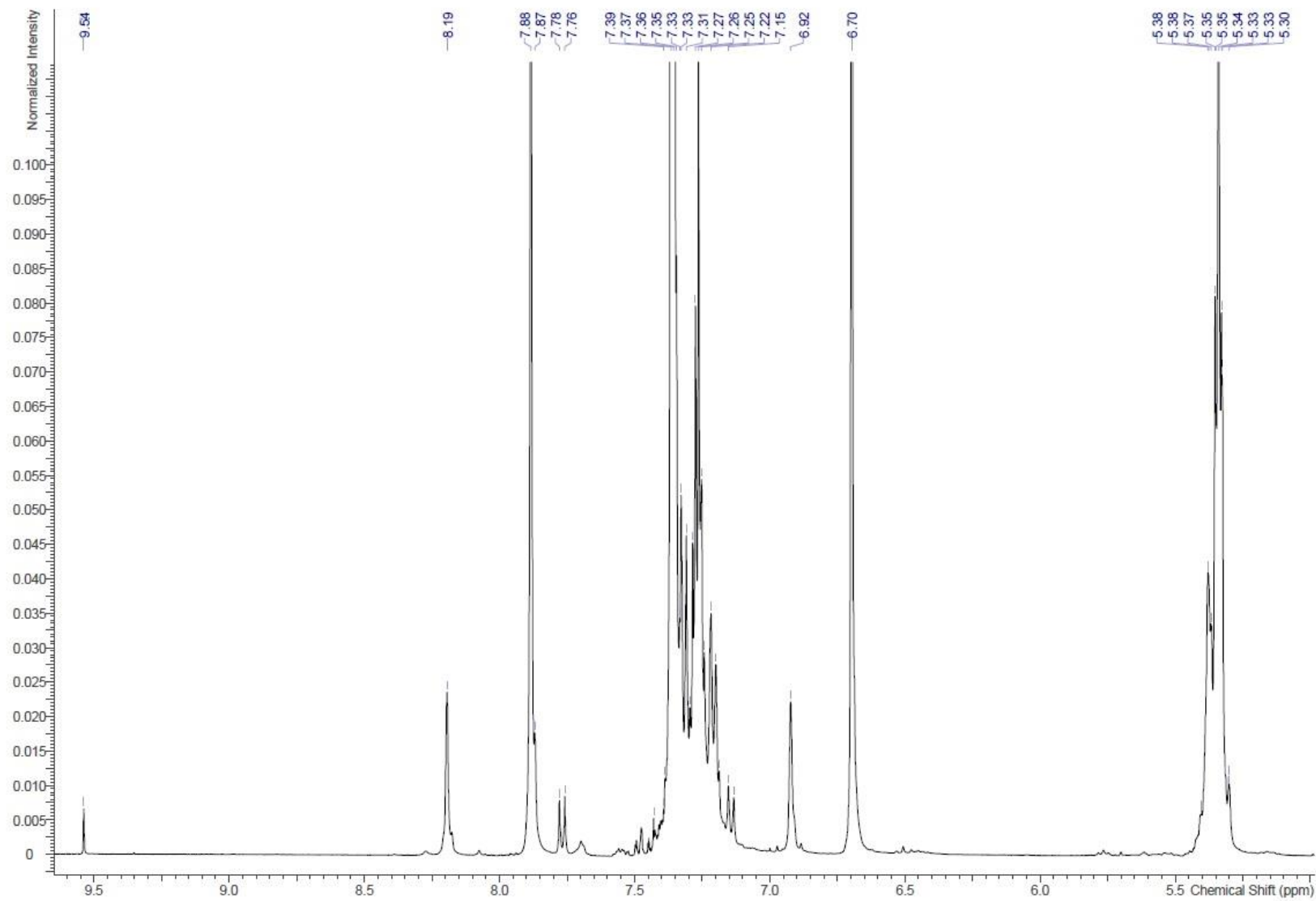


Figure 94: ¹H-NMR of Product 24

HH

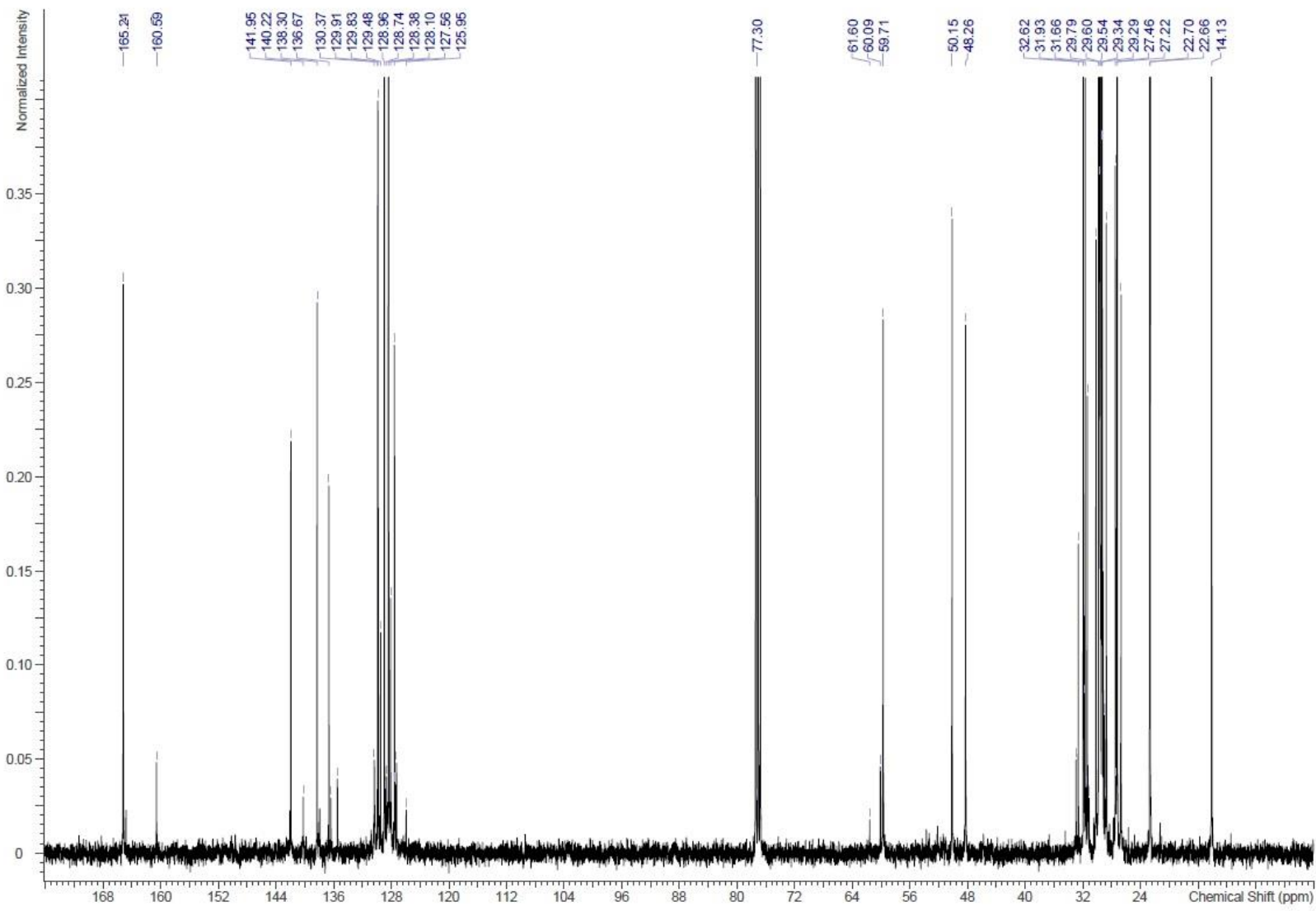


Figure 95: ¹³C-NMR of Product 24

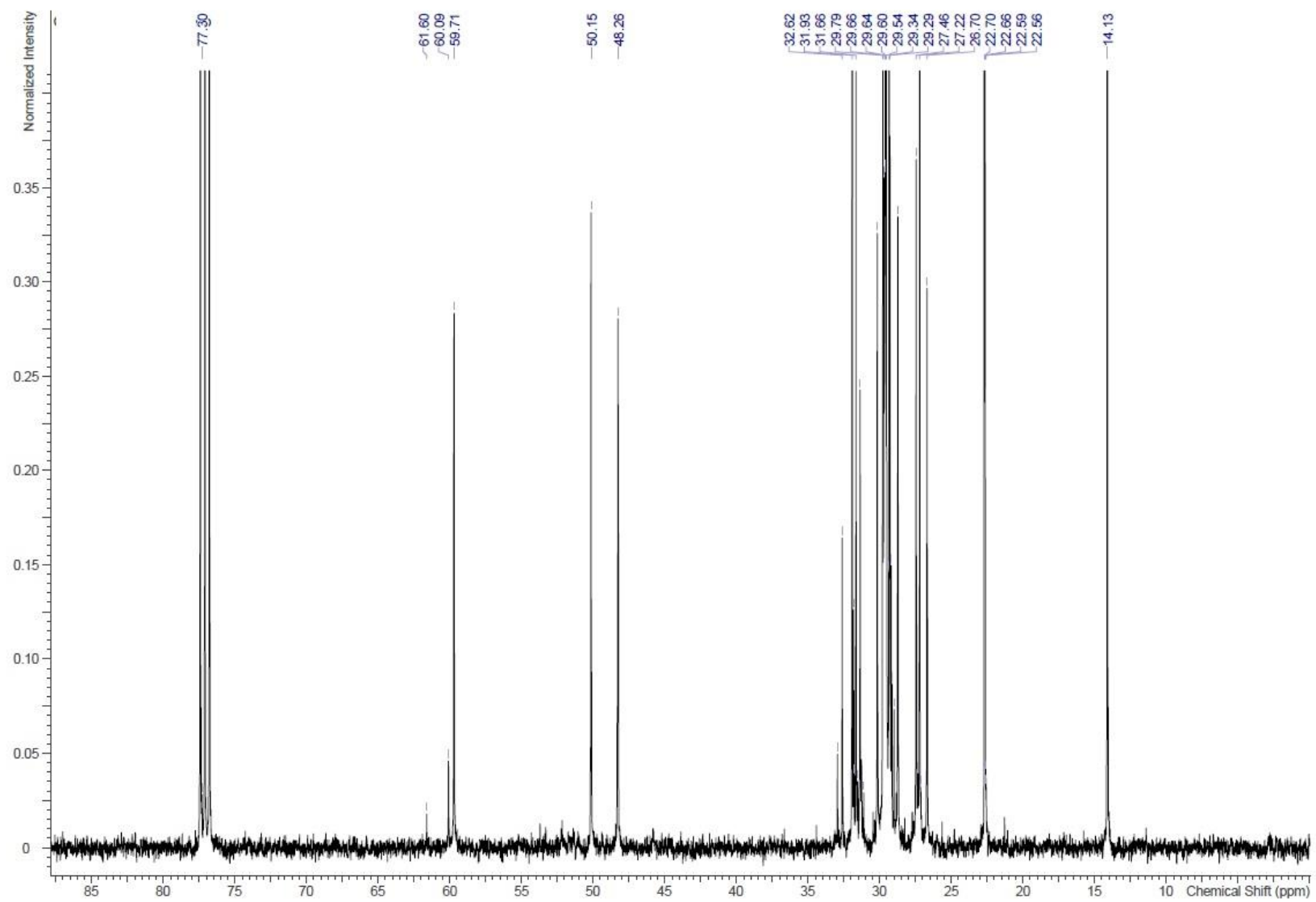


Figure 96: ¹³C-NMR of Product 24

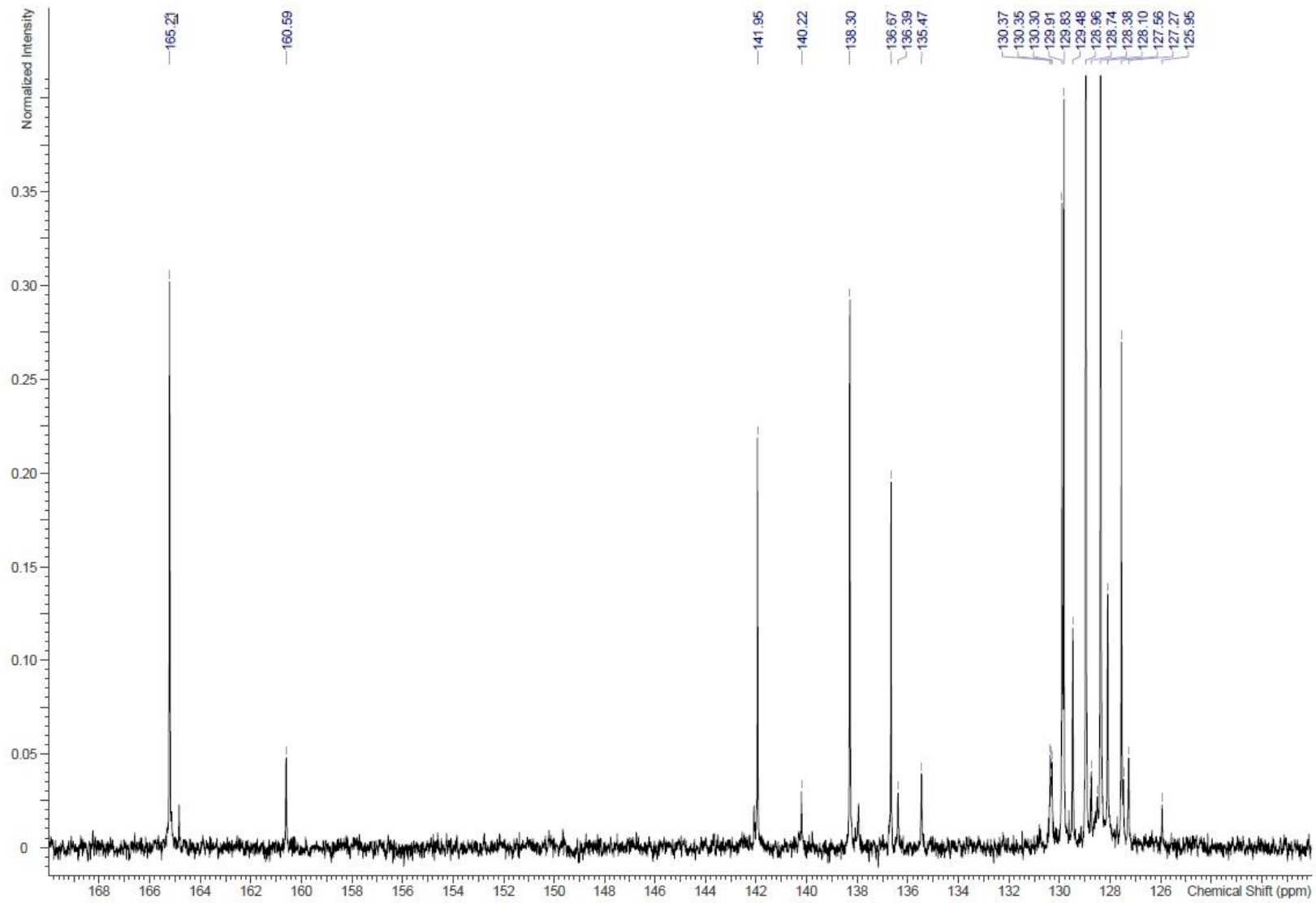


Figure 97: ^{13}C -NMR of Product 24

KK

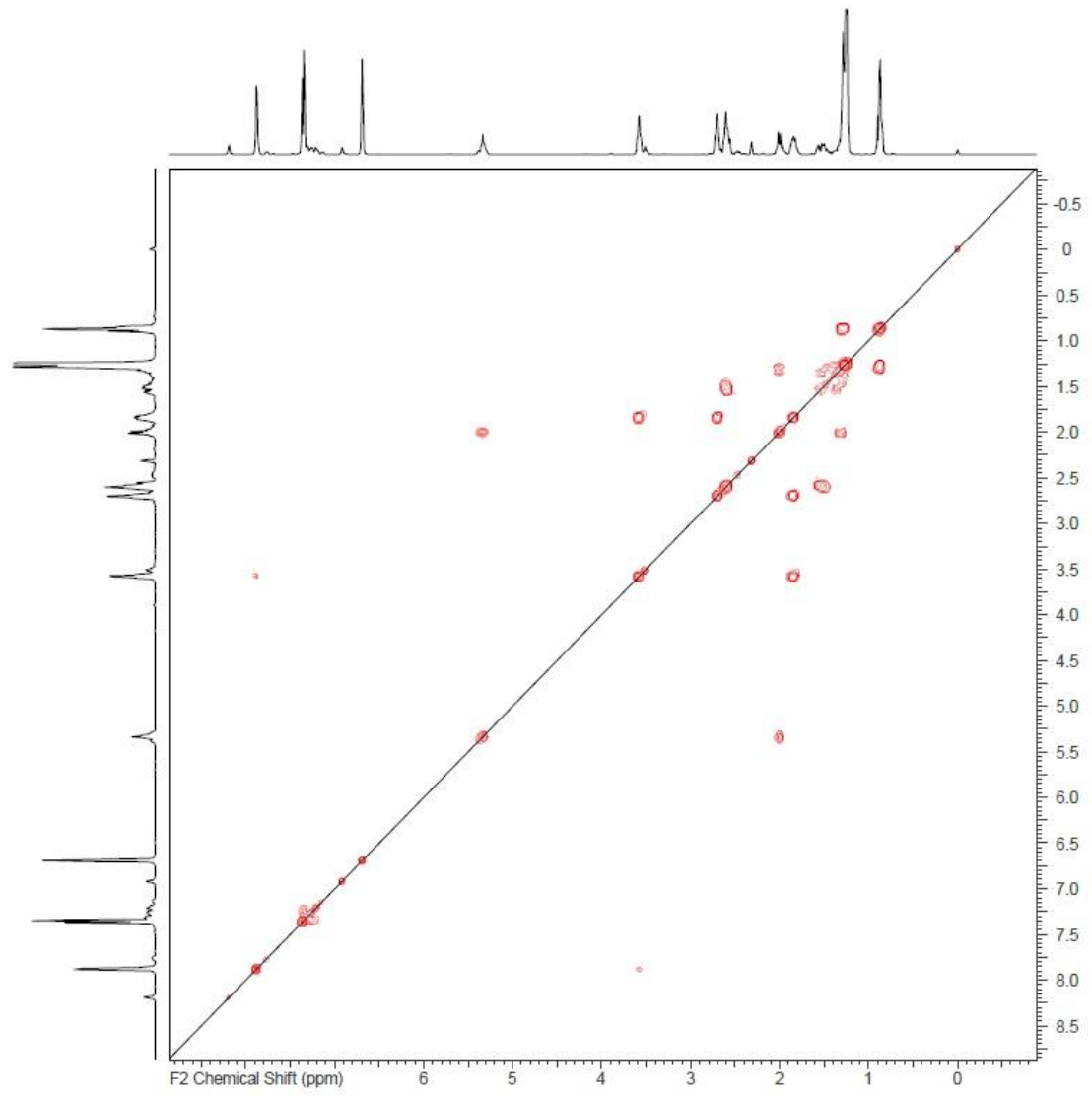


Figure 98: 2D-NMR COSY of Product 24